Transcriptional and posttranscriptional regulation of the microRNA pathway by 5-lipoxygenase

Vom Fachbereich Biologie
der Technischen Universität Darmstadt
zur Erlangung des Grades
Doctor rerum naturalium
(Dr. rer. nat.)

DISSERTATION

von

Stella Andrea Hedrich

Erstgutachterin: Prof. Dr. Beatrix Süß
Zweitgutachter: Prof. Dr. Dieter Steinhilber

Darmstadt 2019

Hedrich, Stella Andrea: Transcriptional and posttranscriptional regulation of the microRNA pathway by 5-lipoxygenase
Darmstadt, Technische Universität Darmstadt
Jahr der Veröffentlichung der Dissertation auf TUprints: 2021
URN: urn:nbn:de:tuda-tuprints-90977
Tag der mündlichen Prüfung: 12.08.2019

Für Lukas

Acknowledgement

Zuerst möchte ich meinen drei Chefs – Beatrix, Dieter und Olle – für die Möglichkeit danken meine Doktorarbeit in ihren Arbeitskreisen durchzuführen sowie für die vielfältigen Erfahrungen, die ich durch meine Aufenthalte in Darmstadt, Stockholm und Jena sammeln durfte.

//

Initially, I would like to thank my three supervisors – Beatrix, Dieter and Olle – for the opportunity to do my PhD in their working groups as well as for the manifold experiences I gained during my stays in Darmstadt, Stockholm and Jena.

Natürlich gilt mein Dank auch meinen vielen Kollegen im AK Süß, AK Steinhilber und AK Werz/Garscha sowie meinen „schwedischen" Kollegen von Kemi II. Um die Gefahr zu umgehen jemanden zu vergessen, möchte ich einfach allen „Danke" sagen – vielen Dank für eure Hilfe, für eure Unterstützung, für die gute Zusammenarbeit, für lustige gemeinsame Pausen und für die schöne Zeit.

//

Of course, I would also like to thank my many colleagues from the Süß working group, the Steinhilber working group, and the Werz/Garscha working group, as well as my "Swedish" colleagues from Kemi II. To avoid the risk of not mentioning someone, I would just like to say "thank you" to everyone – thanks for your help, for your support, for the good cooperation, for the funny breaks, and the good times.

Für die großartige Betreuung während meiner aufregenden Zeit in Jena bedanke ich mich bei Ulrike. Ich danke auch Oliver für die nette Aufnahme in seinen Arbeitskreis.

Mein Dank gilt auch der Else Kröner-Fresenius-Stiftung für die finanzielle Unterstützung.

Danke Julia für die schöne Zeit in Stockholm und die fortwährende Aufmunterung während meiner Promotion. Dein größter Verdienst ist aber meiner Meinung nach, dass du meine Leidenschaft für das Klettern und die Berge aufgeweckt hast.

Ein großes Dankeschön geht an meine Eltern. Ohne eure beständige Unterstützung in allen Lebenslagen wäre der Weg bis zu dieser Arbeit viel mühseliger und vielleicht auch gar nicht möglich gewesen. Dank gilt auch meinem großen Bruder Philipp, der mir stets ein gutes Vorbild war und mich, wie er selbst sagt, für das Leben abgehärtet hat.

Mein allergrößter Dank gilt natürlich meinem Verlobten Lukas - deine bedingungslose Unterstützung und fortwährende Ermunterung in schwierigen Phasen haben mir diese Arbeit ermöglicht, die ich als Zeichen meiner Dankbarkeit dir widme.

II

Ehrenwörtliche Erklärung

Ich erkläre hiermit ehrenwörtlich, dass ich die vorliegende Arbeit entsprechend den Regeln guter wissenschaftlicher Praxis selbstständig und ohne unzulässige Hilfe Dritter angefertigt habe. Sämtliche aus fremden Quellen direkt oder indirekt übernommenen Gedanken sowie sämtliche von Anderen direkt oder indirekt übernommenen Daten, Techniken und Materialien sind als solche kenntlich gemacht. Die Arbeit wurde bisher bei keiner anderen Hochschule zu Prüfungszwecken eingereicht.

Darmstadt, der 11. Juli 2019

Stella Andrea Hedrich

“The summit is what drives us,
but the climb itself is what matters.”

Conrad Anker

Contents

Abbreviations

5-LO	5-lipoxygenase
5-LOΔ	5-lipoxygenase knockout
5-LOkd	5-lipoxygenase knockdown
AA	arachidonic acid
AGO	argonaute
ATP	adenosine triphosphate
AUDA	12-(3-adamantan-1-ylureido)dodecanoic acid
BMP	bone morphogenetic protein
BSA	bovine serum albumin
cDNA	complementary DNA
CO_2	carbon dioxide
COX	cyclooxygenase
$cPLA_2$	cytosolic phospholipase A_2
CTP	cytidine triphosphate
Ctrl	control knockdown
CYP	cytochrome P450
DNA	deoxyribonucleic acid
DAPI	4′,6-diamidino-2-phenylindole
DGCR8	DiGeorge syndrome critical region 8
DTT	dithiothreitol
dsRBD	double-stranded RNA binding domain
dsRNA	double-stranded RNA
DUF	domain of unknown function
EET	epoxyeicosatrienoic acid
EMA	European Medicines Agency
FCS	fetal calf serum
FDA	U.S. Food and Drug Administration
FITC	5/6- fluorescein isothiocyanate
FLAP	5-lipoxygenase activating protein
GSH	glutathione
GTP	guanosine-5'-triphosphate
HA	hemagglutinin
hATTR	hereditary transthyretin-mediated amyloidosis
HBSS buffer	Hank's buffered salt solution
HETE	hydroxyeicosatetraenoic acid
H(p)ETE	hydroperoxyeicosatetraenoic acid
HPLC	high-performance liquid chromatography
HSPC	hematopoietic stem and progenitor cells
IL	interleukin
IR	infrared
IRAK1	interleukin-1 receptor-associated kinase 1
KSRP	KH-type splicing regulatory protein
LPS	lipopolysaccharide
LT	leukotriene
MM6	Mono Mac 6
miRNA	microRNA
mRNA	messenger RNA
NF-κB	nuclear factor kappa B
PACT	protein activator of protein kinase R

PAZ	Piwi-Argonaute-Zwille
P-bodies	processing bodies
PBS	phosphate buffered saline
PBS-T	phosphate buffered saline with Tween 20
PCR	polymerase chain reaction
PDCD4	programmed cell death 4
PG	prostaglandin
piRNA	piwi-interacting RNA
PLA_2	phospholipase A_2
pre-miRNA	precursor miRNA
pri-miRNA	primary miRNA
qRT-PCR	real-time quantitative PCR
RISC	RNA-induced silencing complex
RNA	ribonucleic acid
RP-HPLC	reversed-phase high-performance liquid chromatography
rpm	revolutions per minute
RT	reverse transcription
SBE	SMAD binding element
scRNA	small cytoplasmatic RNA
SDS-PAGE	sodium dodecyl sulfate polyacrylamide gel electrophoresis
sEH	soluble epoxide hydrolase
SHIP1	Src homology 2 domain-containing inositol-5′-phosphatase 1
siRNA	small interfering RNA
snoRNA	small nucleolar RNA
SNP	single nucleotide polymorphism
SOCS1	suppressor of cytokine signalling 1
SPACA6	sperm acrosome-associated 6
SPM	pro-resolving mediators
ssRNA	single-stranded RNA
rRNA	ribosomal RNA
TFA	trifluoroacetic acid
TGF-β	transforming growth factor β
TLR	Toll-like receptor
TNFα	tumor necrosis factor alpha
TNFAIP3	tumor necrosis factor alpha induced protein 3
TRAF6	tumor necrose factor receptor-associated factor 6
TRBP	TAR RNA-binding protein
tRNA	transfer RNA
TX	thromboxane
UTP	uridine triphosphate
UTR	untranslated region

1 Introduction

1.1 RNA silencing

RNA silencing (or RNA interference) refers to post-transcriptional gene silencing pathways implemented by short noncoding double stranded RNAs (dsRNA). The short RNA duplexes interfere with single stranded RNAs (ssRNA), e.g. messenger RNAs (mRNA) or viral RNAs, introducing their cleavage or translational repression and thus silencing the respective endogenous genes or protecting the host from foreign or invasive nucleic acids as defenders of the genome integrity[1,2]. RNA interference was first discovered in *Caenorhabditis elegans* (*C. elegans*) by Andrew Z. Fire and Craig S. Mello, who provided insights into how experimental introduced dsRNA interferes with the function of endogenous genes[3]. In 2006, Fire and Mello got awarded the Nobel Prize in Physiology or Medicine for their discoveries[4].

For the last two decades considerable efforts were made to explore and unveil the mechanisms of RNA silencing. In particular, the family of microRNAs (miRNA), the most prominent class of short noncoding dsRNAs, and its potential as drug targets and biomarkers were extensively studied.

1.1.1 miRNAs

Remarkably, the first miRNA lin-4 was already discovered in *C. elegans* in 1993 and therefore several years before the discovery of the overriding mechanism of RNA interference[5]. The high physiological relevance of miRNAs is emphasized by the fact that miRNAs control most of the human protein-coding genes and are involved in almost every physiological and pathological process. Furthermore, miRNAs are very abundant[6]. This can be nicely illustrated by some numbers: the miRNA database miRbase lists 271 organisms, who in total express ∼38500 miRNAs. 1917 of these miRNAs are annotated to the human genome (status as of May 2019)[7].

Great efforts are undertaken for the development of miRNA therapeutics. The database clinicaltrials.gov by the U.S National Library of Medicine[8] lists 382 interventional clinical trials as a result for the keyword search “microRNA” and “miRNA” (status as of May 2019). This high number of clinical trials emphasizes the potential of miRNA mimics and substances inhibiting miRNA functions (antimiRs) as promising drug candidates for the treatment of various diseases, in particular various types of cancer, as well as the potential of miRNAs as reliable biomarkers. Major challenges for the development of miRNA therapeutics are the *in vivo* stability, the design of delivery systems, and the safety profile[9]. For instance, a phase 1 study of MRX34, a liposomal mimic of miR-34, in patients suffering from primary liver cancer and other types of cancer had to be terminated due to five immune-related serious adverse events[8].

However, in August 2018 the FDA (U.S. Food and Drug Administration) and the EMA (European Medicines Agency) approved marketing authorization for Onpattro® (patisiran), the first commercially available drug interfering with the RNA silencing pathway. Onpattro® is used for the treatment of peripheral nerve disease caused by hereditary transthyretin-mediated amyloidosis (hATTR) in adult patients. The hATTR is a severe genetic disorder caused by a mutation in the amyloid protein transthyretin. The used siRNA patisiran prevents the production of the abnormal amyloid protein by silencing the respective gene leading to a relief of the polyneuropathy[10–12].

1.1.2 Biogenesis of miRNAs

The miRNA biogenesis is tightly controlled both temporally and spatially, as well as regulated at multiple levels, to avoid dysfunctions which are related to severe disorders, most notably cancer. Figure 1.1 illustrates the biogenesis of miRNAs. The first step is the transcription by RNA polymerase II providing the primary miRNA (pri-miRNA). The pri-miRNA is quite long (>1 kb) and forms a hairpin structure, embedding the mature miRNA, with flanking ssRNA segments at both sides[6]. Human miRNAs are encoded either between genes (intergenic) or within a gene (intragenic; intronic or exonic). Transcription of intergenic miRNAs is controlled by their own promotors, whereas expression of intragenic miRNAs is regulated independently or dependent on their host gene. A dual regulation of intronic genes by both, their own as well as their host gene promotor, may also occur[6,13]. Some miRNA genes are located close to others, forming a transcription unit so that these clustered miRNAs are co-transcribed. Moreover, transcription of miRNAs is controlled by transcription factors, such as p53 and MYC, as well as by epigenetic alterations like DNA methylation and histone modifications[6].

The pri-miRNA is subsequently processed by the microprocessor complex consisting of Drosha and DGCR8 (DiGeorge syndrome critical region 8). The microprocessor complex crops the hairpin structure of the pri-miRNA at a distance of ∼11 bp from the dsRNA-ssRNA junction, generating a stem-loop structured precursor miRNA (pre-miRNA) ∼65 nucleotides in length, with a two-nucleotide overhang at the 3' end. Drosha's interaction partner DGCR8 is an essential subunit of the microprocessor complex. Suggested functions of DGCR8 are the recognition of the RNA substrate, as well as stabilizing Drosha via protein-protein interactions[14,15]. Furthermore, the DGCR8 gene was found to be embedded within the DiGeorge syndrome chromosomal region on chromosome 22. The monoallelic microdeletion of chromosome 22q11.2 has been associated with a severe genetic disorder called the DiGeorge syndrome. The clinical phenotype includes learning disabilities, characteristic facial appearance, cleft palate, heart defects, thymic hypoplasia or aplasia, hypocalcaemia, and psychiatric illness[16].

Cleavage of intronic pri-miRNAs by the microprocessor complex does not interfere with the splicing of the host genes, since it is presumed that pri-miRNA processing happens co-transcriptionally. However, processing of exonic miRNAs leads to destabilization of the host mRNA. Remarkably, Drosha cleaves DGCR8 mRNA at a hairpin structure in the second exon, releasing the miR-1306 as part of an autoregulatory loop. It is unclear whether miR-1306 is a canonical miRNA or just functions as a mRNA destabilizing element[15]. In addition to the autoregulation, several factors were reported to modulate the processing activity of the microprocessor complex. For instance, transforming growth factor β (TGF-β) and bone morphogenetic protein (BMP) rapidly induce the expression of 20 different miRNAs, including miR-21 and miR-199a, in human primary pulmonary smooth muscle cells by facilitating the Drosha-mediated cleavage. Upon stimulation with TGF-β and BMP the signal transducers R-smads translocate to the nucleus and associate with the Drosha/DGCR8/p68 microprocessor complex. A majority of the miRNAs regulated by TGF-β and BMP contain a Smad binding element within the stem region of the primary transcript. Smads were found to bind directly to this consensus sequence[17]. Furthermore, the RNA-binding proteins hnRNP A1 and KH-type splicing regulatory protein (KSRP) were reported to promote the Drosha-mediated processing of pri-miR-18a and pri-let-7, respectively[18–20]. Interestingly, KSRP facilitates the Drosha-mediated cleavage, as well as the subsequent Dicer-mediated cleavage, via binding to the terminal loop of the target miRNA precursors (see chapter 1.1.3)[20].

Subsequent to the Drosha-mediated processing, the carrier protein exportin-5 transfers the pre-miRNA from the nucleus to the cytoplasm, where it is in turn processed further by the RNAse III-type endonuclease Dicer to the mature miRNA duplex[6,21]. The functions and structure of Dicer, as well as its regulation, are described in detail in chapter 1.1.3.

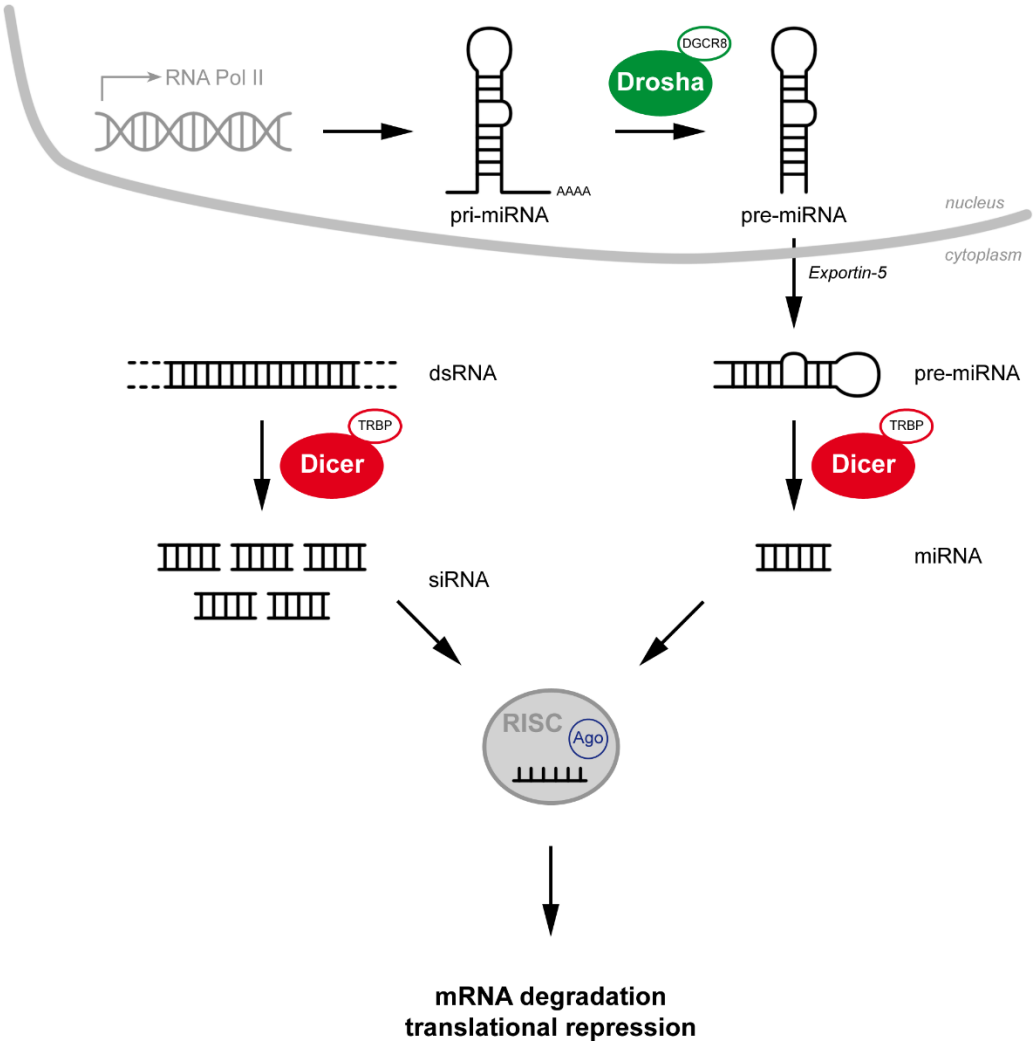

Figure 1.1 The miRNA pathway
After transcription by RNA polymerase II, the pri-miRNA is cleaved by the microprocessor complex, which consists of Drosha and DGCR8. Exportin-5 transfers the resulting pre-miRNA to the cytoplasm, where Dicer in complex with TRBP processes the pre-miRNA to the mature miRNA duplex. The guide strand of the duplex, which is selected by an argonaute protein, guides the RNA-induced silencing complex to the 3'UTR of the target mRNAs facilitating mRNA degradation or translational repression. Dicer also processes long, linear, and perfectly base-paired dsRNA to siRNA. (Figure is adapted from[22]).

Following its generation by Dicer, the miRNA duplex is loaded onto an argonaute (AGO) protein to form the RNA-induced silencing complex (RISC). During the adenosine triphosphate (ATP) consuming AGO loading step, RISC needs to select and unwind the guide strand from the miRNA duplex based on the thermodynamic stability of the two strands. The strand with the more unstable 5' end and preferably a U nucleotide at position 1 is selected as the guide strand, which then leads RISC to the target mRNAs. Meanwhile, the passenger strand is released and degraded, resulting in a miRNA pool enriched with the guide strand[6]. Target recognition by the miRNA occurs through base pairing between the miRNA seed region (nucleotide 2-8) and the 3' untranslated region (UTR) of the mRNA. The base pairing can be supported by additional pairing with little efficacy between the target mRNA and the nucleotides 13 to 16 at the 3' end of the miRNA[23]. Following target recognition, the AGO proteins function as effectors within the RNA-induced silencing complex by inducing translational repression, mRNA decay, or mRNA degradation in processing bodies (P-bodies)[6].

Although the miRNA biogenesis is tightly controlled to avoid dysfunction, there are various options for additional regulation. For instance, the biosynthesis of miRNAs can be regulated by single nucleotide polymorphisms (SNP) of the miRNA sequence, through miRNA tailing and stability, as well as by RNA editing and methylation. In addition to the canonical miRNA pathway, several noncanonical pathways bypassing Drosha or Dicer-mediated processing exist. However, just 1% of the conserved miRNAs in vertebrates are synthesized via a noncanonical pathway and the majority of noncanonical miRNAs are barely conserved and hardly abundant[6].

1.1.3 Dicer

The RNAse III-type endonuclease Dicer is a key enzyme within the RNA silencing pathway due to its dsRNA processing properties. Dicer either cleaves pre-miRNAs into the miRNA duplex (see chapter 1.1.2) or long, linear, and perfectly base paired dsRNAs, that are taken up from the environment or directly introduced into the cytoplasm, into small interfering RNAs (siRNA) (see Fig. 1.1)[2,22].

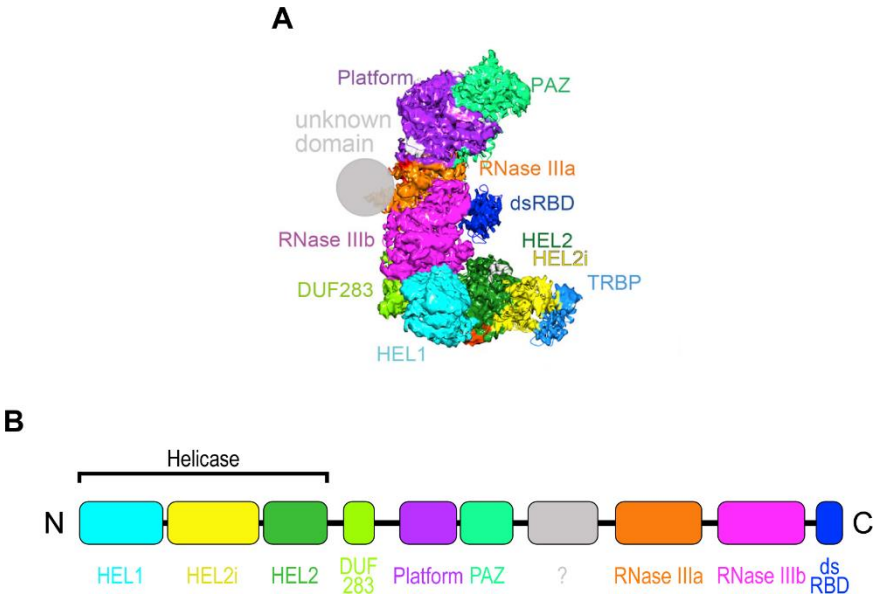

Figure 1.2 Dicer
The multidomain enzyme Dicer exhibits an L-shaped three-dimensional structure and consists of an N-terminal helicase domain (HEL1, HEL2i, HEL2), DUF 283, the PAZ domain, an unknown domain, two RNAse III (RNAse IIIa/b) domains, and a C-terminal dsRNA binding domain, which interacts with 5-LO. (A) EM density map of full-length human Dicer in complex with its cofactor TRBP (figure is taken from[24]). (B) Schematic illustration of full-length human Dicer's domain structure. Each domain is colored as in the EM density map (figure is adapted from[24]).

The protein Dicer is ∼200 kDa in size and comprised of 1922 amino acids. The multidomain enzyme consists of an N-terminal helicase domain, DUF283 (domain of unknown function), the PAZ (Piwi-Argonaute-Zwille) domain, an unknown domain, two RNAse III (RNAse IIIa/b) domains, and a C-terminal

double-stranded RNA binding domain (dsRBD) (see Fig. 1.2 B). Dicer exhibits an L-shaped three-dimensional structure (see Fig. 1.2 A): The two RNAse III domains dimerize to form the nuclease core. The helicase domain binds to the stem-loop of the dsRNA while the PAZ domain interacts with its end. The production of small RNAs of a distinct size is facilitated by the region located between the PAZ and the RNase III domains, which functions as a "molecular ruler". The PAZ domain, which requires a two-nucleotide overhang at the 3' end of the dsRNA for efficient interaction, binds both ends of the substrate and thus enables Dicer to determine its cleavage site by measuring the distance (∼ 22 nucleotides) from the 3' and the 5' ends[6,24–29].

Processing of dsRNAs by Dicer is modulated by its cofactors and RNA binding proteins. For example, the cofactor TAR RNA-binding protein (TRBP) modulates Dicer's processing efficiency and adjusts the length of the cleaved products. Apart from TRBP, Dicer interacts with another cofactor, PACT (protein activator of protein kinase R), the function of which remains unclear. Interestingly, both cofactors, TRBP and PACT, are not essential for Dicer-mediated cleavage[6]. As already mentioned in the previous chapter 1.1.2, the RNA-binding protein KSRP, a key regulator of mRNA decay, was found to regulate the biosynthesis of miRNAs as a component of both processing complexes, the Drosha and the Dicer complex. KSRP promotes the maturation of a subset of miRNAs via its interaction to their terminal loop[20]. LIN28 exerts an opposite effect as it binds to the terminal loop of pre-let-7 in order to induce its oligouridylation, resulting in the prevention of Dicer cleavage[30] (see chapter 1.1.4). Interestingly, the enzymatic activity of Dicer is also regulated by its products via negative feedback loops. For instance, the human DICER1 mRNA contains binding sites for let-7 miRNA[31].

Previous studies discovered that Dicer interacts with 5-lipoxygenase (5-LO), a key regulator of inflammatory processes (see chapter 1.2)[32,33]. A yeast two hybrid system was used with the intention to screen for proteins interacting with 5-LO. The obtained data revealed that the C-terminal 140 amino acids of Dicer interact with the N-terminal C2-like regulatory domain of 5-LO. Furthermore, GST pull-down experiments performed with a mutant, but enzymatically active, W13/75/102A 5-LO (alanine replaces tryptophan residues) demonstrated that 5-LO's tryptophan residues at position 13, 75, and 102 are essential for its ability to interact with Dicer. In addition to this, coimmunoprecipitation of HA-tagged 5-LO and the FLAG-tagged C-terminus of Dicer were interrupted by the same mutations. Furthermore, 5-LO and Dicer were shown to interfere with each other's enzymatic activity *in vitro*. The 5-LO interacting domain of Dicer moderately stimulated Ca^{2+}-induced 5-LO activity, whereas 5-LO modified the Dicer cleavage pattern in favour of the formation of ∼55 bp and 10-12 bp long products[32]. Besides its ability to interact with 5-LO, it was reported that Dicer's dsRBD domain supports the substrate binding and cleavage while also functioning as a nuclear localization signal[24,27,34,35].

1.1.4 Prominent representatives of the miRNA class

The let-7 miRNAs are one of the most prominent and well studied family of miRNAs, which is evolutionarily conserved across different animal species. Although the let-7 miRNAs are expressed ubiquitously in adult tissue of mammals, their expression increases during development in line with

their function in terminal differentiation. Further functions of this miRNA family are self-renewal of stem cells as well as tumor suppressor functions in various types of cancer. In humans, 12 different genomic loci encode for nine mature let-7 miRNAs, some of which are clustered together (see Table 1.1)[36].

Table 1.1 The let-7 miRNA family

let-7a-1	let-7a-2	let-7a-3	let-7c	let-7e	let-7f-2
let-7a	let-7a	let-7a	miR-99a	miR-99b	let-7f
let-7f	miR-100	let-7b	let-7c	let-7e	miR-98
let-7d		miR-4763	miR-125b	miR-125a	

The table displays the following clusters of the let-7 miRNA family: let-7a-1, let-7a-2, let-7a-3, let-7c, let-7e, and let-7f-2. The name of the primary transcript is written in bold letters. The respective mature miRNAs are listed below. The table is based on the miRbase database[7].

Clusters let-7a-2 and let-7c, which are highly expressed in hematopoietic stem cells (HSC), were shown to regulate hematopoietic stem and progenitor cell (HSPC) homeostasis by blocking the TGF-β pathway and simultaneously amplifying Wnt signaling due to stabilizing active β-catenin. The shifted balance between TGF-β and Wnt signaling results in a promoted HSC expansion as well as in an enhanced megakaryocytic differentiation[37]. Additionally, the let-7e cluster, consisting of miR-99b, let-7e, and miR-125a, was also reported to be highly expressed in HSC, but in turn the cluster is down-regulated upon differentiation. Remarkably, miR-125a by itself retains the cells in a primitive state as well as augments stem cell activity. Furthermore, miR-125a amplifies the HSC pool size by reducing apoptosis of HSPCs via the targeting of proapoptotic genes, such as Bak1, in a differentiation stage specific manner[38,39].

The let-7e cluster is subject of many scientific reports, not just limited to the context of stem cell homeostasis. The three miRNAs miR-99b, let-7e, and miR-125a are located on chromosome 19 and form an intronic cluster, which shares its promotor with the SPACA6 (sperm acrosome-associated 6) gene. The promotor harbours a binding site for the p65 subunit of NF-κB (nuclear factor kappa B) and previous reports revealed an increase of the miR-125a expression upon NF-κB activation during monocyte to osteoclast differentiation, as well as in hepatic cells. Interestingly, miR-125a was reported to target TNFAIP3 (tumor necrosis factor alpha induced protein 3), a negative regulator of the NF-κB pathway, providing a positive feedback loop leading to a strengthened miR-125a expression[40,41]. Another report provides an additional link between the let-7e cluster and inflammatory as well as innate immune responses. The miR-99b/let-7e/miR-125a cluster was described as a regulator of the Toll-like receptor (TLR) signaling pathway (see Fig. 1.3) and the mature miR-125a as a modulator of endotoxin tolerance. Exposure of human monocytes to the TLR4 agonist lipopolysaccharide (LPS) was shown to induce the cluster in a delayed manner. The late kinetic is caused by interleukin-10 (IL-10), a second mediator of the LPS response, that potentiates the upregulation by LPS. This study also provided a deeper insight into the transcriptional regulation of the let-7e cluster. LPS, IL-10, and TGF-β facilitate increased recruitment of the polymerase II to the core promotor via activation of the transcription factors NF-κB, STAT3 (signal transducer and activator of transcription 3), or Smad3, resulting in an enhanced expression of the respective mature miRNAs. The mature miRNAs let-7e and miR-125a in turn regulate the TLR pathway on multiple levels by targeting TLR4, as well as signaling molecules (e.g. IRAK1) and

proinflammatory cytokines (e.g. TNFα, IL-6). Thus, both miRNAs act as anti-inflammatory agents, diminishing the proinflammatory impacts of LPS[42].

Various scientific reports describe the let-7 miRNAs as regulators of the oncogenic Ras and HMGA2 (High-mobility group AT-hook 2) proteins, emphasizing their function as tumor suppressors[43–45]. For instance, let-7g reduces growth of non-small cell lung cancer (NSCLC) tumors through suppressing K-Ras and HMGA2[44]. In breast cancer stem cells, let-7 was reported to increase upon differentiation and to target H-Ras and HMGA2 in order to regulate self renewal and multipotent differentiation. Silencing of HMGA2 enhances differentiation, whereas silencing of H-Ras leads to the loss of the ability to self-renew[45]. Moreover, previous studies reported that let-7a downregulates the oncogenic transcription factor Myc and thus reduces Myc-induced cell growth in Burkitt lymphoma cells[46]. Interestingly, Myc itself negatively regulates the expression of several let-7 clusters (e.g. let-7a-1, let-7f-1, and let-7d) via binding to their promoter, providing a negative feedback loop[47,48].

In accordance with their pivotal functions, the biogenesis of let-7 miRNAs is tightly regulated by various factors. As already mentioned in chapter 1.1.3, previous studies described both homologues of the RNA binding protein LIN28 (Lin28a and Lin28b) as posttranscriptional repressors of let-7 processing by Dicer. LIN28 binds to the terminal loop of pre-let-7 to induce its uridylation at the 3' end by terminal uridylyl transferases (TUTase). Then, the U tail prevents Dicer processing and facilitates miRNA degradation[30,49,50]. Other studies provided evidence that LIN28 also prevents Drosha-mediated processing via binding to the loop region of primary let-7 transcripts[51]. Group II pre-miRNAs, to which most of the let-7 miRNAs belong (except pre-let-7a-2, pre-let-7c, and pre-let-7e), exhibit a shorter (1 nucleotide) 3' overhang and thus need an extension for efficient Dicer-mediated processing. Remarkably, TUTases provide this one additional nucleotide at the 3' end through monouridylation in cells lacking LIN28[52]. The discovery that let-7b, miR-125a, and its homologue miR-125b block LIN28's translation via binding to its 3'UTR, enabling a feedback loop, adds more complexity to the regulatory circuit mediated by LIN28[53,54]. As described above, Dicer is also regulated via a negative feedback loop, since let-7 binding sites are located within the human DICER1 mRNA [31].

Besides the already mentioned miR-99b/let-7e/miR-125a cluster, various other miRNAs are involved in inflammatory processes as part of the innate immune response. In literature, two types of inflammatory miRNAs are described. The proinflammatory, miRNAs which facilitate the immune response, e.g. miR-155, and the negative feedback regulators, like miR-146a, miR-146b, and miR-21, that dampen the immune system[55]. Like the miR-99b/let-7e/miR-125a cluster, all four miRNAs are NF-κB-dependent TLR-response genes, whose expression is induced in monocytic cells upon treatment with TLR activators, such as LPS (see Fig. 1.3)[40–42,56–58]. Moreover, miR-146b was also shown to be upregulated via an IL-10 mediated STAT3-dependent loop upon LPS exposure of monocytes[59]. In addition to the classification as pro- and anti-inflammatory, the group of TLR-induced miRNAs are also classified as rapidly induced miRNAs, like miR-155, or late induced ones, for instance miR-21 and the let-7e cluster[42,60].

The rapidly induced miR-155 targets SHIP1 (Src homology 2 domain-containing inositol-5'-phosphatase 1), a negative regulator of TLR-induced responses, in order to inhibit AKT signaling that in turn shuts down miR-155 expression, providing a negative feedback loop[61,62]. PDCD4 (programmed cell death 4), a target of the late induced miR-21, inhibits IL-10, which also stunts miR-155[58,63]. However, miR-21 also targets NF-κB, adding another feedback loop to a complex regulatory circuit. Thus, both miRNAs contribute to the fine tuning of TLR4 signaling. The initial increase in miR-155 enables a proceeding of the TLR4 signaling, which is limited due to a miR-21 dependent cumulation of IL-10[60,63]. Interestingly, IL-10 exhibits no effect on the expression of miR-146a and miR-21[63]. Moreover, SOCS1 (suppressor of cytokine signalling 1), another miR-155 target, regulates sensitivity and tolerance to endotoxins[61].

The miRNAs miR-146a and miR-146b also interfere with the TLR pathway on multiple levels. Both homologues of miR-146 target TRAF6 (tumor necrose factor receptor-associated factor 6) and IRAK1 (interleukin-1 receptor-associated kinase 1), downstream signal transducers of the TLR signaling, leading to a decrease in the proinflammatory cytokines TNFα (tumor necrosis factor alpha) and IL-6[56,59,64,65]. Hence, the feedback mechanisms of miR-21 and miR-146a may feature built in delay switches to the anti-inflammatory response, since already synthesized signal transducers still exist at the time of the TLR-induced expression of the respective miRNAs[55].

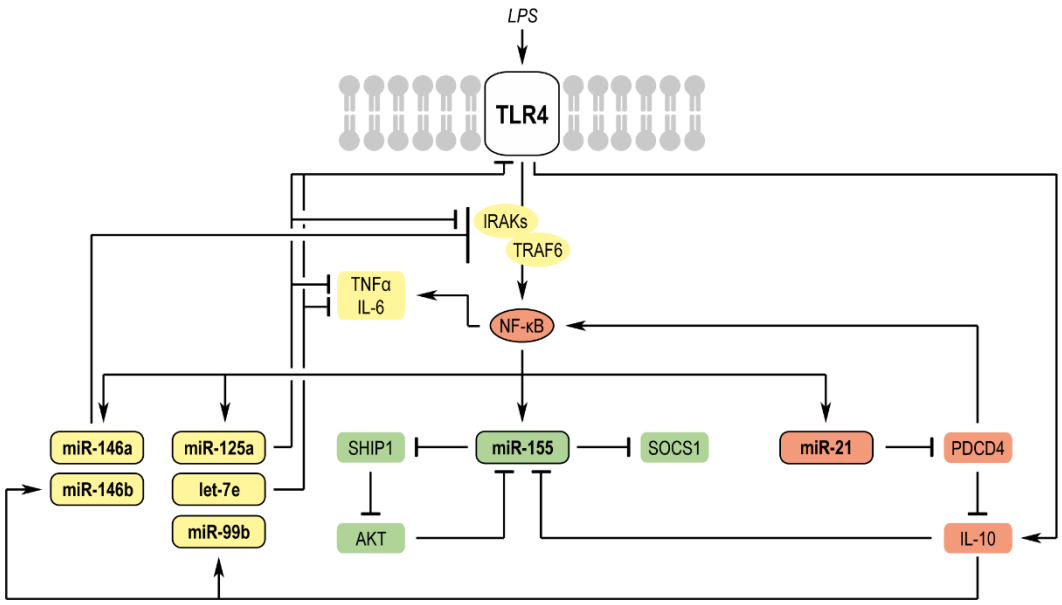

Figure 1.3 TLR-induced miRNAs
Scheme of the mutual regulation of miRNAs and Toll-like-receptor signaling[40–42,56–65]. The miRNAs miR-146a/b, miR-125a, let-7e, and miR-99b, as well as their respective targets (IRAKs, TRAF6, TNFα, IL-6), are indicated in yellow. The targets of miR-155 (SHIP1, SOCS1, AKT) and the miRNA itself are indicated in green, whereas the miRNA-21 and its targets (PDCD4, IL-10, NF-κB) are indicated in orange.

1.2 The 5-lipoxygenase pathway

Acute and chronic inflammatory diseases are a worldwide health issue with an estimated prevalence of 5-7% for chronic inflammatory diseases in the western society[66]. For many decades great efforts have been undertaken to explore and uncover the mechanisms underlaying inflammatory processes. The discovery of eicosanoids marked a milestone in the history of research related to inflammation. In 1982, Bengt I. Samuelsson, Sune K. Bergström, and John R. Vane received the Nobel Prize in Physiology or Medicine for their important findings within the field of eicosanoids[67].

Eicosanoids are a class of signaling lipid mediators, which are mainly derived from arachidonic acid (AA). Because of their participation in inflammation, as well as in its resolution, eicosanoids play a pivotal and manifold role in homeostatic and inflammatory processes linked to various pathophysiological disorders[68].

Arachidonic acid, which is released from the phospholipids in the nuclear membrane by phospholipase A_2 (PLA_2) enzymes, in particular by the cytosolic Ca^{2+}-dependent PLA_2 ($cPLA_2$), enters one of three possible eicosanoid producing metabolic cascades: the lipoxygenase (LO), the cyclooxygenase (COX), or the cytochrome P450 pathway[68] (see Fig. 1.5).

1.2.1 Canonical functions

The human protein 5-LO is encoded by the ALOX5 gene, which is located on chromosome 10. The main 5-LO transcript consists of 14 exons and encodes for 673 amino acids, which are translated to a protein ∼78 kDa in size[69]. The 5-LO protein is described as a monomeric iron-containing protein that consists of a β-sheet forming N-terminal regulatory C2-like domain and a helical structured C-terminal catalytic domain[70] (see Fig. 1.4 A). The 5-LO catalyzes the first two steps of the leukotriene biosynthesis by converting AA to the unstable epoxide leukotriene A_4 (LTA_4), which in turn is either metabolized to LTB_4 by the LTA_4 hydrolase or converted to LTC_4 via conjugation to glutathione (GSH) by the LTC_4 synthase. Subsequent peptide cleavage of the GSH residue facilitates conversion of LTC_4 to LTD_4 or LTE_4[70] (see Fig. 1.4 B and Fig. 1.5).

The enzyme 5-LO is not only involved in the onset of inflammation, but also in its resolution, as it converts oxidized fatty acids derived from arachidonic acid, eicosapentaenoic acid, or docosahexaenoic acid to specialized pro-resolving mediators (SPM), even though 5-LO prefers arachidonic acid as a substrate[69].

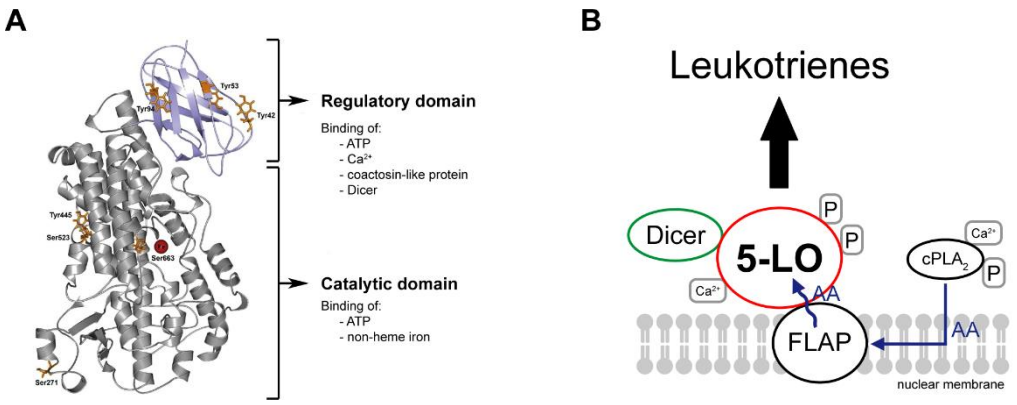

Figure 1.4 5-lipoxygenase
(A) Structure of 5-LO displays the N-terminal regulatory domain (purple), the C-terminal catalytic domain (grey), the non-heme iron (red), and the phosphorylation sites (orange) (figure is taken from[69]). (B) The figure illustrates the mode of action of the leukotriene synthesis: FLAP transfers arachidonic acid, which is liberated from the phospholipids by $cPLA_2$, to the active centre of 5-LO. Subsequently, 5-LO catalyzes the synthesis of leukotrienes (figure is adapted from[70]).

1.2.2 Leukotrienes

The functions of leukotrienes are mediated via binding to G-protein coupled receptors. LTB_4 binds to BLT1/2, while the cysteinyl LTs (LTC_4, LTD_4, LTB_4) bind to CysLT1/2 and GPR17, respectively[71]. Consequently, the effects of LTs depend on the receptor distribution and expression in various cell types. For instance, LTB_4 increases cellular adhesion and motility, while also functioning as a potent chemo attractant for several types of leukocytes by facilitating the recruitment and accumulation of neutrophils, dendritic cells, and T-cells. Furthermore, highly concentrated LTB_4 causes degranulation of phagocytes and a release of lysosomal enzymes. LTC_4 and LTD_4 are very potent broncho-contricting substances that are actually 1000 times more potent than histamine. Additionally, both cysteinyl LTs induce exudation of plasma and mucus production in the lung. Moreover, LTC_4 causes an increased vascular permeability and leukotrienes are also involved in functions of antigen presenting cells[70–72].

Although several substances targeting the LT pathway have been tested as potential drugs, not many have received approval to enter the market. The antileukotrienes zafirlukast (Accolate®) and montelukast (Singulair®) are used as add on therapeutics for the treatment of asthma. Both drugs are competitive and selective antagonists of the CysLT1 receptor and therefore prevent mucus production, edema formation, bronchoconstriction, and damage of the bronchial epithelium, while also exhibiting anti-inflammatory effects to a limited extent[72,73]. The only direct 5-LO inhibitor that has entered the market is zileuton (Zyflo®)[74], which is commercially available in the USA[75] and is also indicated for the treatment of asthma like the antileukotrienes. In Germany, montelukast is the only drug that targets the LT pathway and is both authorized by the medicine agency and prescribable[76].

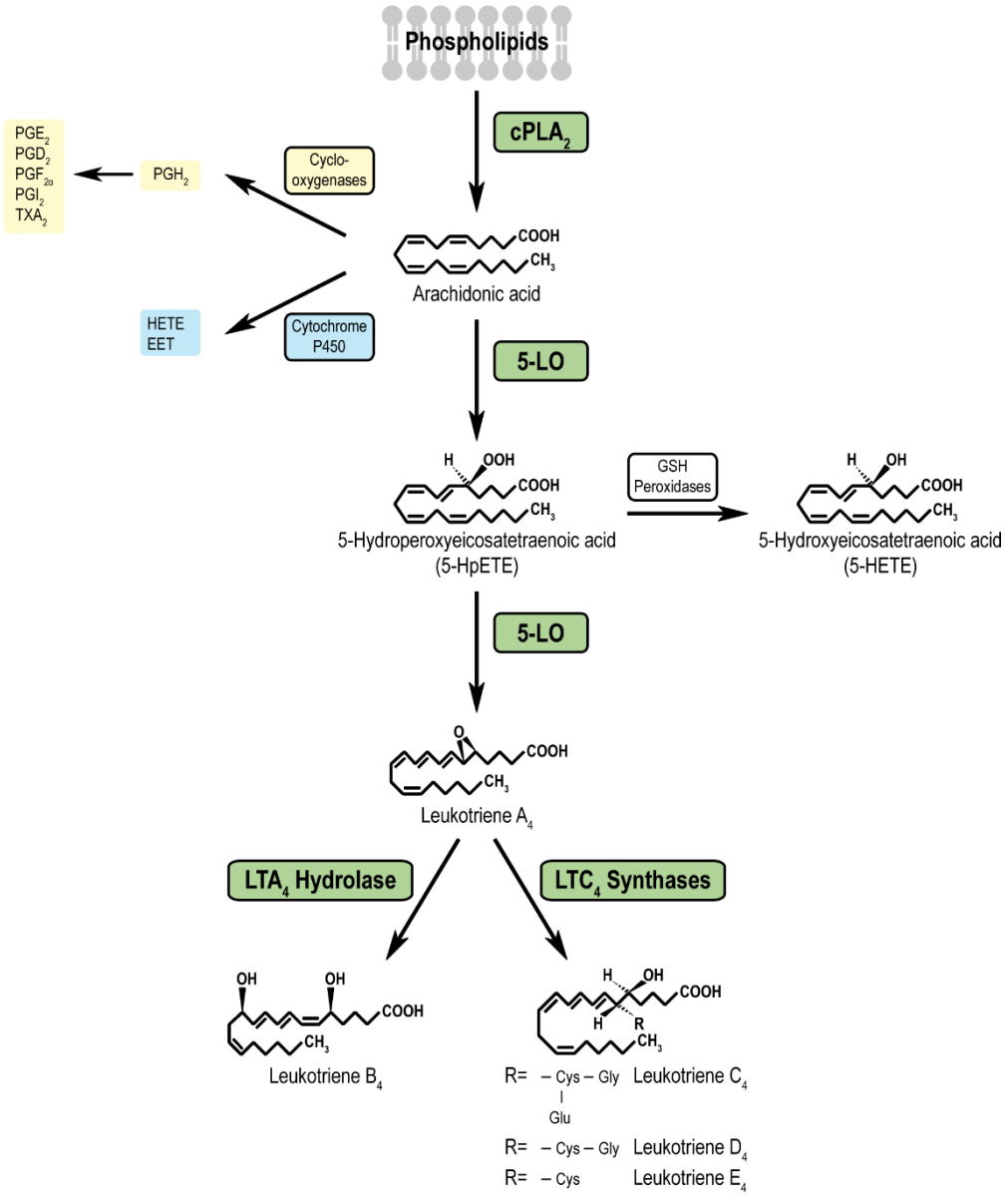

Figure 1.5 Biosynthesis of eicosanoids
The figure displays the conversion of arachidonic acid to prostaglandins by cyclooxygenases (yellow), to hydroxyeicosatetraenoic acid (HETE) or epoxyeicosatetraenoic acid (EET) by cytochrome P450 (blue), or to leukotrienes by 5-LO (green) (figure is adapted from[68,70]).

1.2.3 Gene expression and enzymatic activity

The enzymatic activity of 5-LO is tightly regulated by phosphorylation, the subcellular localization, and other factors. For instance, upon cell activation, 5-LO translocates from the soluble compartments in the cytosol or in the nucleus to the nuclear membrane, supported by the scaffold proteins 5-LO activating protein (FLAP) and coactosin-like protein (CLP)[69,77]. The transfer of 5-LO from the cytoplasm to the nucleus results in a higher enzymatic activity and was observed for various cell types, such as differentiating monocytes[78]. Nuclear localization sequences and a nuclear export sequence, all of which contain phosphorylation sites, regulate 5-LO's cellular localization and therefore also its activity[69]. Phosphorylation of the serine residue at position 523 blocks 5-LO activity by inhibiting the function of the nuclear localization sequence located around Ser-523, leading to a cytosolic localization of the enzyme[79]. Moreover, phosphorylation at Ser-271 results in maintaining the nuclear localization of 5-LO due to a blockade of the nuclear export sequence containing Ser-271[80]. Phosphorylation of the serine residue at position 663, just like phosphorylation at Ser-271, augments 5-LO activity. Other factors activating 5-LO are the direct binding of ATP and Ca^{2+} signaling[70].

In accordance with its function in the host defense within the innate immune system, 5-LO is predominantly expressed in leukocytes. In particular, monocytes, macrophages, mast cells, neutrophils, granulocytes, dendritic cells, and B-lymphocytes express 5-LO[70,81]. In myeloid cells, 5-LO expression is upregulated in a differentiation-dependent manner. Previous studies revealed a strong increase in 5-LO expression upon four-day treatment of the monocytic cell line Mono Mac 6 (MM6) with the differentiation stimuli transforming growth factor β and calcitriol[82]. These results indicate that 5-LO is a TGF-β and vitamin D response gene. It is known that activation of the TGF-β receptor leads to phosphorylation of Smad proteins and their subsequent translocation to the nucleus, where they act as transcription factors. Two functional Smad binding elements (SBE) are located within the 5-LO core promotor, allowing a Smad-dependent stimulation of transcriptional initiation and elongation[69]. Furthermore, several vitamin D response elements were identified within the ALOX5 gene and previous studies revealed that the calcitriol effect is mediated via a vitamin D receptor-dependent stimulation of the transcriptional elongation[69,83]. Other transcription factors, especially regulators of stem cell regeneration and differentiation (e.g. Smad1, Wnt, p53, RUNX1, C/EBPα, and GATA2), are reported to bind to the 5-LO gene and to drive its expression in myeloid and lymphocytic cell lineages[69].

1.2.4 Noncanonical functions

Besides its key function in the biosynthesis of LTs and SPMs, 5-LO was also associated with noncanonical functions. Many cancer tissues are reported to express 5-LO, suggesting an involvement of the 5-LO pathway in cancer development. 5-LO and its metabolites might stimulate the growth of cancer cells as well as promote escape mechanisms for tumors from the immune system by modulating the cross talk between the tumor microenvironment and infiltrating immune cells[84,85]. Additionally, 5-LO was reported as an effector and regulator of p53, since 5-LO expression seems to be regulated by p53, while in turn 5-LO might regulate p53 trafficking and its transcriptional activity[69].

Furthermore, 5-LO was linked to the development of acute and chronic myeloid leukemia. It was reported, that in AML1/ETO-positive acute myeloid leukemia 5-LO is highly upregulated, whereas in a murine BCR/ABL chronic myeloid leukemia model 5-LO is required for the aberrant self-renewal capacity of leukemic stem cells[86,87]. In line with the previous reports, another study characterized 5-LO as an important player for the maintenance of leukemic stem cells in a PML/RARα-positive cell model of acute myeloid leukemia. Enzymatically active 5-LO was reported to be expressed in the hematopoietic stem cell compartments. Moreover, the stem cell capacity of PML/RARα-positive hematopoietic stem and progenitor cells (HSPC) is impaired by a selective inhibition of 5-LO by CJ13610. Inactive 5-LO directly interacts with β-catenin, preventing the signaling molecule from entering the nucleus and therefore resulting in an inhibition of the Wnt signaling, a pathway which is essential for the maintenance of cancer stem cell-like cells. Remarkably, a knockout of the 5-LO gene did not alter the stem cell capacity in the PML/RARα model, indicating that either the β-catenin/inactive 5-LO complex is crucial for inhibiting Wnt signaling or that CJ13610 has more targets than 5-LO[69,88].

1.2.5 Interference between the 5-LO pathway and the miRNA pathway

Various scientific reports linked the 5-LO pathway to the miRNA pathway by discovering miRNAs that target 5-LO or proteins associated with the 5-LO pathway. For instance, the 5-LO mRNA 3'UTR is directly targeted by miR-19a-3p, miR-125b-5p, and miR-216-3p[89,90]. Treatment of T-lymphocytes with the lectin phytohaemagglutinin caused an induction of miR-19a-3p, as well as a strong decrease in 5-LO mRNA expression. Interestingly, 5-LO mRNA expression was strongly upregulated in T-lymphocytes when miR-19a-3p was inhibited by an antagomir[89]. In addition to targeting 5-LO, miR-216-3p was also shown to target COX-2 as well as to inhibit colorectal cancer proliferation by downregulating both enzymes, 5-LO and COX-2, respectively[90]. Furthermore, the specialized pro-resolving mediator resolvin D1 was found to induce miR-219, which in turn regulates 5-LO expression in macrophages[91,92]. Moreover, FLAP was shown to be targeted by miR-135a and miR-199a[93].

As already mentioned in chapter 1.1.3, 5-LO itself might interfere with the miRNA pathway due to its binding properties to Dicer[32]. A possible impact of 5-LO on miRNA formation and a further characterization of its interaction with Dicer is subject of this study.

1.3 Aim of the study

RNA silencing pathways, especially the miRNA pathway, largely contribute to posttranscriptional gene silencing and thus are extensively studied. Complex regulatory networks controlling the miRNA pathway were unveiled in the past and dysfunctions were related to severe disorders[6]. Amongst others, miRNAs coordinate the innate immune response to inflammatory stimuli, whereas inflammatory signaling pathways in turn interfere with the miRNA biosynthesis, demonstrating the interrelationship between the posttranscriptional regulators of gene expression and inflammation[55,60,69]. More than two decades ago Dicer, a protein catalyzing the final steps of the miRNA pathway, was first discovered as an interaction partner of the proinflammatory enzyme 5-LO, which is a catalyst of the leukotriene synthesis[69,94]. In recent years, various scientific studies have provided more links between the two proteins by unveiling 5-LO as a miRNA target as well as describing the 5-LO-Dicer protein-protein interaction in a more detailed manner[32,69,89,95]. Although some scientific findings have already been gathered, many questions still stay unanswered and secure knowledge about the functional impact of the interaction remains to be elucidated.

Thus, the aim of this study is to provide new insights into the modulation of the miRNA pathway by 5-LO in order to better understand how inflammation is linked to posttranscriptional gene regulation. For instance, a proximity ligation assay is performed for the purpose of investigating whether the endogenous proteins Dicer and 5-LO interact in their natural environment. Furthermore, sequencing of small noncoding RNAs and the subsequent validation of its results by both real-time quantitative PCR (qRT-PCR) and an *in vitro* Dicer assay are utilized to examine a functional impact of the protein-protein interaction and to gain a deeper insight into the mechanism by which 5-LO alters the miRNA expression, as well as to better characterize the noncanonical 5-LO functions. Ideally, the new insights will contribute to a better understanding of the miRNA pathway in the context of inflammatory responses, more precisely to a better understanding of how 5-LO regulates the miRNA pathway.

2 Results

2.1 5-LO and Dicer protein expression in MM6 cells

The 5-LO enzyme is known to be highly expressed in differentiated myeloid cells. In particular, the monocytic cell line Mono Mac 6 was reported to exhibit a strong increase in 5-LO expression upon four-day treatment with the differentiation stimuli TGF-β and calcitriol[82] (see chapter 1.2.3). Thus, those cells are highly suitable for investigating a possible interference of 5-LO with the miRNA pathway. In addition to the wildtype, 5-LO knockout (5-LOΔ) MM6 cells generated using the CRISPR/Cas method[96] were utilized as a control in most of the experiments described here.

To analyze the 5-LO and Dicer protein expression, western blots were performed in wildtype and 5-LOΔ MM6 cells, which were differentiated for four days with 1 ng/mL TGF-β and 50 nM calcitriol. Additionally, cells were stimulated for four days with 1 µg/mL LPS or 25 ng/mL zymosan. Furthermore, qRT-PCR experiments were carried out to determine the mRNA levels of 5-LO and Dicer. For this purpose, cells were differentiated for four days, but treated with LPS and zymosan for just the last 24 h.

In accordance with previous results[82] the 5-LO protein (see Fig. 2.1 A) and mRNA expression (see Fig. 2.1 B) is strongly increased upon differentiation (12.5-fold and 16.1-fold, respectively) and even stronger upon additional stimulation with LPS or zymosan (16.3-fold and 15.7 to 19.2-fold, respectively). To assess whether 5-LO protein is measurable in the 5-LOΔ MM6 cells, two different single cell clones, clone 3 and clone 15, were examined. The 5-LO protein is undetectable for both cell clones, as already described[97]. Although 5-LO mRNA is measurable, the successful knockout of the 5-LO gene is confirmed by the absence of the 5-LO protein, since the detected mRNA transcripts are not translated to functional proteins[97]. Thus, the mRNA levels are negligible. Since both clones exhibit similar results, the data obtained for clone 3 and clone 15 are summarized as 5-LOΔ in the following chapters.

The Dicer protein expression (see Fig. 2.1 C) is slightly augmented by differentiation (2.2 to 2.8-fold). However, the Dicer protein levels are rather stable regarding the additional stimuli LPS and zymosan (2.5 to 2.7-fold) in comparison to the differentiated samples. Dicer mRNA levels (see Fig. 2.1 D) are rather stable as well. However, the Dicer mRNA level in the differentiated and LPS-treated wildtype is slightly, but significantly, decreased (0.9-fold).

In summary, 5-LO gene expression is upregulated by differentiation and increases even stronger upon additional treatment with LPS or zymosan. However, Dicer gene expression remains unaffected by these stimuli.

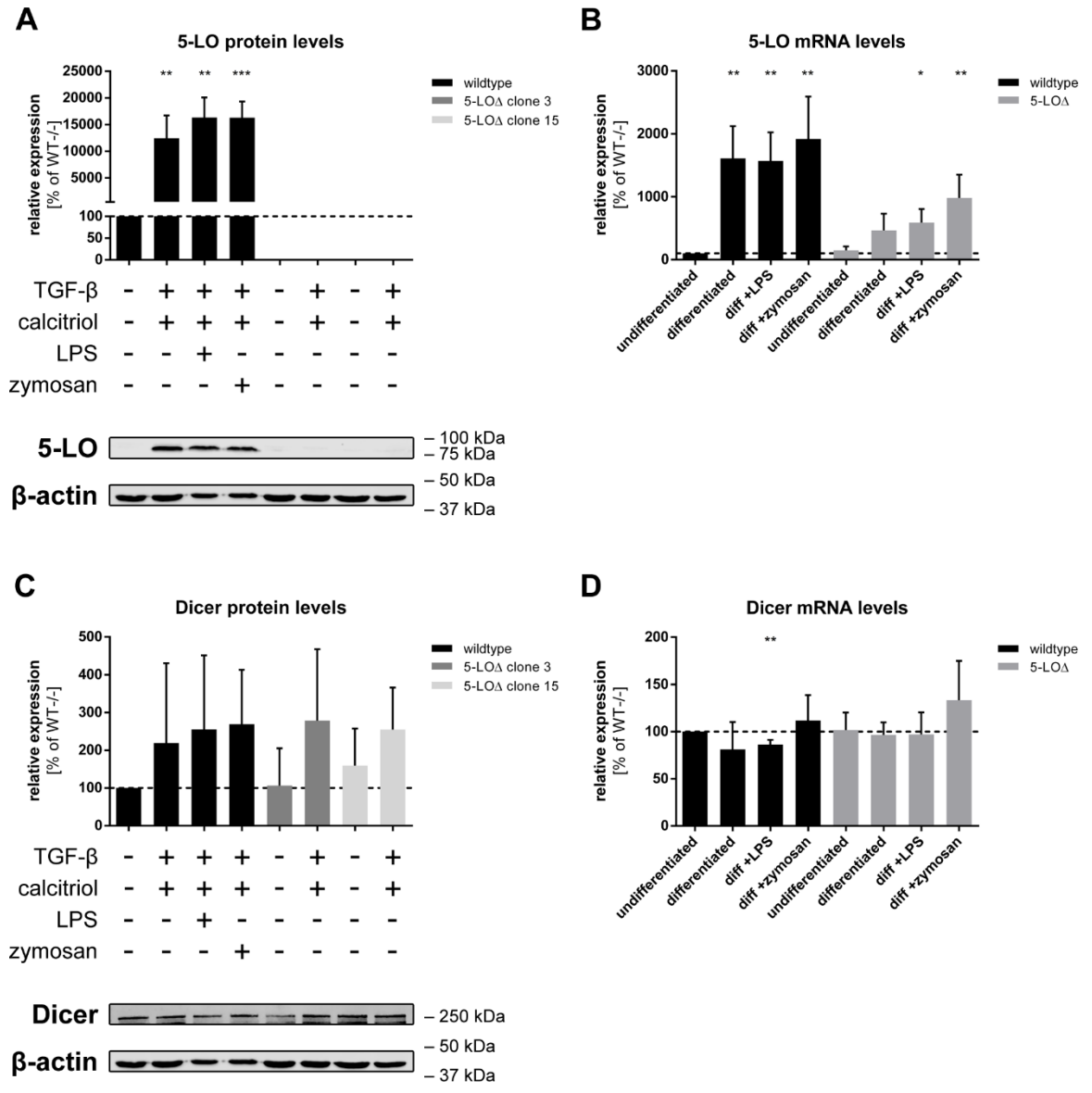

Figure 2.1 5-LO and Dicer protein expression and mRNA levels in MM6 cells

(A-D) 5-LO (A) and Dicer (C) protein expression was determined via western blot. Real-time quantitative PCR was used to determine the mRNA expression levels of 5-LO (B) and Dicer (D). Wildtype and 5-LOΔ MM6 cells were differentiated with 1 ng/mL TGF-β and 50 nM calcitriol for four days. Additionally, if indicated, cells were stimulated with 1 µg/mL LPS or 25 ng/mL zymosan for four days (A; C) or for the last 24 h (B; D). The data is presented relative to undifferentiated wildtype MM6 cells (WT-/-), set as 100%. β-actin was used as the reference. Results are displayed as mean + SD and are representative for three independent experiments. (*p < 0.05, **p < 0.01, ***p < 0.001, ****p < 0.0001; two-tailed unpaired t test)

2.2 *In situ* interaction of 5-LO and Dicer

In vitro assays have shown that 5-LO interacts, amongst other proteins, with Dicer[32,33] (see chapter 1.1.3). Despite the strong evidence for an *in vitro* interaction, the question whether the two endogenous proteins also bind *in situ* remained to be elucidated. In order to address this question, immunofluorescence (IF) microscopy was performed as a preliminary experiment to monitor the subcellular localisation of 5-LO and Dicer. Experiments were carried out in wildtype MM6 cells, which were differentiated for four days with 1 ng/mL TGF-β and 50 nM calcitriol. If indicated, cells were also stimulated with 1 µg/mL LPS or 25 ng/mL zymosan for four days.

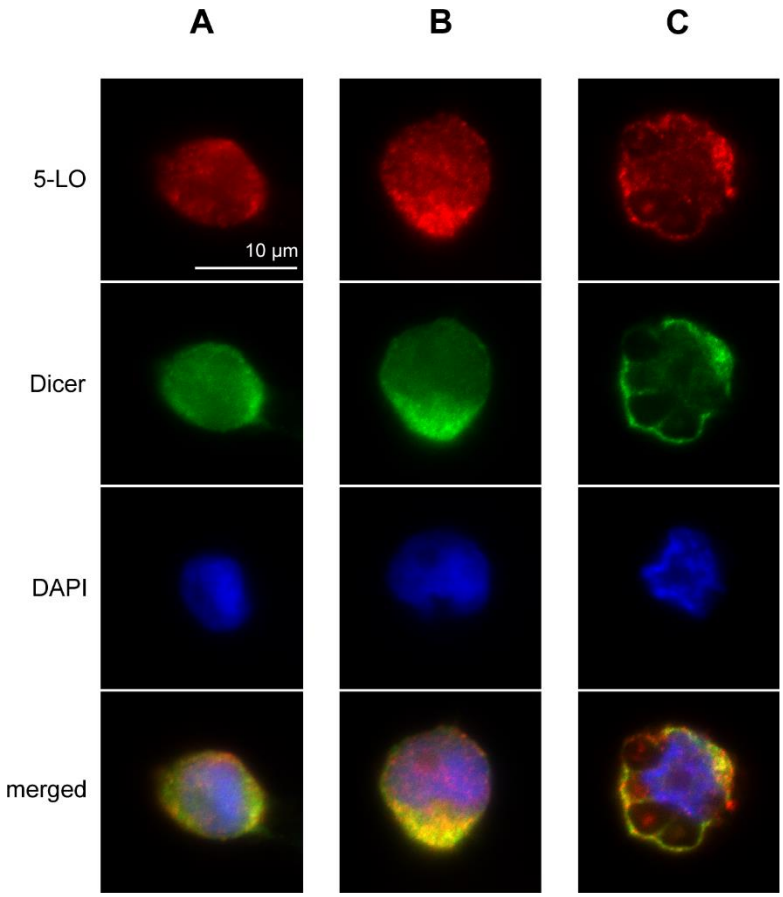

Figure 2.2 Colocalization of 5-LO and Dicer
(A-C) Subcellular localization of 5-LO and Dicer was monitored by indirect immunofluorescence microscopy in wildtype MM6 cells. Cells were differentiated with 1 ng/mL TGF-β and 50 nM calcitriol for four days (A), as well as additionally stimulated with 1 µg/mL LPS (B) or 25 ng/mL zymosan (C). Cells were fixed, permeabilized, and incubated with antibodies against 5-LO (Alexa Fluor 555, red) and Dicer (Alexa Fluor 488, green). Results are representative for approximately 100 individual cells of three independent experiments. The scale bar represents 10 µm.

MM6 cells were fixed on coated cover slips, permeabilized with acetone and triton X-100, and incubated with antibodies against 5-LO (red fluorescence signals) and Dicer (green fluorescence signals). IF results illustrated in Fig. 2.2 A-C reveal that differentiated wildtype MM6 cells express both target proteins. The

proteins are localized predominantly in the cytosol, with less 5-LO and Dicer inside the nucleus. It is not possible to state for certain whether the proteins are localized within the nucleus or in the cytosol overlaying the nucleus, since z-stacking was used. Z-stacking combines several images taken at different focus distances to improve the depth of field in the resulting image. The used microscope did not allow to take images with adequate sharpness focusing on only one optical layer. Nevertheless, an overlay of the Dicer and 5-LO distribution within the cell reveals a colocalization of both proteins in differentiated wildtype MM6 cells (see Fig. 2.2 A). Moreover, the proteins still colocalize despite additional treatment with LPS (see Fig. 2.2 B) or zymosan (see Fig. 2.2 C). Interestingly, the cells treated with zymosan exhibit morphological changes, as bubble-shaped structures next to the nucleus were observed. This observation was further investigated in Chapter 2.3.

In order to investigate whether the colocalized proteins 5-LO and Dicer interact *in situ,* proximity ligation assays (PLA) were carried out in wildtype and 5-LOΔ MM6 cells. Cells were treated just as described for the IF experiments. The PLA is a tool which monitors protein-protein interactions in intact cells (see Fig. 2.3). The method enables to observe endogenous proteins interacting in their natural environment without the necessity to disrupt the cells, which is a great advantage of the PLA[98]. If the target proteins are in close proximity (< 40 nm), the oligonucleotides, which are attached to secondary antibodies, ligate to new circular DNA. Positive PLA signals are visible under the microscope after amplifying the circular DNA and hybridizing it with a fluorophore[99,100].

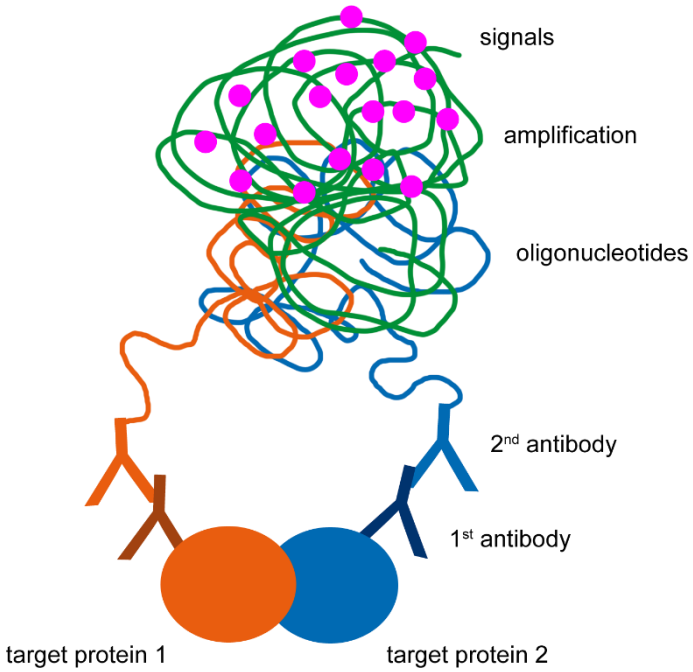

Figure 2.3 Scheme of the proximity ligation assay
Oligonucleotides (blue and orange), that are attached to the secondary antibodies, ligate to new circular DNA if the target proteins are in close proximity (< 40 nm). After the circular DNA is amplified (green) and hybridized with a fluorophore (magenta), positive PLA signals are detected under the microscope. (figure is adapted from[100]).

The PLA reveals strong signals in differentiated wildtype MM6 cells (see Fig. 2.4 B). As expected, cells lacking 5-LO display no PLA signals (see Fig. 2.4 A; no magenta dots). Differentiated wildtype MM6 cells also exhibit strong PLA signals upon additional stimulation with LPS (see Fig. 2.4 C) or zymosan (see Fig. 2.4 D). It seems like these cells, especially those treated with LPS, show even more signals compared to the differentiated wildtype. This observation can be explained with the increase in 5-LO protein expression upon stimulation with LPS or zymosan. The Dicer protein levels are rather stable in this experimental setup (see chapter 2.1). However, since the PLA does not allow quantification, no final conclusions can be drawn. Moreover, z-stacking was also used for the PLA image acquisition. Therefore, no statement can be made whether the interaction of 5-LO and Dicer takes place in the cytosol or the nucleus.

Taken together, these results demonstrate that 5-LO and Dicer colocalize and that the endogenous proteins interact *in situ* in differentiated wildtype MM6 cells.

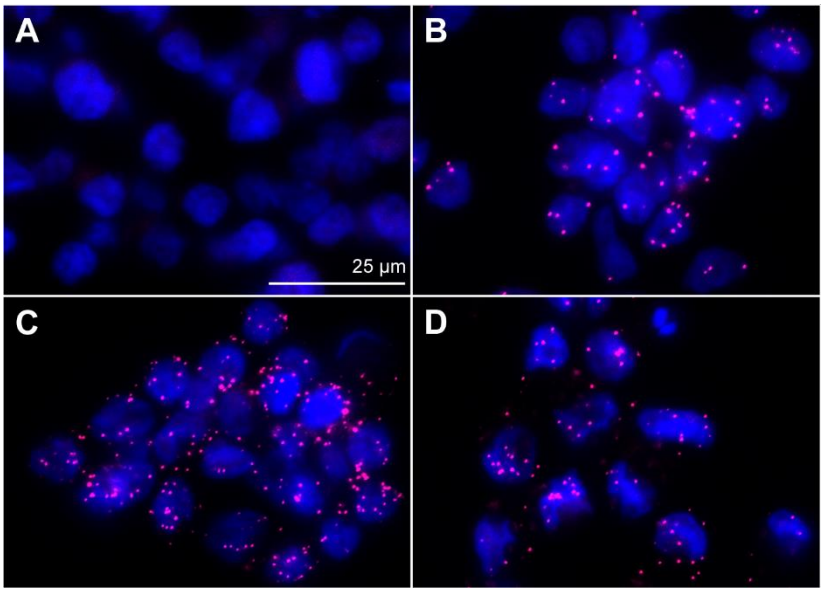

Figure 2.4 *In situ* interaction of 5-LO and Dicer
(A-D) *In situ* PLA was performed in wildtype (B) and 5-LOΔ MM6 cells (A), both differentiated with 1 ng/mL TGF-β and 50 nM calcitriol for four days. Cells were also stimulated with 1 µg/mL LPS (C) or 25 ng/mL zymosan (D). Proximity probes against mouse anti 5-LO and rabbit anti Dicer were used. *In situ* PLA signals (magenta-coloured dots) visualize 5-LO-Dicer protein-protein interactions and DAPI (blue) was used to stain the nucleus. Results are representative for approximately 100 individual cells of three independent experiments. The scale bar represents 25 µm.

2.3 Uptake of FITC-labeled opsonized zymosan by MM6 cells

While performing IF microscopy experiments, morphologic changes, bubble-shaped structures that appeared next to the nucleus, were observed in MM6 cells treated with zymosan (see chapter 2.2). Since these changes seemed to be a result of the zymosan-treatment, the substance was tracked under the microscope. First, zymosan was labelled with fluorescein isothiocyanate (FITC) and then opsonized with serum dilution, enabling its tracking under the microscope. Wildtype MM6 cells were differentiated with 1 ng/mL TGF-β and 50 nM calcitriol and simultaneously treated with 25 ng/mL FITC-labeled opsonized zymosan. Samples were collected at different time points (0, 0.5, 1, 3, 6, 24, 48, 72 and 96 h) and analyzed by IF microscopy.

Endocytosis of the FITC-labeled zymosan occurs already after 24 h (see Fig. 2.5 B). After 48 h the cells seem to have taken up even more zymosan. However, treatment with zymosan for only six hours is not sufficient for its uptake (see Fig. 2.5 A). Comparison of the microscopic pictures revealed that the endocytic vesicles look similar to the bubble-shaped structures observed in chapter 2.2. Thus, those results suggest, that the morphologic changes are caused by zymosan.

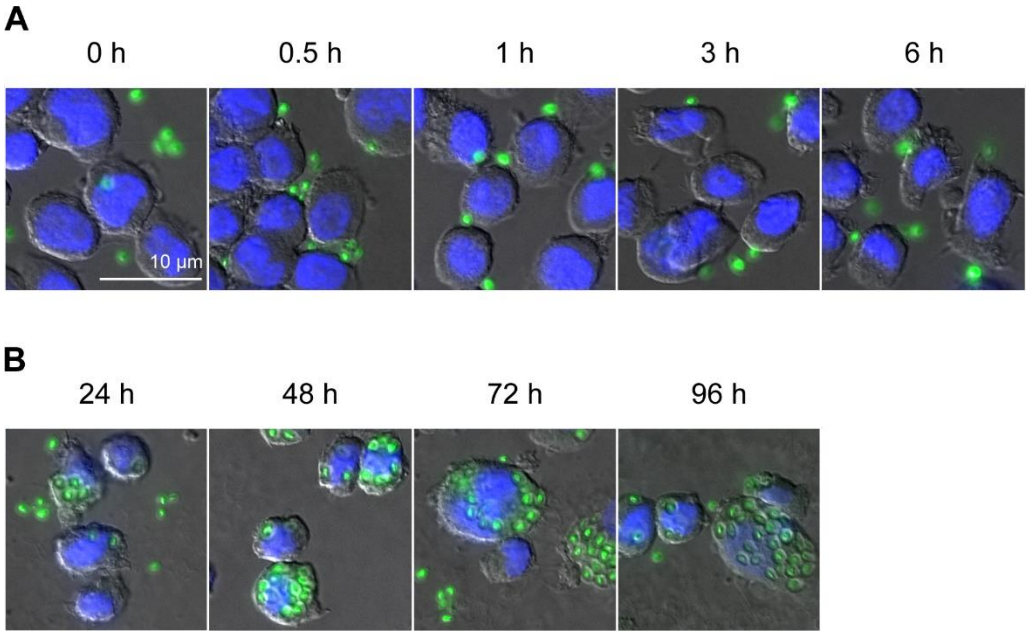

Figure 2.5 Pick-up of FITC-labeled opsonized zymosan by differentiated wildtype MM6 cells
(A-B) Wildtype MM6 cells, differentiated for the indicated period of time with 1 ng/mL TGF-β and 50 nM calcitriol, were simultaneously stimulated with 25 µg/mL FITC-labeled zymosan. Samples were collected at indicated time points and analyzed by IF microscopy. Results are representative for approximately 100 individual cells of one (A) or three (B) independent experiments. The scale bar represents 10 µm.

2.4 Sequencing of small noncoding RNAs

Since the protein-protein interaction of 5-LO and Dicer was proven *in situ* (see Chapter 2.2), further experiments were performed to investigate whether the 5-LO-Dicer interaction impacts the miRNA biogenesis. For this, sequencing of small noncoding RNAs was carried out to screen for miRNAs whose expression profile is changed by 5-LO or LPS.

Next generation sequencing was performed on an Illumina platform in wildtype and 5-LOΔ MM6 cells, differentiated for three days with 1 ng/mL TGF-β and 50 nM calcitriol. If indicated, cells were also stimulated with 1 µg/mL LPS for the last 6 h. The web tool omiRas was used to analyze the differential expression of the detected miRNAs[101]. Approximately 940 sequences were aligned to the human genome, of which 20.7% were identified as mature miRNAs. Small nucleolar RNA (snoRNA, 30.29%), piwi-interacting RNA (piRNA, 24.01%), precursor miRNA (pre-miRNA, 18.4%), transfer RNA (tRNA, 5.86%), small cytoplasmatic RNA (scRNA, 0.42%), and ribosomal RNA (rRNA, 0.32%) were also detected (see Fig. 2.6 B), but omitted from further analysis. Differential expression between two conditions was calculated as the logarithm of the x-fold change of the mean expression. The compared conditions were differentiated wildtype and differentiated 5-LOΔ, as well as differentiated wildtype and differentiated wildtype stimulated with LPS, in order to report the 5-LO effect and the LPS effect, respectively (see Table S1 and Table S2).

A

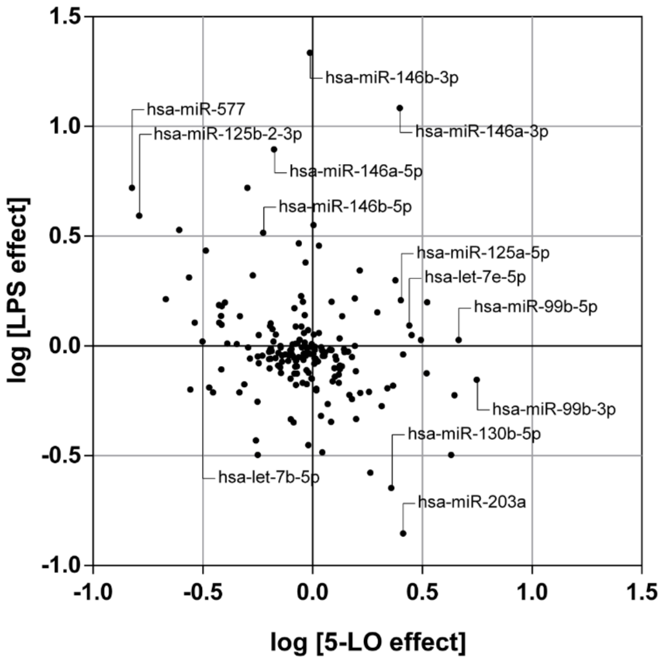

B

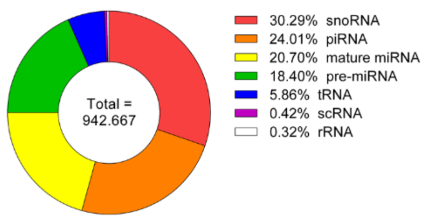

C

id	log [5-LO effect]	log [LPS effect]
hsa-let-7a-5p	-0.194	-0.016
hsa-let-7b-5p	-0.501	0.020
hsa-let-7d-5p	-0.139	-0.043
hsa-let-7e-5p	0.441	0.094
hsa-let-7f-5p	-0.147	0.001
hsa-miR-125a-5p	0.402	0.208
hsa-miR-146a-5p	-0.175	0.896
hsa-miR-146b-5p	-0.225	0.516
hsa-miR-155-5p	-0.168	0.052
hsa-miR-21-5p	-0.192	0.103
hsa-miR-99b-5p	0.665	0.027

Figure 2.6 miRNA expression profiles altered by 5-LO and LPS
(A-C) Sequencing of small noncoding RNAs was performed on an Illumina platform in wildtype and 5-LOΔ MM6 cells, differentiated for three days with 1 ng/mL TGF-β and 50 nM calcitriol. (A, C) Differentiated wildtype MM6 cells were also stimulated with 1 µg/mL LPS for the last 6 h. The data was analyzed with the omiRas tool[101]. (A, C) Differences in the miRNA expression profile were calculated as the base 10 logarithm of the x-fold change of the mean expression. (A, C) The effect of 5-LO and LPS on the miRNA expression profile are reported. (B) Proportional distribution of the non-coding RNAs mapped to the human genome is displayed. Results are representative for three independent experiments.

Both strands of the mature miR-99b duplex, miR-99b-3p and miR-99b-5p, display the strongest increase in the presence of 5-LO (see Fig. 2.6 A, C and Fig. 2.7 A). Those strands share one common transcript with the miRNAs let-7e and miR-125a. The clustered miRNAs, whose expression is regulated by NF-κB[41], are very well studied. For instance, the cluster is known to be involved in stem cell functions and TLR signaling, as well as in the regulation of primitive hematopoietic cells[38,39,42,45] (see chapter 1.1.4). Just like miR-99b, the expression of let-7e-5p and miR-125a-5p is also strongly increased by 5-LO. In contrast, 5-LO also exhibits a decreasing effect on miRNAs, e.g. let-7b-5p. This miRNA, as well as let-7e, are members of the well studied let-7 miRNA family, which was shown to play crucial roles in self-renewal of stem cells, developmental timing, and tumor suppressor functions[36] (see chapter 1.1.4).

Furthermore, LPS also modulates the expression profile of miRNAs (see Fig. 2.6 A, C and Fig. 2.7 B). The non-functional strands miR-146b-3p and miR-146a-3p were most heavily increased upon stimulation with LPS. However, also the functional strands, miR-146a-5p and miR-146b-5p, were strongly enhanced. This observation is in line with already known functions of the miRNAs miR-146a and miR-146b, since they belong to the group of NF-κB dependent TLR-response genes, just like the miR-99b/let-7e/miR-125a cluster, and function as negative feedback regulators of the innate immune response, which in turn is activated, amongst others, by the TLR4 activator LPS[42,60] (see chapter 1.1.4). Remarkably, miR-125a-5p is the only member of the miR-99b/let-7e/miR-125a cluster whose expression level is slightly increased by LPS. Surprisingly, in the used experimental setup, LPS neither affects miR-99b-5p or let-7e-5p nor miR-155-5p or miR-21-5p, all of which are also TLR-response miRNAs involved in the regulation of the innate immune response[60] (see chapter 1.1.4).

In brief, the sequencing of small noncoding RNAs revealed a functional impact of the 5-LO-Dicer protein-protein interaction on the miRNA biosynthesis. The expression profiles of several miRNAs with relevant biological functions are altered by 5-LO and LPS.

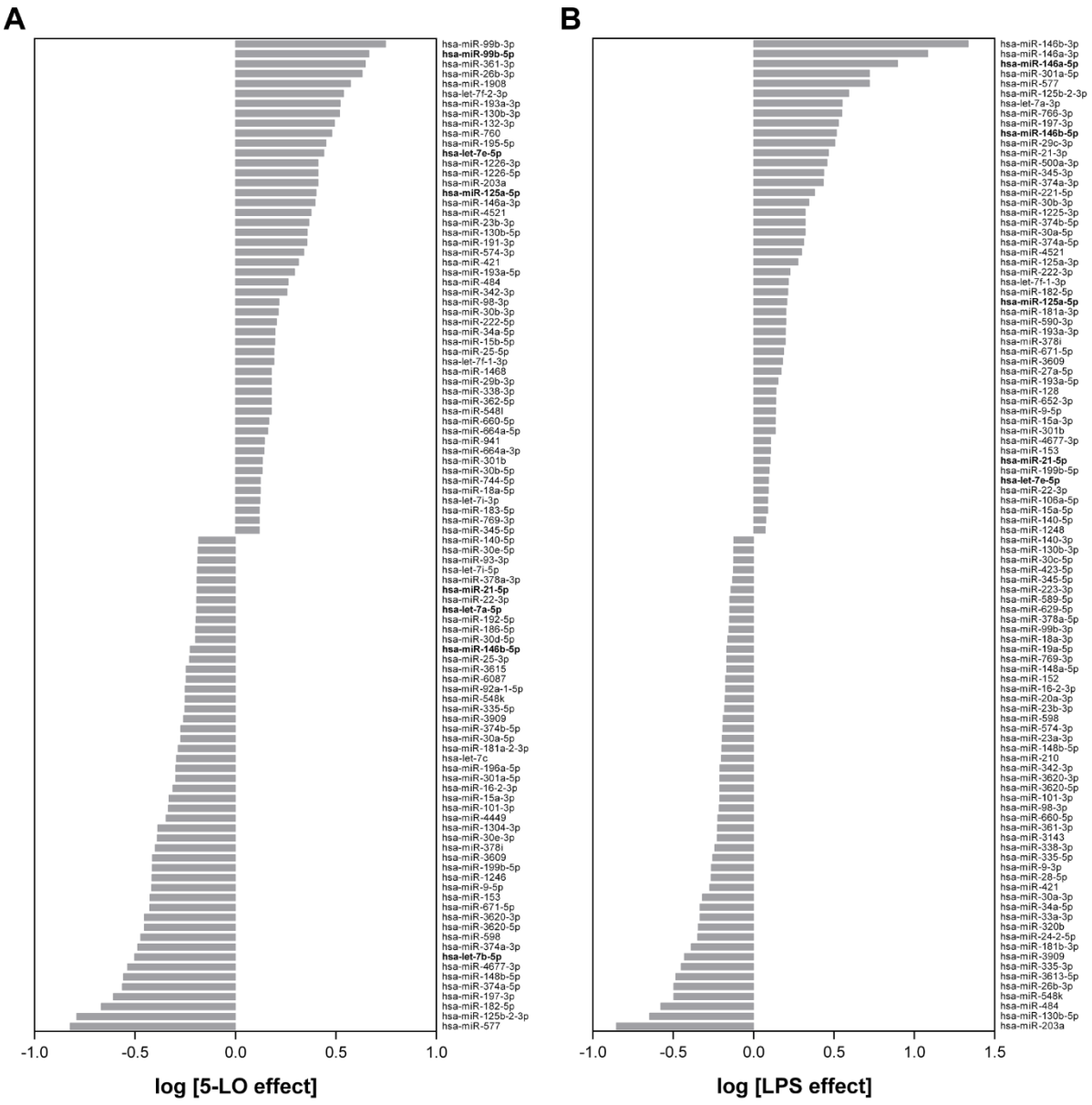

Figure 2.7 miRNA expression profiles altered by 5-LO and LPS

(A-B) Sequencing of small noncoding RNAs was performed on an Illumina platform in wildtype and 5-LOΔ MM6 cells, differentiated with 1 ng/mL TGF-β and 50 nM calcitriol for three days. (B) Differentiated wildtype MM6 cells were also stimulated with 1 µg/mL LPS for the last 6 h. The data was analyzed with the omiRas tool[101]. (A-B) Differences in the miRNA expression profile were calculated as the base 10 logarithm of the x-fold change of the mean expression. The effect of 5-LO (A) or LPS (B) on the miRNA expression profiles are reported. Graphs display only the 100 most influenced miRNAs. Results are representative for three independent experiments.

2.5 5-LO modulates the processing of miRNAs

Sequencing of small noncoding RNAs (see chapter 2.4) revealed an impact of 5-LO and LPS on the expression of several miRNAs. Especially the levels of the miR-99b/let-7e/miR-125a cluster and let-7b seem to be regulated by 5-LO. To further investigate the impact of 5-LO and LPS on the processing of miRNAs and to validate the results from the sequencing of small noncoding RNAs, real-time quantitative PCR experiments were performed with special focus on the miR-99b/let-7e/miR-125a cluster and the let-7 family.

The experiments were carried out in wildtype and 5-LOΔ MM6 cells, differentiated with 1 ng/mL TGF-β and 50 nM calcitriol for four days, to measure the relative expression levels of several mature miRNAs and their precursors. If indicated, cells were also stimulated with 1 µg/mL LPS or 25 ng/mL zymosan for the last 24 h, or either treated twice (day 0 and after 48 h) with 1 µM Zileuton, 0.1 µM MK886, or 0.1 µM or 1 µM CJ13610. In order to demonstrate the effect of 5-LO on the maturation of miRNAs, the mature miRNA levels were normalized to their corresponding primary miRNA. However, for the purpose of displaying the overall effect of 5-LO on the expression profile of miRNAs, the mature miRNA levels were not normalized to their primary transcript. This enables to distinguish between the overall effect of 5-LO on the expression profile of miRNAs and its effect on the transcription and the maturation of distinct miRNAs. Normalization to the primary transcript is indicated as $^{+}$ and only occurs if just one primary transcript exists (this is not the case for let-7a and let-7f).

5-LO regulates the transcription of the let-7 family members diversely (see Fig. 2.8 A). On the one hand, the primary miRNA levels of the let-7a/let-7b/miR-4763 cluster (15-fold) and the let-7f/miR-98 cluster (1.2-fold) are augmented in cells lacking 5-LO. On the other hand, the levels of the miR-99a/let-7c/miR-125b cluster (0.7-fold) and the miR-99b/let-7e/miR-125a cluster (0.2-fold) are decreased. The let-7a/miR-100 cluster was not detected in MM6 cells, although several different primers were tested. Therefore, it is likely that the cluster is not expressed in this monocytic cell line.

Since the 5-LO-Dicer interaction most likely modulates the Dicer processing step, mature miRNA levels were also determined (see Fig. 2.8 B-D). Interestingly, 5-LO only regulates the maturation of the miRNAs let-7e-5p and let-7e-3p, which is enhanced (6.7-fold and 8.2-fold, respectively) in cells lacking 5-LO. Interestingly, neither the maturation of another let-7 family member (see Fig. 2.8 B), nor that of miR-99b-5p and miR-125a-5p (see Fig. 2.8 C), are impacted significantly by 5-LO - at least not under the used experimental conditions. Thus, 5-LO exhibits an inhibiting effect on the maturation of let-7e with both strands of the miRNA duplex being equally affected. However, 5-LO slightly inhibits (2.3-fold) the processing of let-7a-5p, which is located on three different miRNA clusters (see Table 1.1). Cluster 3 was shown to be positively regulated by 5-LO, while cluster 2 was not detected and cluster 1 was unaffected. Therefore, only the mature miRNA levels of cluster 3 were assessed for further analysis (see Fig. 2.8 D). Remarkably, the maturation of miR-4763-3p is strongly reduced (0.1-fold) in cells lacking 5-LO, showing a stimulating effect of 5-LO on the processing of miRNAs.

The shown data reveals opposing and specific effects of 5-LO on the transcription and the maturation of miRNAs. Whenever the transcription is stimulated, the maturation is inhibited (e.g. hsa-let-7e), and vice versa (e.g. hsa-miR-4763). This counteracting regulation leads to different overall effects (see Fig. 2.8 E-F). Finally, the expression levels of the mature miRNAs miR-99b-5p and miR-125a-5p are greatly decreased (0.1-fold and 0.2-fold, respectively) in cells lacking 5-LO. The expression level of let-7e remains unchanged due to the counteracting regulation by 5-LO. It increases let-7e transcription but inhibits its processing to the same extent. Let-7a-5p, let-7b-5p, and miR-4763-3p exhibit an increase (2.3-fold, 18.8-fold, and 1.8-fold, respectively) in their expression levels as an overall effect caused by

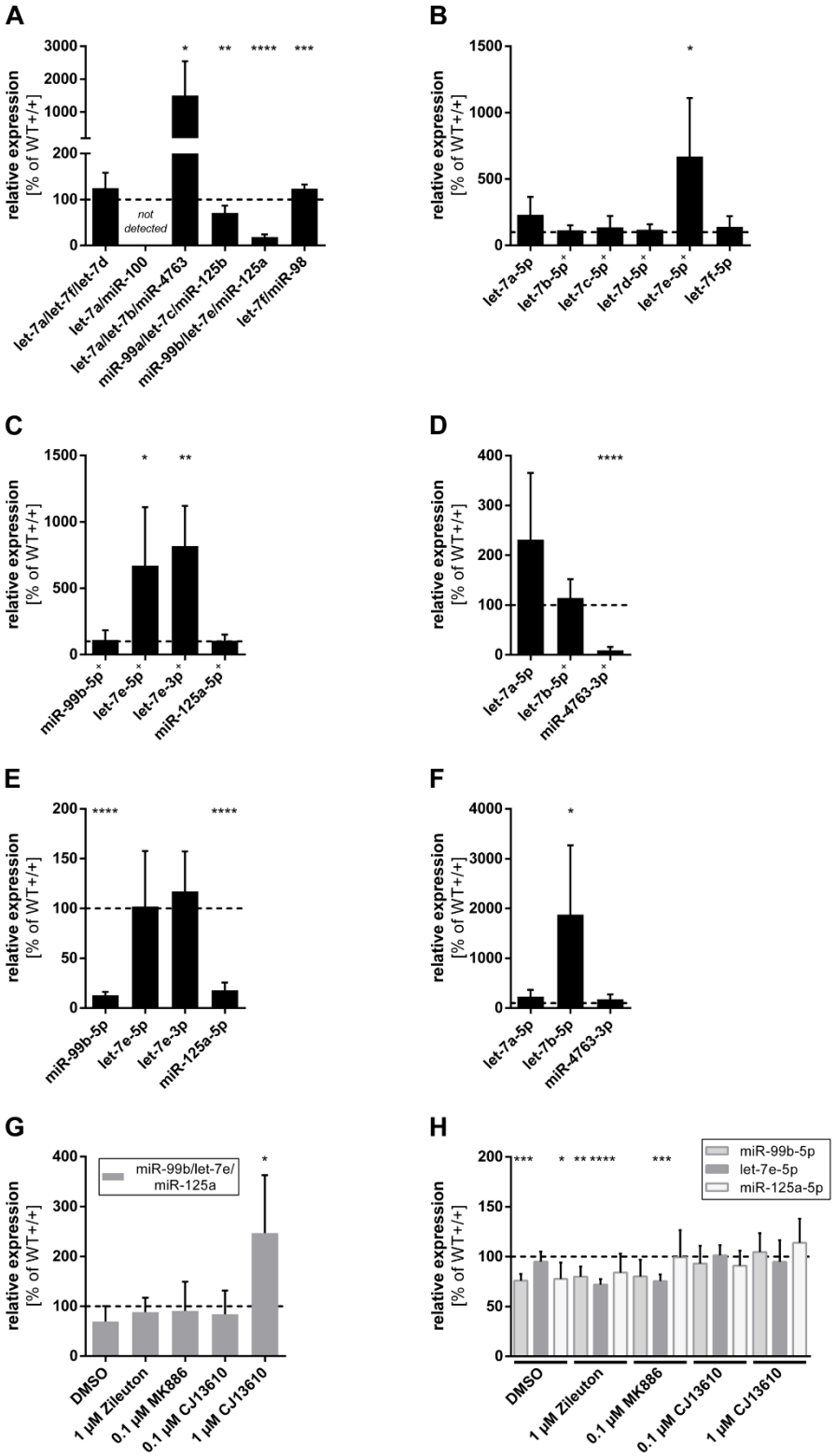

Figure 2.8 5-LO modulates the processing of miRNAs

(A-F) Real-time quantitative PCR was used to determine the expression levels of primary miRNA (A; G) and mature miRNA (B-F; H) in wildtype and 5-LOΔ MM6 cells, differentiated with 1 ng/mL TGF-β and 50 nM calcitriol for four days. Additionally, the differentiated wildtype MM6 cells were treated twice (day 0 and after 48 h) with 1 µM Zileuton, 0.1 µM MK886, or 0.1 µM or 1 µM CJ13610. The data is presented relative to differentiated wildtype MM6 cells (WT+/+), set as 100%. If indicated (+), mature miRNA levels are also normalized to the corresponding primary miRNA levels. U6 (mature miRNA) and β-actin (primary miRNA) were used as reference genes. Results are displayed as mean + SD and are representative for at least three independent experiments. (*$p < 0.05$, **$p < 0.01$, ***$p < 0.001$, ****$p < 0.0001$; two-tailed unpaired t test)

5-LOΔ, with let-7b-5p showing the strongest regulation within the cluster. Considering the specific and divergent regulation of different miRNAs' transcription and processing by 5-LO, these results may uncover a mechanism to regulate each member within a miRNA cluster individually.

In order to investigate whether the modulation of miRNA processing by 5-LO requires an enzymatically active form of the protein, several inhibitors of the leukotriene formation (for detailed description of the inhibitors see chapter 1.2.2 and 2.7) were tested (see Fig. 2.8 G-H). Inhibition of 5-LO's enzymatic activity seems to not interfere with its miRNA pathway modulating activity, although significant, but rather small, changes (0.7 to 1.1-fold) of the mature miRNA levels of miR-99b-5p, let-7e-5p, and miR-125a-5p were observed (see Fig. 2.8 H). The small reduction of the mature miR-99b/let-7e/miR-125a cluster members in cells treated with Zileuton or MK886 (0.7 to 1-fold) are negligible in comparison to the prominent effects caused by 5-LOΔ (see Fig. 2.8 E). Furthermore, the minor changes are possibly triggered by DMSO, which was utilized as the solvent. Interestingly, CJ13610, a potent and selective inhibitor of 5-LO that was reported to interfere with 5-LO's noncanonical function as a transcriptional regulator of the Wnt signaling[88], increases the levels of the primary transcript (2.4-fold), if the inhibitor is applied in high concentrations (see Fig. 2.8 G). Thus, CJ13610 seems to potentiate the stimulatory effect of 5-LO on the transcription of the miR-99b/let-7e/miR-125a cluster.

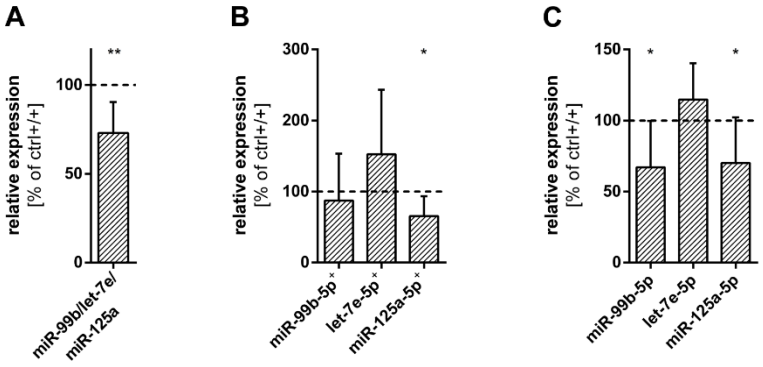

Figure 2.9 5-LO modulates the processing of miRNAs

(A-C) Real-time quantitative PCR was used to determine the expression levels of primary miRNA (A) and mature miRNA (B-C) in control and 5-LOkd MM6 cells, differentiated with 1 ng/mL TGF-β and 50 nM calcitriol for four days. The data is presented relative to differentiated ctrl MM6 cells (ctrl+/+), set as 100%. If indicated (+), mature miRNA levels are also normalized to the corresponding primary miRNA levels. U6 or miR-20a-5p (mature miRNA) and β-actin (primary miRNA) were used as reference genes. Results are displayed as mean + SD and are representative for at least five independent experiments. (*p < 0.05, **p < 0.01, ***p < 0.001, ****p < 0.0001; two-tailed unpaired t test)

A previous study revealed a reduced biosynthesis of the miR-99b/let-7e/miR-125a cluster in 5-LO knockdown (5-LOkd) MM6 cells compared to the control knockdown (ctrl) MM6 cells, which are wildtype MM6 cells transfected with an shRNA against a non-target control[95]. The transcription of the cluster was unaffected in these experiments. However, qRT-PCR experiments were performed in ctrl and 5-LOkd MM6 cells, that were differentiated with 1 ng/mL TGF-β and 50 nM calcitriol for four days, in order to validate those results.

The primary transcript level of the miR-99b/let-7e/miR-125a cluster (0.7-fold), as well as the level of the mature miR-125a-5p (0.7-fold), are decreased in 5-LOkd MM6 (see Fig. 2.9 A-B). The maturation of miR-99b-5p and let-7e-5p is not significantly affected by the 5-LO knockdown, although let-7e-5p levels are

slightly augmented (1.5-fold). This results in an overall 5-LO effect of a decreased expression of miR-99b-5p and miR-125a-5p (both 0.7-fold) in 5-LOkd MM6 cells (see Fig. 2.9 C). The overall expression of let-7e-5p remains unchanged. Thus, the 5-LOkd MM6 cells exhibit similar, but less pronounced, effects as the 5-LOΔ cells. This can be explained due to the fact that the 5-LOkd MM6 cells still express small amounts of mRNA transcripts, which can be translated to functional 5-LO proteins[77]. Therefore, the 5-LOkd cells barely express 5-LO, whereas the 5-LOΔ cells do not express 5-LO at all. This minor difference in the 5-LO expression causes a much stronger modulation of the miRNA processing in 5-LOΔ MM6 cells. Furthermore, the results from the previous study[95] could hardly be confirmed even though the results of this study seem to refute the previous findings in parts. The discrepancy is discussed in detail in chapter 3.3.

Previously in this thesis, it was shown that LPS and zymosan increase 5-LO protein expression (see Chapter 2.1) and possibly strengthen the 5-LO-Dicer interaction (see Chapter 2.2). Furthermore, the data from the sequencing of small noncoding RNAs shows a strong increase in the expression profiles of miR-146a and miR-146b upon LPS stimulation. Hence, the influence of LPS and zymosan on differentiated wildtype and 5-LOΔ MM6 cells was examined.

LPS treatment stimulates the transcription of miR-146a, miR-146b, and miR-21 (1174.6-fold, 2.7-fold, and 6.6-fold, respectively) in differentiated wildtype MM6 cells (see Fig. 2.10 A). However, LPS regulates the transcription of miR-155 negatively (0.2-fold). Remarkably, LPS, like 5-LO, displays contrasting effects on the transcription and the maturation of miRNAs, since the maturation of miR-146a-5p and miR-21-5p is decreased (0.1-fold and 0.3-fold, respectively), while miR-155-5p processing is increased (2.8-fold) (see Fig. 2.10 D). The processing of miR-146b-5p is not affected by LPS. In the case of miR-146a, miR-146b, and miR-21 the reduced processing of these miRNAs just dampens their enhanced transcription, leading to an increased overall expression level (miR-146a-5p: 62.2-fold, miR-146b-5p: 2.7-fold, miR-21-5p: 2.2-fold) (see Fig. 2.10 G). The LPS regulation of the transcription also overrules its impact on the processing in the case of miR-155-5p, resulting in a reduced overall expression (0.7-fold). The same applies for the miR-99b/let-7e/miR-125a cluster (see Fig. 2.10 B-C, E-F, H-I). The primary expression levels are highly increased (10 to 16.3-fold) due to the stimulation of differentiated wildtype MM6 cells with LPS or zymosan. Apart from that, both stimuli have reducing effects on the further processing of the cluster members (0.2 to 0.6-fold). The stimulating regulation on the transcriptional level overrules the inhibiting influence on the processing and consequently results in an augmented overall expression profile of miR-99b-5p, let-7e-5p, and miR-125a-5p upon LPS or zymosan stimulation (1.9 to 5.8-fold). Moreover, the influence of LPS and zymosan on the 5-LOΔ MM6 cells was assessed as well. Cells lacking 5-LO exhibit a similar regulation by LPS and zymosan compared to cells expressing 5-LO (see Fig. 2.10 B-C, E-F, H-I). Both stimuli enhance the transcription of the miR-99b/let-7e/miR-125a cluster (15.3 to 13.5-fold) but decrease the processing of the corresponding mature miRNAs miR-99b-5p, let-7e-5p, and miR-125a-5p (0.1 to 0.5-fold). Furthermore, the overall expression profiles of miR-99b-5p, let-7e-5p, and miR-125a-5p in stimulated 5-LOΔ MM6 cells display the same effects as their profiles in wildtype MM6 cells (see Fig. 2.10 H-I). Thus, those results indicate an independency of the regulation by LPS or zymosan from 5-LO's effects.

Taken together, LPS and zymosan regulate the miRNA biogenesis on the transcriptional and the processing level in opposing directions. In most cases, the regulation on the transcriptional levels overrules the regulation on the processing level resulting in a negatively (e.g. miR-155) or positively (e.g. miR-146a, miR-146b, miR-21, miR-99b, let-7e, and miR-125a) altered miRNA expression. The common characteristic of the 5-LO-, LPS-, and zymosan-effect on the miRNA biogenesis described here seems to be the opposing effects on the transcriptional and the processing level.

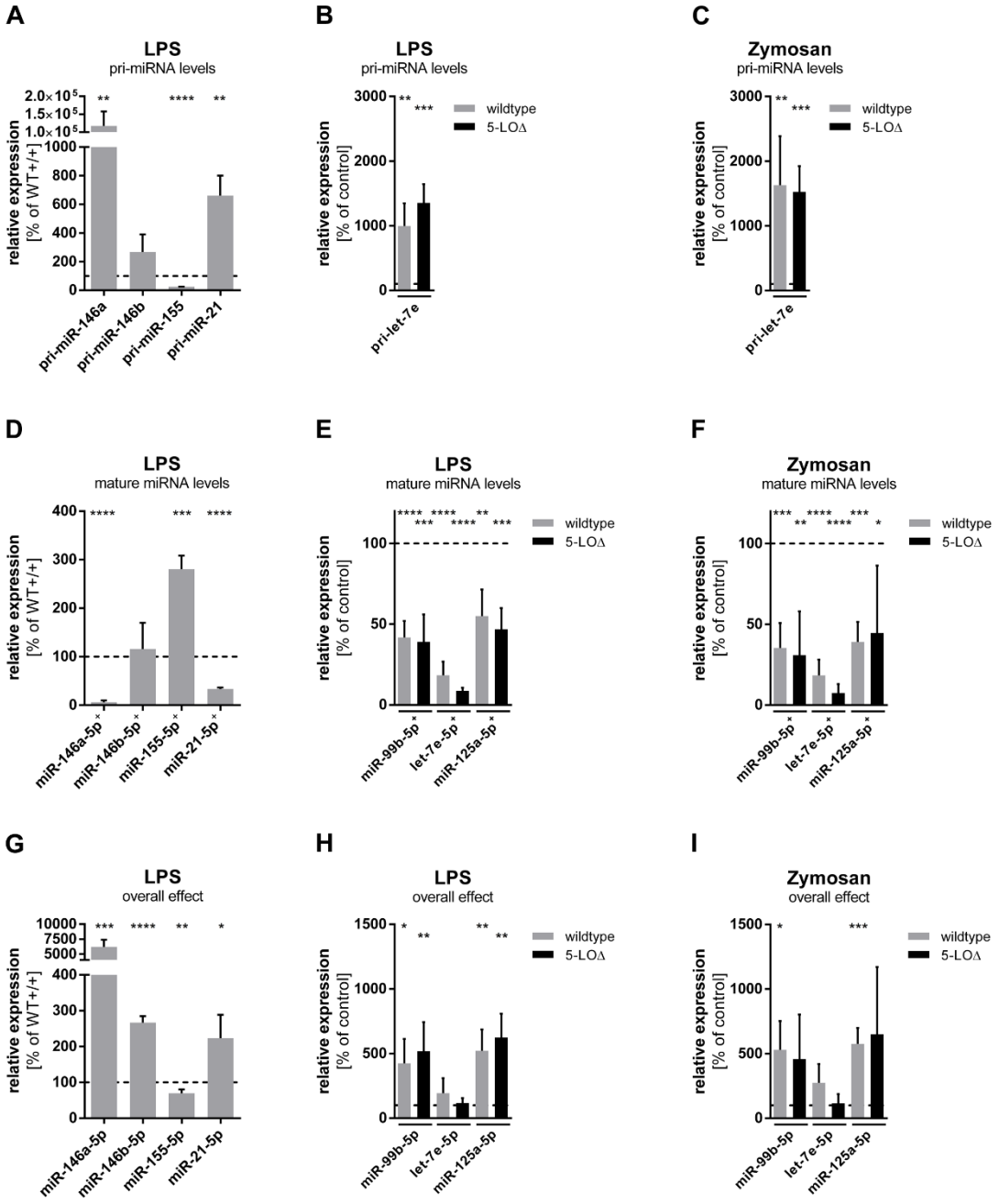

Figure 2.10 5-LO modulates the processing of miRNAs

(A-I) Real-time quantitative PCR was used to determine the expression levels of primary miRNA (A-C) and mature miRNA (D-I) in wildtype (grey) and 5-LOΔ MM6 cells (black), differentiated with 1 ng/mL TGF-β and 50 nM calcitriol for four days. Additionally, cells were stimulated with 1 µg/mL LPS (A-B, D-E, G-H) or 25 ng/mL zymosan (C, F, I) for the last 24 h. The data is presented relative to the respective control, set as 100%. (The controls for the wildtype and 5-LOΔ MM6 cells are the differentiated wildtype MM6 cells and the differentiated 5-LOΔ MM6 cells, respectively.) If indicated (+), mature miRNA levels are also normalized to the corresponding primary miRNA levels. U6 (mature miRNA) and β-actin or GAPDH (primary miRNA) were used as reference genes. Results are displayed as mean + SD and are representative for at least three independent experiments. (*$p < 0.05$, **$p < 0.01$, ***$p < 0.001$, ****$p < 0.0001$; two-tailed unpaired t test)

2.6 5-LO modulates pre-miRNA processing activity of human Dicer dose-dependently

In Chapter 2.5 it was shown that the biogenesis of the miR-99b/let-7e/miR-125a cluster is highly influenced by 5-LO both on the transcriptional and the processing level. To focus on the processing level, especially on the Dicer processing step, *in vitro* Dicer assays were performed as previously described[32]. This enables a closer look on the modulation of pre-miRNA processing by 5-LO.

Recombinant human Dicer 1650-1912 fragment was used for the *in vitro* Dicer assay. This fragment, comprising the C-terminal 262 amino acids, consists of one RNAse IIIb motif and the double-stranded RNA binding domain, which is essential for binding to 5-LO. Other important domains, e.g. the helicase, PAZ, and RNase IIIa domain, are missing. Nevertheless, it was shown that Dicer 1650-1912 is capable of cleaving double-stranded RNA, although it does not cleave the dsRNA exactly at the determined size[32]. This can be explained by the fact that the missing PAZ domain is crucial to produce RNAs approximately 22 nt in length since the PAZ domain functions as a "molecular ruler" for the correct placement of the pre-miRNAs[6,25]. A previous study[32] reported that 5-LO requires the tryptophan residues at position 13, 75, and 102 for binding to Dicer. Therefore, a mutant W13/75/102A 5-LO (5-LO_3W), where alanine replaces the tryptophan residues, was also tested in the *in vitro* Dicer assay.

Dicer 1650-1912 was incubated at 21°C for 5 min without or with increasing amounts of human 5-LO (wildtype or mutant 5-LO_3W) prior to addition of radioactive 5'-endlabeled pre-let-7e, pre-miR-125a, or pre-miR-99b. After incubation at 37°C for 1 h samples were analyzed by denaturing PAGE and autoradiography. An alkaline and a T1 ladder were used as size markers for determination of the exact product length. Pre-miRNA was produced via T7 polymerase. Hence, nucleotides at the 5' end of the pre-miRNAs were changed to guanine residues, if necessary. Corresponding nucleotides were also changed, so that the secondary structure of the pre-miRNA remained unaffected (see Figure 2.11 B).

The results displayed in Fig. 2.11 A and Fig. 2.11 C reveal that wildtype 5-LO inhibits the processing of pre-let-7e by Dicer 1650-1912 dose-dependently, since the band intensity of the unprocessed pre-let-7e (blue arrow) increases, while the band intensity of the cleaved product (20 nt; green arrow) decreases with increasing 5-LO concentrations. Remarkably, wildtype 5-LO enhances processing of pre-miR-125a (blue arrow) and pre-miR-99b (green arrow) (see Fig. 2.12 A-C), since the intensity of the uncleaved pre-miRNAs is reduced with increasing 5-LO concentration. Thus, wildtype 5-LO exhibits a pre-miRNA specific and dose-dependent modulation of Dicer processing *in vitro*.

Lane 3 of Fig. 2.11 A was incubated in the absence of Dicer 1650-1912 and wildtype 5-LO. Interestingly, an unexpected strong band (31 nt in length) appeared. A cytosine residue is located at position 31 (see black arrow) at the very end of the last loop of pre-let-7e (see Fig. 2.11 B). Hence, pre-let-7e seems to be unstable at this position and self-cleaves. The dose inhibition curve (see Fig. 2.11 D) displays the inhibitory effect of wildtype 5-LO and mutant 5-LO_3W. Although it was proposed that 5-LO_3W cannot interact with Dicer[32], it inhibits pre-let-7e processing slightly more efficient than wildtype 5-LO. Since the results for wildtype 5-LO and mutant 5-LO_3W are very similar, the gel for 5-LO_3W is not shown.

To sum up, the dose inhibition curve (see Fig. 2.12 D) displays the modulation of pre-let-7e, pre-miR-125a, and pre-miR-99b by wildtype 5-LO. The Dicer 1650-1912 processing of pre-let-7e is strongly inhibited, but otherwise wildtype 5-LO augments cleavage of pre-miR-125a. Processing of pre-miR-99b is also slightly enhanced. Thus, the *in vitro* Dicer assay revealed that 5-LO modulates the pre-miRNA processing activity of human Dicer in a dose-dependent and pre-miRNA specific manner.

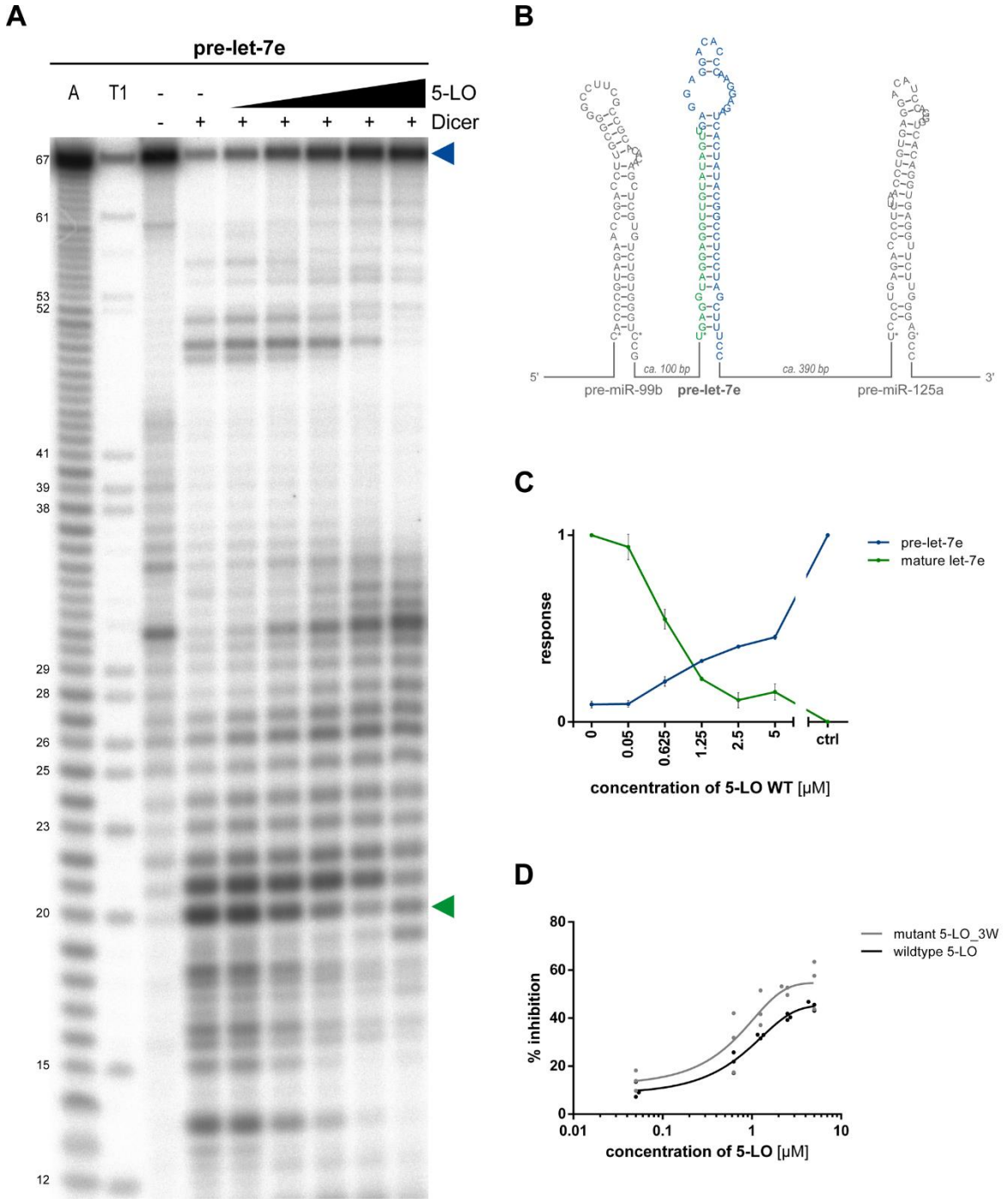

Figure 2.11 5-LO inhibits pre-let-7e processing by human Dicer dose-dependently

(A) *In vitro* Dicer assay was performed according to *Dincbas-Renqvist et al.*[32]. (Lane 4-9) Recombinant human Dicer 1650-1912 fragment (0.05 µM) was incubated at 21°C for 5 min without or with increasing amounts of human 5-LO (0.05, 0.625, 1.25, 2.5, and 5 µM) prior to addition of ^{32}P-labeled pre-let-7e. After incubation at 37°C for 1 h samples were analyzed by denaturing PAGE and autoradiography. Lane 3 was incubated in the absence of 5-LO and Dicer 1650-1912. An alkaline (lane 1) and a T1 ladder (lane 2) were used as size markers. (B) Illustration of the secondary structure of the pre-miR-99b/let-7e/miR-125a cluster with the letters representing the respective pre-miRNAs. RNA folding was predicted based on the Zuker algorithm[102]. To allow effective RNA production via T7 polymerase with unaffected secondary structure of the precursor miRNA, nucleotides were changed to guanine residues (*) or to uracil residues ($^+$), if indicated. (C) The data is displayed as a dose response curve (the strongest bands of the precursor miRNA or the cleaved miRNA, respectively, were normalized to 1). (D) The data is presented as dose response curve showing the effect of wildtype or mutant 5-LO_3W on the processing of pre-let-7e by Dicer. Results are representative for three independent experiments.

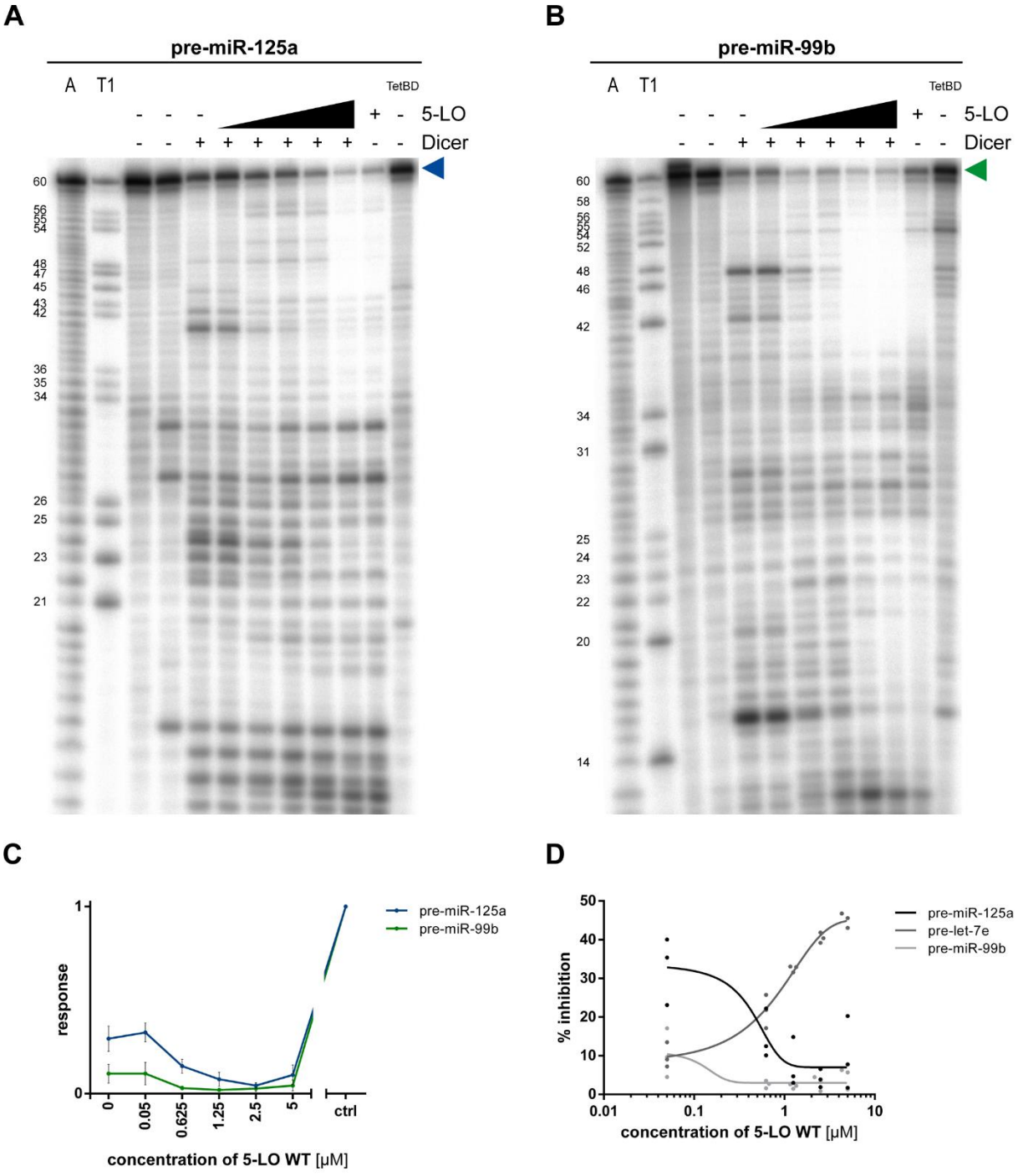

Figure 2.12 5-LO modulates pre-miRNA processing activity of human Dicer dose-dependently

(A-B) *In vitro* Dicer assay was performed according to *Dincbas-Renqvist et al.*[32]. (Lane 5-10) Recombinant human Dicer 1650-1912 fragment (0.05 µM) was incubated at 21°C for 5 min without or with increasing amounts of human 5-LO (0.05, 0.625, 1.25, 2.5, and 5 µM) prior to addition of ^{32}P-labeled pre-miR-125a (A) or pre-miR-99b (B). After incubation at 37°C for 1 h samples were analyzed by denaturing PAGE and autoradiography. Lane 4 was incubated in the absence of 5-LO and Dicer 1650-1912. Precursor miRNA was loaded directly onto the gel without any incubation (lane 3) or after incubation with 5 µM 5-LO or 5 µM TetBD, respectively (lane 11 and lane 12). An alkaline (lane 1) and a T1 ladder (lane 2) were used as size markers. (C) The results are presented as a dose response curves (the strongest bands of the precursor miRNA were normalized to 1). (D) The data is presented as dose response curve displaying the modulation of pre-miRNA processing activity of human Dicer by wildtype 5-LO. Results are representative for three independent experiments.

2.7 5-LO product formation in MM6 cells

To further investigate the effects of the applied stimuli TGF-β, calcitriol, LPS, and zymosan on MM6 cells, 5-LO activity assays were performed. The 5-LO activity assay utilizes reversed-phase high-performance liquid chromatography (RP-HPLC) to measure the 5-LO products leukotriene B_4 (LTB_4), trans isomers of leukotriene B_4, leukotriene C_4 (LTC_4), and 15/12/5-hydroperoxyeicosatetraenoic acid (H(p)ETE). The 5-LO product formation is calculated as the sum of the 5-LO products in proportion to the internal standard prostaglandin B_1 (PGB_1).

Differentiated wildtype MM6 cells, as well as differentiated cells stimulated with LPS or zymosan, were treated with PMA, Ca^{2+}-ionophore A23187, and arachidonic acid prior to the measurement of the 5-LO product formation. PMA and A23187 treatment are essential for the translocation of 5-LO to the nucleus, which in turn is important for 5-LO product formation, since the conversion of arachidonic acid predominantly takes place at the nuclear membrane [71].

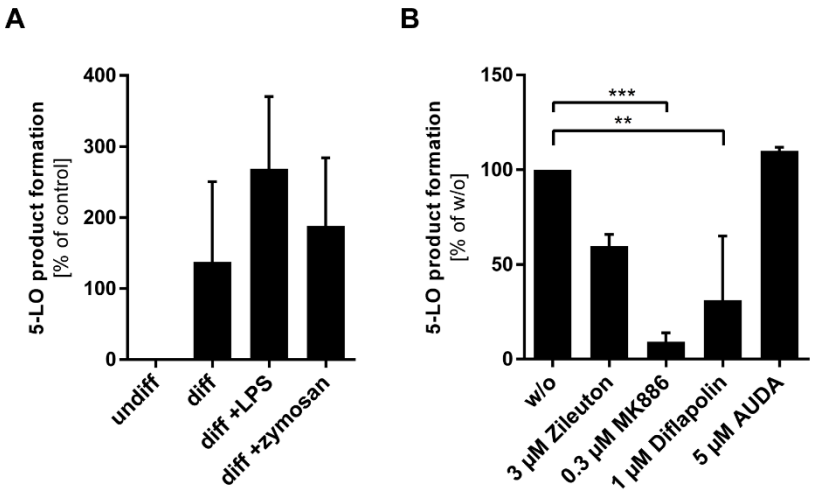

Figure 2.13 5-LO product formation in wildtype MM6 cells
(A) 1 Mio wildtype MM6 cells (differentiated for four days with 1 ng/mL TGF-β and 50 nM calcitriol and stimulated with 1 µg/mL LPS or 25 ng/mL zymosan, if indicated) were preincubated (37°C, 10 min) with 100 nM PMA prior to the incubation (37°C, 10 min) with 2.5 µM Ca^{2+}-ionophore A23187 and 10 µM arachidonic acid. 5-LO product formation was determined by reversed-phase HPLC. (B) 5-LO product formation was analyzed by reversed-phase HPLC in wildtype MM6 cells that were differentiated with 1 ng/mL TGF-β and 50 nM calcitriol for four days. 1 Mio cells were incubated (37°C, 10 min) with 2.5 µM Ca^{2+}-ionophore A23187 and 10 µM arachidonic after preincubation (37°C, 10 min) with both 100 nM PMA and 3 µM Zileuton, 0.3 µM MK886, 1 µM diflapolin, or 5 µM AUDA. (A-B) Results are displayed as mean + SD and are representative for three independent experiments. (*$p < 0.05$, **$p < 0.01$, ***$p < 0.001$; one-way ANOVA with Bonferroni correction)

It was previously described that differentiation of MM6 cells with TGF-β and calcitriol strongly induces 5-LO activity[82]. The presence of zymosan during the entire differentiation period was reported to prevent late upregulation of LTC_4 formation due to reduced LTC_4 synthase activity, caused by phosphorylation of the enzyme[103]. In accordance with these previous findings, 5-LO product formation (trans isomers of LTB_4, LTB_4, and 5-H(p)ETE) is slightly increased upon differentiation (1.4-fold) and upon additional stimulation with LPS (2.7-fold) or zymosan (1.9-fold) (see Fig. 2.13 A). The increase in 5-LO

product formation is most probably caused by the augmented amount of 5-LO protein (see chapter 2.1). Although LTC_4 amounts were not quantified in this experimental setup, the HLPC chromatogram reveals that the LTC_4 peak was detectable in the differentiated cells but disappeared upon additional stimulation with LPS or zymosan (see Fig. S1). This observation indicates that LPS might potentially prevent upregulation of LTC_4 in differentiated MM6 cells, as already reported for zymosan[103].

Next, the effects of several inhibitors of 5-LO, 5-LO activating protein (FLAP), and soluble epoxide hydrolase (sEH) were tested to further characterize 5-LO product formation (trans isomers of LTB_4, LTB_4, LTC_4, and 5-H(p)ETE) in differentiated wildtype MM6 cells.

Zileuton (Zyflo®) is the only direct 5-LO inhibitor that has entered the market[74]. The orally active compound has been shown to be a potent inhibitor of the leukotriene biosynthesis *in vitro* and *in vivo*[104]. MK886 is a competitive inhibitor of FLAP, which in turn is required for leukotriene formation[70]. Thus, MK886 efficiently suppresses production of leukotrienes[105]. Diflapolin is the first described dual inhibitor of FLAP and sEH and inhibits the formation of H(p)ETE and LTB_4, as well as the formation of its isomers, in intact monocytes and neutrophils from human peripheral blood stimulated with Ca^{2+}-ionophore[106]. AUDA inhibits the sEH[106] and functions as a control inhibitor in this experimental setup.

The results displayed in Fig. 2.13 B reveal strong inhibitory effects of MK886 (0.1-fold) and diflapolin (0.3-fold) on the 5-LO product formation in differentiated MM6 cells. These findings are in line with previous reports[105,106]. As expected, Zileuton (0.6-fold) also decreases 5-LO product formation in MM6 cells, while AUDA exhibits no effect.

3 Discussion

The expression of genes is controlled by a complex regulatory network to allow the human body to adjust to internal and external impacts. Silencing of genes after transcription largely contributes to the complexity of the regulatory mechanisms controlling gene expression. MicroRNAs are a major player of RNA silencing since they target hundreds of mRNAs, which in turn harbour binding sites for multiple miRNAs. Thus, the miRNA/mRNA regulatory circuit itself is very complex and requires a tight regulation. Various scientific studies have focused on mechanisms altering the biosynthesis of miRNAs as well as on relating dysfunctions to severe human diseases[6,38].

Especially the innate immune response to inflammatory stimuli and inflammatory disorders have been linked to the miRNA pathway[55]. Several scientific reports provided evidence that 5-LO, a key enzyme of the leukotriene synthesis, interferes with the miRNA biogenesis through its binding to Dicer, a major player within this pathway, and that in turn 5-LO is controlled by miRNAs[32,33,69,89,95]. Thus, the aim of this study is to further investigate the interaction between 5-LO and Dicer and its impact on the miRNA biosynthesis.

3.1 5-LO affects biosynthesis of miRNAs at multiple levels

3.1.1 *In situ* interaction of 5-LO and Dicer

In 1999, *Provost et al.* utilized a yeast two hybrid approach to screen for cellular interaction partners of 5-LO. They discovered a protein named ΔK12H4.8 homologue, which displays high homology to the helicase K12H4.8 from *C. elegans*[33]. Later, the *C. elegans* helicase K12H4.8 was identified as Dicer and shown to be essential for the production of small RNAs involved in the developmental timing[107]. In 2009, *Dincbas-Renqvist et al.* further characterized the 5-LO binding to Dicer. By using *in vitro* methods, namely a yeast two hybrid system, GST pull-down assays, and coimmunoprecipitation, they revealed that the N-terminal C2-like domain of 5-LO interacts with the C-terminal 140 amino acids of Dicer[32].

Despite the strong evidence for an interaction it remained unclear whether the two proteins also bind *in situ* or rather in intact cells. A suitable approach to address this issue is the proximity ligation assay, which is an excellent tool for monitoring interactions of endogenous proteins without the necessity to disrupt intact cells[98]. In short, primary and secondary antibodies are utilized to trigger positive PLA signals (for detailed description of the PLA see chapter 2.2)[100]. Since the average diameter of antibodies is around 10 nm, positive PLA signals are still detected at a maximum distance of 40 nm[108]. So, theoretically, there is a rare chance that the proteins are just in very close proximity, but do not interact. Regardless of this methodological limitation, positive PLA signals are interpreted as proof for a protein-protein interaction[98]. Thus, respective PLA experiments were performed in the course of this study and the obtained positive results provide evidence that 5-LO and Dicer interact under natural conditions *in situ* in differentiated MM6 cells (see chapter 2.2).

3.1.2 Functional impact of the 5-LO-Dicer interaction

The main aim of this thesis is to address the question whether the 5-LO-Dicer interaction alters the processing of miRNAs. Therefore, sequencing of small noncoding RNAs was performed to screen for miRNAs whose expression profile is modified by 5-LO (see chapter 2.4). The outcome of the sequencing data revealed the miR-99b/let-7e/miR-125a cluster as a promising candidate. In order to validate the miRNAs miR-99b, let-7e, and miR-125a as 5-LO targets, and to closer investigate the impact of 5-LO on the miRNA processing, qRT-PCR experiments and *in vitro* Dicer assays were carried out (see chapter 2.5 and 2.6).

Notably, the 5-LO enzyme acts both as a transcriptional as well as a posttranscriptional regulator since it modifies the processing of distinct miRNAs on multiple levels in opposing directions. On the one hand, 5-LO exhibits stimulatory effects on the transcription of the primary miRNA encoding for the miR-99b/let-7e/miR-125a cluster. On the other hand, 5-LO inhibits the processing of pre-let-7e by Dicer specifically and dose-dependently, whereas the Dicer-mediated cleavage of the other clustered miRNAs is unaffected or slightly enhanced. The opposing effects on the processing of the miR-99b/let-7e/miR-125a cluster just described result in a strong upregulation of mature miR-99b and miR-125a with simultaneously unchanged let-7e levels. This is of special interest not only because this regulatory mechanism adds even more complexity to the already very complex regulatory circuits modifying the miRNA pathway, but also because the miR-99b/let-7e/miR-125a cluster is a well studied regulator of Toll-like receptor signaling, suggesting an involvement of this cluster in the coordination of innate immune responses triggered by inflammatory stimuli[42].

Interestingly, 5-LO's action as a transcription factor is less specific compared to its effect as a Dicer interacting partner, since the primary miRNA expression levels of several let-7 family members are altered, whereas the modulation of the Dicer processing step is very specific for let-7e and miR-4763. Considering the data obtained from the qRT-PCR experiments (see chapter 2.5), neither the maturation of any other let-7 family member nor that of miRNAs clustered with let-7e was regulated by 5-LO. Remarkably, 5-LO exerts inhibitory as well as stimulatory effects on both regulatory levels but the modulation is counteracting. Whenever the transcription is stimulated the Dicer processing is inhibited, and vice versa. Thus, further studies are needed to elucidate how 5-LO exerts opposing effects on each regulatory level separately and how the opposingly regulated transcriptional and processing levels interplay, as well as if more determinants other than 5-LO are involved within this regulatory network. Nevertheless, these findings may uncover a mechanism to modulate the expression of each member within the miRNA clusters individually.

As already mentioned above, 5-LO interferes with the miRNA processing at multiple levels. The transcriptional and the post-transcriptional modulation by 5-LO mutually overlap. To enable focusing on the Dicer processing step in order to distinguish the overlapping effects from each other, *in vitro* Dicer assays according to *Dincbas-Renqvist et al.* were performed (see chapter 2.6). *Dincbas-Renqvist et al.* discovered that 5-LO alters Dicer's enzymatic activity dose-dependently. At low concentrations 5-LO enhances Dicer's processing activity up until a concentration at which 5-LO exhibits inhibitory effects. Additionally, 5-LO modifies the cleavage pattern of Dicer in terms of facilitating the conversion of pre-let-7a-3 to ∿55 bp and 10-12 bp long cleavage products. Within the scope of this thesis, it was investigated how 5-LO modulates Dicer-mediated cleavage of pre-miR-125a, pre-let-7e, and pre-miR-99b.

The obtained data reveals that human wildtype 5-LO strongly inhibits the processing of pre-let-7e, whereas the cleavage of pre-miR-99b is slightly and that of pre-miR-125a considerably stimulated.

Moreover, the effect of 5-LO is related to its concentration. Hence, 5-LO acts pre-miRNA specific and in a dose-dependent manner on Dicer's enzymatic activity. The observation that 5-LO modulates Dicer-mediated processing specific for distinct pre-miRNAs and for each in a different way is supported by the fact that *Dincbas-Renqvist et al.* obtained results for pre-let-7a-3 which differ from those results obtained for pre-miR-99b, pre-let-7e, and pre-miR-125a. For the three investigated pre-miRNAs, the modified cleavage pattern could not be confirmed either. For instance, processing of pre-let-7e resulted in products of the correct size (22 bp), although bands, which were 21 bp and 20 bp long, were more prominent. The small discrepancy is due to the usage of a Dicer fragment consisting only of one RNAse III motif and the 5-LO binding domain. The missing PAZ domain, which functions as a "molecular ruler" by facilitating the correct placement of pre-miRNAs, most probably causes the inaccurate cleavage by the Dicer fragment[6,25]. Recently, the structure of the Dicer-TRBP complex bound with pre-let-7 was described, revealing a binding of the dsRBD domain to the middle portion of the RNA substrate. Since 5-LO interacts with Dicer via the dsRBD domain, a further characterization of the this domain might clarify how 5-LO exerts its pre-miRNA specific modulation of the Dicer-mediated processing[24,32].

Dincbas-Renqvist et al. further investigated the 5-LO-Dicer binding process and revealed that 5-LO's tryptophan residues at position 13, 75, and 102 are essential for the 5-LO binding to Dicer. Replacement of these tryptophan residues with alanine disrupted the interaction between the two proteins in GST-pull-downs and coimmunoprecipitation experiments[32]. In contrast to these results, the mutant W13/75/102A 5-LO inhibits pre-let-7e processing by Dicer even more efficiently than the wildtype 5-LO (see chapter 2.6). To elucidate the contradictory results, overexpression of the mutant W13/75/102A 5-LO in 5LOΔ cells and subsequent performance of qRT-PCR experiments to check whether the cells behave like the wildtype could be a viable approach.

Furthermore, it was tested whether the leukotriene formation catalyzing property of 5-LO is essential for its miRNA regulating activity (see chapter 2.5). It turned out that both the 5-LO inhibitor Zileuton[74] and the FLAP inhibitor MK886[70] interfere neither with the transcription of the miR-99b/let-7e/miR-125a cluster nor with its processing. Remarkably, CJ13610, a selective and potent 5-LO inhibitor, only enhances the transcription of pri-let-7e if the inhibitor is applied at a concentration of 1 µM. At lower concentrations CJ13610 exhibits no effect. The 5-LO inhibitor was recently characterized as a transcriptional regulator of the Wnt signaling pathway. Enzymatically inactive 5-LO binds to β-catenin preventing its translocation into the nucleus and thus inhibiting transcriptional activation of Wnt target genes. Interestingly, a knockout of the 5-LO gene had no effects, leading to the assumption that trapping of β-catenin outside the nucleus is indispensable or that CJ13610 interacts with further targets other than 5-LO[88]. However, CJ13610 seems to impact 5-LO's function as a transcriptional regulator in more pathways than just the Wnt signaling pathway, since the inhibitor potentiates 5-LO's stimulatory effect on the let-7e transcription.

3.1.3 Potential consequences of the altered miRNA expression profiles

Besides its role in TLR signaling the miR-99b/let-7e/miR-125a cluster was also linked to stem cell maintenance and functions in previous studies. The miR-99b/let-7e/miR-125a cluster was shown to be highly expressed in hematopoietic stem cells and its expression is down-regulated upon differentiation. Interestingly, miR-125a by itself was reported to increase stem cell activity and retain the cells in a

primitive state, as well as to amplify the HSC pool size by targeting proapoptotic genes (e.g. Bak1) in a differentiation state specific manner reducing the apoptosis of hematopoietic stem and progenitor cells[38,39]. Unlike miR-125a, let-7, whose expression increased upon differentiation of breast cancer stem cells, facilitated multipotent differentiation and contributed to the cancer stem cells' lost ability of self-renewal through targeting of HMGA2 or H-Ras, respectively[45].

Remarkably, previous findings also linked 5-LO to the maintenance of stem cells. Hematopoietic stem cell compartments were shown to express enzymatically active 5-LO and the stem cell capacity of PML/RARα-positive HSPCs was impaired by selective 5-LO inhibition. As already mentioned above, direct interaction of enzymatically inactive 5-LO with β-catenin inhibited Wnt signaling, a key signaling pathway for the maintenance of cancer stem cell-like cells[88].

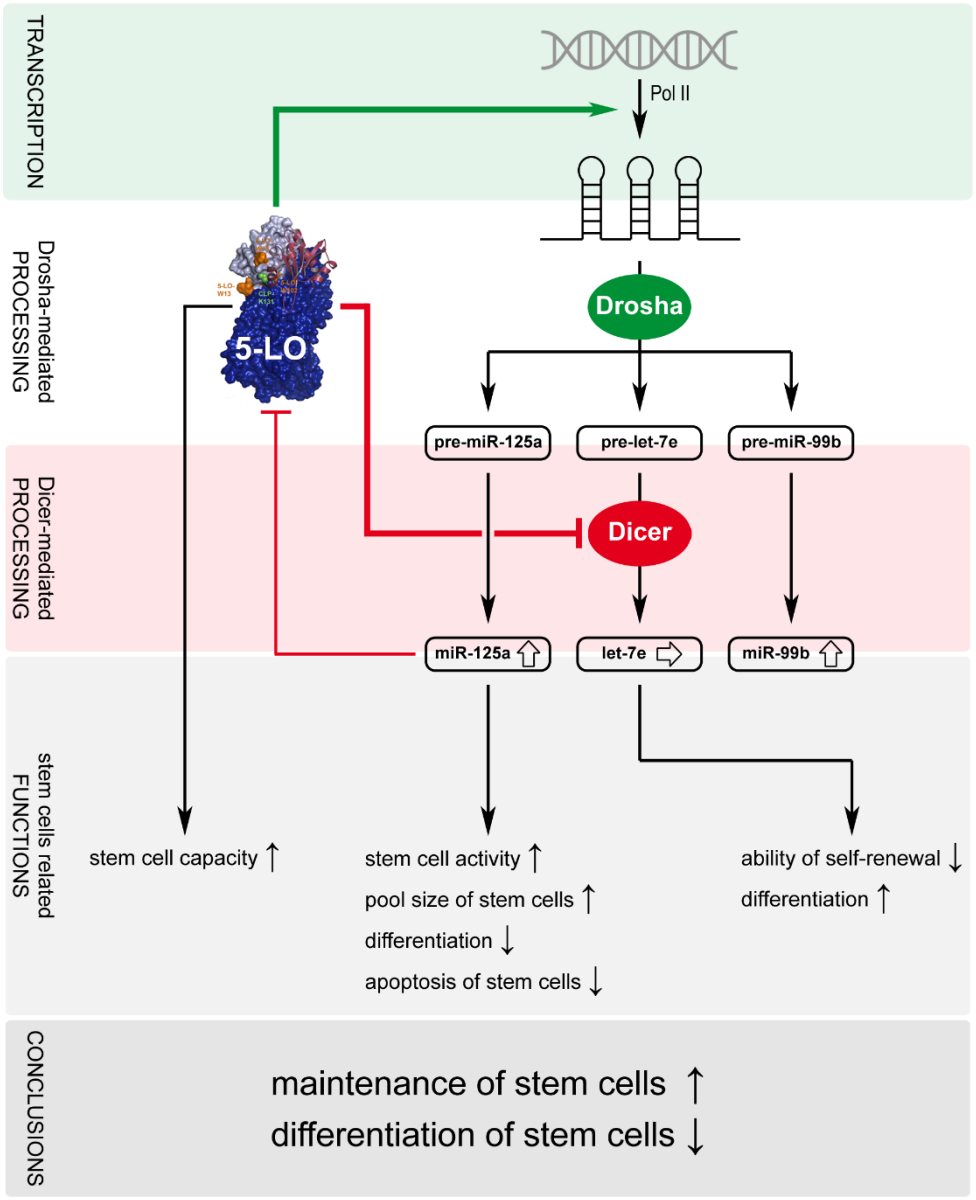

Figure 3.1 Potential consequences of the altered miR-99b/let-7e/miR-125a expression profile
5-LO alters the expression of the miR-99b/let-7e/miR-125a cluster, which is involved in the coordination of diverse stem cell functions[38,39,45,88,89]. This figure summarizes the parts of chapter 3.1.3, which are related to functions of stem cells.

Table 3.1 Regulation of the miR-99b/let-7e/miR-125a and the let-7a/let-7b/miR-4763 cluster by 5-LO

	miR-99b	let-7e	miR-125a	let-7a	let-7b	miR-4763
Transcription		↑			↓	
Processing	→	↓	→	→	→	↑
Final outcome	↑	→	↑	→	↓	→

This table summarizes 5-LO's contrasting effects on the transcription and the processing of the miR-99b/let-7e/miR-125a and the let-7a/let-7b/miR-4763 cluster resulting in different final outcomes. 5-LO's effects on the levels of the primary transcripts or the mature miRNAs is displayed by arrows (↑: increased; ↓: reduced; →: constant)

Given 5-LO's role in stem cell maintenance, as well as considering the opposing effects of the single cluster members on stem cell functions, their specific and divergent modulation by 5-LO may be a mechanism to promote maintenance of stem cells and suppress cell differentiation (see Fig. 3.1). It is worth noting that this assumption is supported by 5-LO's regulation of the let-7a/let-7b/miR-4763 cluster (see Table 3.1 and chapter 2.5). Interestingly, 5-LO contrastingly modulates this cluster compared to the miR-99b/let-7e/miR-125a cluster. More precisely, 5-LO decreases the transcription of the let-7a/let-7b/miR-4763 cluster while simultaneously increasing the processing of miR-4763-3p, resulting in reduced let-7b-5p levels with unchanged levels of let-7a-5p and miR-4763-3p. Taking into account that the let-7 miRNAs contribute to the differentiation of stem cells and their lost ability to self-renew[45], the regulation of the let-7a/let-7b/miR-4763 cluster by 5-LO may contribute to the maintenance of stem cells just like 5-LO's modulation of the miR-99b/let-7e/miR-125a cluster. Furthermore, these findings illustrate the manifold options of 5-LO to regulate the miRNA pathway on multiple levels, allowing a very specific modulation of the expression profile of individual miRNAs. This is of special interest since the promotors of both the miR-99b/let-7e/miR-125a and the let-7a/let-7b/miR-4763 cluster contain NF-κB binding sites. Overexpression of the NF-κB subunits p50 or p65, or rather recruitment of NF-κB to the promotor upon exposure to LPS, leads to an increased expression of both clusters[42,109]. Thus, further studies are needed to elucidate how 5-LO is capable of positively as well as negatively regulating two different promotors, both of which are regulated by the same transcription factor in the same way.

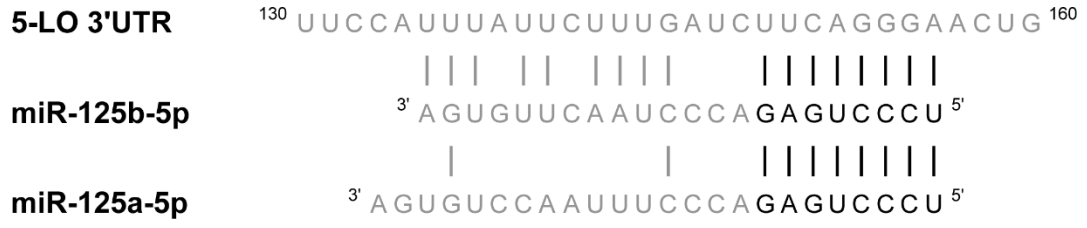

Figure 3.2 Sequence homology of miR-125a/b with the 5-LO 3'UTR
The figure (adapted from[89]) displays the sequence homology of miR-125b-5p and miR-125a-5p, especially of their seed regions (indicated in black), as well as the predicted binding sites within the 5-LO 3'UTR of both miR-125 homologues.

An effective tool to add another adjustment option to regulatory networks is a negative feedback loop. *Busch et al.* characterized the 3'UTR of 5-LO as a direct target of the miRNAs miR-19a-3p and miR-125b-5p[89]. Since the homologues miR-125b-5p and miR-125a-5p share the same seed sequence at the 5' end (see Fig. 3.2), it is likely that miR-125a-5p also targets 5-LO, enabling such a regulatory negative feedback loop. Hence, 5-LO augments the overall expression of mature miR-125a-5p by enhancing its transcription rate as well as the Dicer-mediated processing, but miR-125a-5p in turn can target 5-LO mRNA in order to lower the amount of 5-LO protein (see Fig. 3.1).

3.1.4 Comparison to other proteins modulating the miRNA pathway

It has already been known, that auxiliary factors facilitate transcriptional as well as posttranscriptional regulation of specific miRNAs and thus provide additional regulatory levels to the already complex network coordinating miRNA biosynthesis[19].

For instance, the RNA-binding proteins KSRP and LIN28 interfere with the miRNA pathway on both posttranscriptional levels: the Drosha-mediated as well as the Dicer-mediated cleavage[20,30,49–51]. KSRP, which is part of both processor complexes and also functions within the mRNA decay, promotes the processing of a subset of miRNAs (e.g. let-7 family members) by interacting with their terminal loop[20].

In contrast to KSRP, LIN28 exerts inhibitory effects on the posttranscriptional processing of miRNAs since it binds to the terminal loop of pri-let-7 or pre-let-7, respectively, in order to prevent Drosha-mediated cleavage or to induce oligouridylation which results in the inhibition of Dicer-mediated processing[30,49–51]. Interestingly, LIN28 translation is regulated by its targets (e.g. let-7b, miR-125a, miR-125b) via a negative feedback loop[53,54]. Due to the consistent seed regions of miR-125a and the 5-LO 3'UTR binding miR-125b[89] it can be assumed that 5-LO expression is also modulated by the 5-LO regulated miRNAs via a negative feedback loop, just like LIN28.

Smads, signal transducers of the TGF-β pathway, were reported to alter the miRNA biogenesis on the transcriptional level and even on both posttranscriptional levels[17,110,111]. As transcription factors, Smad proteins control the expression of various miRNA genes, for instance by binding to the Smad binding elements within the promotor regions[111]. Moreover, *Davis et al.* reported that Smad proteins promote the Drosha-mediated maturation of a subset of miRNAs (e.g. miR-21). Those primary miRNAs harbour a conserved consensus sequence within their stem region to which the Smad protein can directly bind and thus facilitate cleavage of the respective pri-miRNAs by Drosha[17]. Additionally, *Garcia et al.* revealed that p-Smad2/3 interacts with Dicer in order to promote pre-miR-21 processing in cardiac fibroblasts under pressure overload. The interaction of these two proteins was confirmed by performing PLAs[110]. Hence, the Smad proteins are indeed multifunctional as they act as both transcriptional and posttranscriptional regulators, just like 5-LO. However, the Smad proteins exert mutually reinforcing effects while, in contrast, 5-LO exhibits opposing effects on miRNA transcription and maturation, which balance out in the case of let-7e.

3.2 Modulation of miRNA processing by the TLR agonists LPS and zymosan in MM6 cells

Many scientific reports linked miRNAs and their biogenesis to TLR signaling pathways, especially to TLR4 signaling which is activated by bacterial LPS[55]. Moreover, the TLR2 and TLR6 agonist zymosan, a part of the fungal cell wall, was previously reported to suppress LTC_4 synthase activity and thus to interfere with the leukotriene pathway[103]. These points of contacts lead to the investigation of a possible modulation of the miRNA processing by LPS and zymosan in MM6 cells.

PLA experiments were performed to check LPS' and zymosan's impact on the 5-LO-Dicer interaction. Neither LPS nor zymosan disturb the interaction. In contrast, both stimuli seem to strengthen it since more PLA signals appear, most probably due to an increased amount of 5-LO protein (see chapter 2.1 and 2.2). However, as already discussed in chapter 2.2, the PLA does not allow any quantification in the used experimental setup and thus, even though assumptions can be made based on the visual impression, no final conclusions can be drawn. Interestingly, the fungal zymosan causes morphological changes, likely due to the formation of endocytic vesicles (see chapter 2.3).

The sequencing of small noncoding RNAs revealed that the expression profile of various miRNAs was modified by LPS (see chapter 2.4). In particular, the expression of the TLR-inducible miRNAs miR-146a and miR-146b is altered by the bacterial agent. The performing of qRT-PCR enabled a closer look on how the TLR agonists LPS and zymosan impact the miRNA pathway (see chapter 2.5). The obtained data revealed an increased transcription of miR-146a, miR-146b, the miR-99b/let-7e/miR-125a cluster, and miR-21, as well as a decreased transcription of miR-155. Remarkably, just like 5-LO, LPS and zymosan exert contrary effects on the transcriptional and the Dicer processing level. The maturation of miR-146a, miR-99b, let-7e, miR-125a, and miR-21 is reduced, whereas the maturation of miR-155 is augmented. It is worth noting that the opposite regulation of the Dicer processing step dampens the strong transcriptional effect without fully compensating it, resulting in a total outcome of less enhanced (e.g. miR-146a/b, miR-21, and the let-7e cluster) or decreased (e.g. miR-155) mature miRNA levels. This compensating regulatory mechanism raises the complexity of the already very complex regulatory network coordinating TLR signaling and contributes to the fine tuning of the innate immune response. Interestingly, in the absence of 5-LO, a less pronounced but similar effect could be observed.

The miRNAs investigated within the course of this thesis, namely miR-146a/b, miR-155, miR-21, and the let-7e cluster, are known to be encoded by NF-κB-dependent TLR-response genes. Previous publications reported an induced expression of these miRNAs in monocytic cell lines other than Mono Mac 6 upon treatment with the TLR4 agonist LPS[40–42,56–58]. Except for miR-155, the findings reported here are in line with the previous publications.

The TLR response miRNAs are classified as rapidly induced proinflammatory miRNAs (e.g. miR-155) and late induced negative feedback regulators (e.g. miR-146a, miR-21, let-7e cluster)[42,57,58]. In the used experimental setup, the cells were stimulated with LPS and zymosan for the last 24 h. This is quite a long period of time in terms of the innate immune response to hostile invaders. The rapidly induced miR-155 already exerts high expression levels after 6 h while the late induced miRNAs were not strongly enhanced until after 24 h[42,57,58]. Furthermore, miR-155 expression is regulated via a negative feedback loop[60]. Additionally, cumulation of IL-10 induced by miR-21 also stunts the initial increase of miR-155, reinforcing the negative feedback loop[57,58,61]. Considering all these aspects, the experimental setup

applied here represents inflammatory conditions at later time points at which the late induced miRNAs are highly increased, whereas the regulatory mechanisms repressing miR-155 are already activated at this point, resulting in a reduced expression.

Although the scientific research on TLR signaling in the context of the miRNA pathway is rather focused on TLR4, the TLR2 agonist Pam3CSK4 was reported to increase the expression of miR-99b, let-7e, and miR-125a[42]. However, zymosan, a TLR2 and TLR6 agonist[103], also increases the expression of the let-7e cluster members in MM6 cells (see chapter 2.5). Considering that zymosan and LPS exert similar effects, this thesis provides evidence that activation of TLR2, TLR4, or TLR6 results in similar outcomes, at least regarding the let-7e cluster and under the used experimental conditions.

Thus, the findings obtained within the course of this thesis provide more evidence that TLR signaling and the miRNA pathway are closely interconnected and mutually affect one another. Negative feedback loops and regulation at multiple levels further complicate the regulatory network. The dampening of the strong transcriptional effects through modulation of miRNA maturation described here adds a compensating regulatory mechanism to the TLR signaling, which expands the possibility to fine tune the TLR-miRNA-pathway.

3.3 Comparison to preliminary work

This thesis was started based on findings from a previous PhD project done by *Friederike Scholl*[95]. In the beginning, many experiments were planned in order to confirm the previous findings. However, these experiments revealed a huge discrepancy between the results obtained within the scope of the current project and those previously gained.

Microarray and qRT-PCR experiments performed within the course of the previous PhD project revealed a decrease of mature miR-99b-5p, let-7e-5p, and miR-125a-5p in the absence of 5-LO. The primary transcript levels remained unchanged but lowered pre-miRNA levels were observed in cells expressing hardly any 5-LO, suggesting a regulation of the Drosha activity. Furthermore, expression of miR-99b-5p and miR-125a-5p was shown to be independent of leukotriene levels as well as of inhibitors of the leukotriene synthesis. LPS stimulation led to an increase of pri-let-7e and the mature miRNAs miR-99b-5p and miR-125a-5p. In 5-LO knockdown cells a minor increase of the mature miRNA levels was detected and the enhanced pri-let-7e expression was fully prevented, indicating a 5-LO-dependent LPS effect. Moreover, the amount of 5-LO protein was not enhanced upon LPS stimulation[95].

However, the results of the present thesis refute these previous findings in parts. Firstly, the qRT-PCR data gained here revealed a very strong transcriptional regulation by 5-LO (see chapter 2.5). The transcription of several let-7 family members was altered in 5LOΔ MM6 cells, with the expression of pri-let-7e showing an especially heavy decrease. An overall effect of reduced mature miRNA levels in the absence of 5-LO could be confirmed in the case of miR-125a-5p and miR-99b-5p, but not for let-7e-5p, whose levels remained unchanged. In addition, a close investigation of the Dicer cleavage step discovered a specific and inhibitory modulation of pre-let-7e processing by 5-LO, counteracting the transcriptional upregulation. In line with the previous findings is the observation that the inhibitors Zileuton and MK886 do not impair 5-LO's miRNA modulating activity, although those substances do inhibit its catalyzing properties[70,74]. Just the selective 5-LO inhibitor CJ13610[88], which was not tested with regards to a possible modulation of the miRNA pathway before, interferes with the transcriptional regulation of pri-let-7e by 5-LO. Moreover, LPS treatment leads to an overall increase in mature miR-99b, let-7e, and miR-125a levels, as well as to a stimulation of pri-let-7e transcription. In contrast to the previous findings, the results obtained here suggest a 5-LO-independent LPS effect. Furthermore, the wildtype MM6 cells displayed an enhanced amount of 5-LO protein upon LPS stimulation (see chapter 2.1).

A possible explanation for the differing results is the usage of different types of MM6 cells. *Friederike Scholl* utilized MM6 cells transfected with non-target control shRNA or 5-LO knockdown shRNA, whereas wildtype and 5-LO knockout MM6 cells were used for the recent project. The 5-LO knockdown still expresses small amounts of functional 5-LO protein, while 5-LO knockout cells do not express any 5-LO at all. Experiments performed with both control and 5-LO knockdown MM6 cells within the course of this thesis resulted in similar, but less pronounced, effects compared to the wildtype and 5-LO knockout cells (see chapter 2.5). Therefore, the small difference in 5-LO expression seems to cause a much stronger, or even different, modulation of the miRNA processing.

3.4 Outlook

The present thesis characterizes a novel mechanism regulating the miRNA biosynthesis on the transcriptional and post-transcriptional level, unveiling the possibility to obtain a precise regulation of clustered miRNAs through divergent modulation at multiple levels by a single determinant within a pathway. By describing how 5-LO and inflammatory stimuli alter miRNA expression profiles, further proof is provided for the extensive and complex interrelation between posttranscriptional gene silencing and inflammatory processes.

However, further investigations are indispensable to detect more miRNAs regulated by 5-LO. Analyzing various miRNAs controlled by 5-LO will possibly enable the uncovering of determinants (e.g. sequence homology or similarity of secondary structures) defining which miRNAs are regulated by 5-LO, and which are not. More studies are also needed to further investigate 5-LO's counteracting effects on the different regulatory levels in order to gain deeper insights into the interplay between the opposed regulated transcriptional and processing levels, as well as to clarify whether more factors other than 5-LO are part of this complex regulatory network. Additionally, more efforts must be undertaken in order to better understand the noncanonical functions of 5-LO as well as how the inflammatory enzyme acts as a transcriptional regulator.

In general, the regulators of the posttranscriptional gene expression, such as miRNAs and siRNAs, are promising drug candidates for the treatment of severe diseases, namely cancer and inflammatory disorders. Clarification of the underlaying basic mechanisms of pathological conditions within the miRNA signaling will simplify the development of safe and efficient drugs. Thus, the findings gained within the course of this thesis, which shed some light on 5-LO's role within the miRNA pathway, could potentially be a starting point for the development of innovative drug therapies in the future.

4 Materials and methods

4.1 Materials

In the following, the materials and devices used for the work presented in this thesis are listed. Water refers to purified water from a Purelab flex 2 purification machine (ELGA LabWater). Oligonucleotides (desalted, lyophilized) were purchased from Sigma-Aldrich (Merck). If necessary, buffers were autoclaved (121°C, 2 bar, 20 min) or filtrated (pore size 0.22 µm) for sterilization.

4.1.1 Chemicals

Table 4.1 Chemicals

Name	Supplier
[γ-^{32}P] ATP	Hartmann Analytics, Braunschweig
Acetone	AppliChem, Darmstadt
Agarose	Carl Roth GmbH, Karlsruhe
Ammonium acetate	Carl Roth GmbH, Karlsruhe
Arachidonic acid	Cayman Chemical (Biomol), Hamburg
AUDA	Cayman Chemical (Biomol), Hamburg
Bovine serum albumin (BSA)	New England Biolabs, USA
Bradford reagent	Bio-Rad Laboratories, USA
Calcitriol	Sigma-Aldrich (Merck), Darmstadt
Calcium chloride ($CaCl_2$)	AppliChem (Darmstadt, Germany)
Ca^{2+}-ionophore (A23187)	Sigma-Aldrich (Merck), Darmstadt
Chloroform	Carl Roth GmbH, Karlsruhe
CJ13610	Goethe-University Frankfurt
DAPI (4',6-diamidino-2-phenylindole)	Life Technologies GmbH, Darmstadt
Dithiothreitol (DTT)	Roche, Switzerland
Ethylenediaminetetraacetic acid (EDTA)	Carl Roth GmbH, Karlsruhe
Ethanol	Carl Roth GmbH, Karlsruhe
FCS	Life Technologies GmbH, Darmstadt
FITC (5/6- fluorescein isothiocyanate)	Thermo Fisher Scientific, USA
Formamide	Carl Roth GmbH, Karlsruhe
L-glutamine	BioChem GmbH, Karlsruhe
Goat serum	Invitrogen, Darmstadt
Hank's buffered salt solution (HBSS)	Life Technologies GmbH, Darmstadt
Human serum AB	Lonza, Switzerland
Diflapolin	University Innsbruck, Austria
Insulin	Sigma-Aldrich (Merck), Darmstadt
Isopropanol	Carl Roth GmbH, Karlsruhe
Lipopolysaccharide (LPS) from *E.coli* 0111:B4	Sigma-Aldrich (Merck), Darmstadt
Magnesium acetate	Carl Roth GmbH, Karlsruhe
Magnesium chloride	Carl Roth GmbH, Karlsruhe
MEM non-essential amino acids	Sigma-Aldrich (Merck), Darmstadt
Methanol	Fisher Scientific, Schwerte
MK886	Cayman Chemical (Biomol), Hamburg
Mowiol	Calbiochem, Bad Soden

N-propyl gallate	AppliChem, Darmstadt
NTPs (ATP, CTP, GTP, UTP)	PeqLab, Erlangen
Odyssey blocking buffer	LI-COR Bioscience, USA
Oxaloacetate	Sigma-Aldrich (Merck), Darmstadt
Paraformaldehyde	AppliChem, Darmstadt
Penicillin streptomycin solution	GE Healthcare Life Science, Freiburg
PGB_1	Cayman Chemical (Biomol), Hamburg
PMA	Sigma-Aldrich (Merck), Darmstadt
Polyacrylamide (rotiphorese gel 40, 19:1)	Carl Roth GmbH, Karlsruhe
RPMI 1640 medium	Sigma-Aldrich (Merck), Darmstadt
Sodium acetate	Carl Roth GmbH, Karlsruhe
Sodium carbonate	Carl Roth GmbH, Karlsruhe
Sodium bicarbonate	Carl Roth GmbH, Karlsruhe
Sodium dodecyl sulfate	Carl Roth GmbH, Karlsruhe
Sodium pyruvate	GE Healthcare Life Science, Freiburg
Spermidine	Sigma-Aldrich (Merck), Darmstadt
Trifluoroacetic acid (TFA)	AppliChem, Darmstadt
TK04a	Karolinska Institute, Sweden
T-PER tissue protein extraction reagent	Life Technologies GmbH, Darmstadt
Transforming growth factor β (TGF-β)	PeproTech, UK
Tris	Carl Roth GmbH, Karlsruhe
Triton X-100	Carl Roth GmbH, Karlsruhe
TRIzol	Invitrogen, Darmstadt
Tween 20	Sigma-Aldrich (Merck), Darmstadt
Urea	Carl Roth GmbH, Karlsruhe
Zileuton	Sequoia Research Products, UK
Zymosan A (from *S. cerevisiae*)	Sigma-Aldrich (Merck), Darmstadt

4.1.2 Buffers

Table 4.2 Buffers

Name	Concentrations
PBS (pH 7.4)	
Water	
Dulbecco's Buffer Substance	9.55 g/L
PBS-T	
PBS (pH 7.4)	
Tween 20	0.1% (v/v)
Acidified PBS	
PBS (pH 7.4)	500 µL
HCl 1 N	30 µL

PG-buffer	
PBS (pH 7.4)	
Glucose	1 g/L
Tris-HCl (pH 8.0/pH 7.5)	
Water	
Tris	121.14 g/L
HCl 1 M	Adjust to pH 8.0 or pH 7.5

4.1.3 Antibodies and enzymes

Table 4.3 Antibodies and enzymes

Name	Supplier
5-LO (human, wildtype or 5-LO_3W)	Goethe-University Frankfurt
5-LO antibody, 6A12	Goethe-University Frankfurt
5-LO antibody, C49G1	Cell Signaling Technology, USA
Alkaline phosphatase	Roche, Switzerland
Dicer 1650-1912 fragment (human)	Karolinska Institute, Sweden
Dicer antibody, A301-936A	Bethyl Laboratories, USA
EcoRI	New England Biolabs, USA
Fast SYBR Green PCR Master Mix	Qiagen, Hilden
Green fluorescent Alexa Fluor 488 anti-mouse II antibody	Invitrogen, Darmstadt
HindIII	New England Biolabs, USA
IRDye conjugated secondary antibody	LI-COR Bioscience, USA
Mouse anti 5-LO	Goethe-University Frankfurt
NcoRI	New England Biolabs, USA
Polynucleotide kinase	Roche, Switzerland
Power SYBR Green PCR Master Mix	Qiagen, Hilden
Red fluorescent Alexa Fluor 555 anti-mouse II antibody	Invitrogen, Darmstadt
RNase T1	Thermo Fisher Scientific, USA
T7 polymerase	New England Biolabs, USA
TURBO DNase	Invitrogen, Darmstadt

4.1.4 Devices

Table 4.4 Devices

Name	Supplier
1409 liquid scintillation counter	Wallac (LKB Instruments), Australia
2100 Bioanalyzer	Agilent, USA
7300 Real-Time PCR System	Applied Biosystems, USA
AxioCam MR camera	Carl Zeiss Jena GmbH, Jena
Axiovert 200 M Microscope	Carl Zeiss Jena GmbH, Jena
Benchtop Centrifuge Micro Star 17	VWR International, Darmstadt
Consort EV243 power supply	Wolflabs, UK
Eppendorf Centrifuge 5424R	Eppendorf AG, Hamburg
Eppendorf ThermoStat Plus	Fisher Scientific, Schwerte
Filtropur S 0.2	Sarstedt, Nümbrecht
Heraeus Multifuge X3R Centrifuge	Thermo Fisher Scientific, USA
Heating block	VWR International, Darmstadt
HPLC System LaChrome Elite®	VWR International, Darmstadt
NanoDrop ND-1000	PeqLab, Erlangen
NextSeq 500	Illumina, USA
Nova-Pak C18 Radial-Pak Column	Waters, Eschborn
Odyssey Infrared Imaging System	LI-COR Bioscience, USA
Peqstar XS PCR Cycler	PeqLab, Erlangen
pH-meter 766 calimatic	Knick, Berlin
Plan Neofluar X100/1.30 Pol (DIC III) objective	Carl Zeiss Jena GmbH, Jena
Purelab flex 2	ELGA LabWater, Celle
StepOnePlus Real-Time PCR System	Applied Biosystems, USA
T100 Thermal Cycler	Bio-Rad Laboratories, USA
Tecan Infinite M 200	Tecan Group, Switzerland

4.1.5 Others

Table 4.5 Others

Name	Supplier
Clean-Up Extraction Columns	UCT, USA
Duolink In Situ Red Starter Kit Mouse/Rabbit	Sigma-Aldrich (Merck), Darmstadt
High Capacity RNA-to-cDNA kit	Applied Biosystems, USA
HyBond ECL nitrocellulose membrane	Amersham, UK
miRNeasy Mini Kit	Qiagen, Hilden
miScript Primer Assay	Qiagen, Hilden
miScript II RT kit	Qiagen, Hilden
miScript SYBR Green PCR kit	Qiagen, Hilden
Poly-D-Lysine coated cover slips	Kleinfeld Labortechnik GmbH, Gehrden
RNase-Free DNase Set	Qiagen, Hilden
Small RNA-Seq Library Prep Kit	Lexogen, USA
Standard microscope slides	Carl Roth GmbH, Karlsruhe

4.2 Cell lines

Mono Mac 6 (MM6) cells were originally purchased from DSMZ (Deutsche Sammlung von Mikroorganismen und Zellkulturen; DSMZ no.: ACC 124).

The CRISPR-Cas system was used[96] to generate a knockout of the 5-LO gene (5-LOΔ) in MM6 cells. The experimental procedure was carried out by Duran Sürün as previously described[112]. The establishment of the cell line and its validation via western blot and sequencing was performed by Marius Kreiß as described in his master thesis[97]. Only cell clones expressing no 5-LO protein and exhibiting a frameshift on both chromosomes were used for further experiments.

MM6 cells were also transfected with lentiviral constructs expressing a shRNA against 5-LO or a shRNA against a non-target control in order to obtain 5-LO knockdown (5-LOkd) and control knockdown (ctrl) MM6 cells. The cells were kindly provided by the Rådmark group[77].

4.3 Cell culture

MM6 cells were grown in glutamine containing RPMI 1640 medium, supplemented with 10% (v/v) heat inactivated FCS, 10 µg/mL insulin, 1x MEM non-essential amino acids, 1 mM sodium pyruvate, 1 mM oxaloacetate, 100 U/mL penicillin, and 100 µg/mL streptomycin at 37°C in a humidified atmosphere with 5% CO_2. Optimal growth conditions are at a density of 0.3 Mio cells per mL. The cell density should not exceed 1 Mio cells per mL.

Wildtype and 5-LOΔ MM6 cells or ctrl and 5-LOkd MM6 cells were stimulated with 1 ng/mL TGF-β and 50 nM calcitriol for differentiation experiments. If indicated, the cells were also stimulated with 1 µg/mL LPS or 25 ng/mL zymosan for the entire time period or only for the last 24 h. Additionally, the differentiated wildtype MM6 cells were treated twice (day 0 and after 48 h) with 1 µM Zileuton, 0.1 µM MK886, or 0.1 µM or 1 µM CJ13610, if indicated. Unstimulated wildtype MM6 cells were kept at a density of 0.3 Mio cells per mL, while stimulated MM6 cells were seeded at 0.2 Mio cells per mL. The cells were harvested after 96 h.

4.4 RNA isolation

Stimulated MM6 cells (see chapter 4.2) were spun down by centrifugation (2000 rpm, 5 min) and the cell pellet was washed once with PBS. Then, the cells were lysed by incubation with TRIzol at room temperature for 5 min. After adding chloroform, the samples were vortexed, incubated on ice for 15 min, and centrifuged (13300 rpm, 4°C, 15 min). The upper aqueous phase was transferred to a new tube. In order to precipitate the RNA, the same solution volume of isopropanol and 0.1x solution volume

of 3 M sodium acetate pH 6.5 were added. The mixture was then incubated on ice for 15 min and afterwards spun down by centrifugation (13300 rpm, 4°C, 15 min). The RNA pellet was washed once with 70% (v/v) ethanol and resuspended in water. Then, DNase digestion was performed using TURBO DNase according to the manufacturer's protocol. Total RNA was precipitated again by adding 5x solution volume of ethanol and 0.1x solution volume of 3 M sodium acetate pH 6.5. The mixture was incubated at -20°C overnight and spun down by centrifugation (13300 rpm, 4°C, 30 min). The RNA pellet was washed once with 70% (v/v) ethanol and resuspended in water. The miRNeasy Mini Kit including DNase digestion was also used according to the manufacturer's protocol to isolate total RNA. The quality and the amount of total RNA was assessed via agarose gel electrophoresis and NanoDrop.

4.5 Sequencing of small noncoding RNAs

The Small RNA-Seq Library Prep Kit for Illumina (Lexogen) was used according to the manufacturer's protocol to generate the cDNA libraries from 1000 ng of total RNA. The libraries were mixed equimolarly and restricted to a size of 5-135 bp by agarose gel electrophoresis. The quality and purity of the RNA and cDNA was verified using the 2100 Bioanalyzer (Agilent). The single end sequencing was carried out on a NextSeq500 platform (Illumina) with a read length of 75 bp. The web tool omiRas[101] was used for alignment of the sequences to the human genome and for differential expression analysis. The experimental procedure described here was carried out by Marius Kreiß. The bioinformatical analysis was performed by Ann-Kathrin Häfner.

4.6 cDNA synthesis

For analysis of miRNAs 1000 ng of total RNA was reverse transcribed using the miScript II RT kit. For analysis of mRNA and primary miRNA levels the High Capacity RNA-to-cDNA kit was used for reverse transcription of 1000 ng total RNA. Both kits were handled according to the manufacturer's protocol.

4.7 Real-time quantitative PCR

Mature miRNA levels were analyzed using the miScript SYBR Green PCR kit according to the manufacturer's protocol. U6 or miR-20a-5p served as an endogenous control. If indicated, the mature miRNA levels were normalized to the corresponding primary miRNA levels in addition to normalizing to the endogenous control and the control sample.

The Power SYBR Green PCR Master Mix or the Fast SYBR Green PCR Master Mix and the primers listed below were used to analyze mRNA and primary miRNA levels according to the manufacturer's protocols. β-actin or GAPDH (see Table 4.6) served as an endogenous control. All quantitative PCR experiments were carried out on a 7300 or a StepOnePlus device.

Table 4.6 Primer sequences

Name	Sequence (5'→3')
5-LO_fwd	TGGCATCTGGGTGCAGTGT
5-LO_rev	GCCCAGGAACAGCTCGTTT
β-actin_fwd	CGGGACCTGACTGACTACCTC
β-actin_rev	CTTCTCCTTAATGTCACGCACG
Dicer_fwd	TGGAGACAGTCTGGCAGGTGTA
Dicer_rev	TCCCGTCGTAAGTTCTCTCAGC
GAPDH_fwd	TGAGAACGGGAAGCTTGTCA
GAPDH_rev	ATCGCCCCACTTGATTTTGG
pri-146a_fwd	GCCGATGTGTATCCTCAGCT
pri-146a_rev	AGAGCCTGAGACTCTGCCTT
pri-146b_fwd	CAATGCCCTGTGGACTCAGT
pri-146b_rev	AAGATGTGGGCCTGCAGAAG
pri-21_fwd	GTGACATCTCCATGGCTGTACCA
pri-21_rev	CAAAATGTCAGACAGCCCATCGAC
pri-155_fwd	AGGGAAACTGAAAGGCTATG
pri-155_rev	TGAACCTAGATTTGGGACTTC
pri-let-7a-1_fwd	GTTTTGGGTGGTCTTGGAGA
pri-let-7a-1_rev	TGAGGGCAAAGCTGAAATCT
pri-let-7a-2_#1_fwd	AGGGGAAGGGCAGTAAGTGT
pri-let-7a-2_#1_rev	TGACCCCCAGAATAAGAACG
pri-let-7a-2_#2_fwd	TACCCATTCCATTTCCTCCA
pri-let-7a-2_#2_rev	TTGAGGCTCCCTCAGAGTGT
pri-let-7a-2_#3_fwd	GTGCTGGAGCAGGAGATAGG
pri-let-7a-2_#3_rev	CAGCCTTTACTGGGCAAAAC
pri-let-7a-3_fwd	GTCACAGGGCTGCGAGTATT
pri-let-7a-3_rev	TGTCTGCCTTCAGATTGTGC
pri-let-7c_fwd	TGAGGCTGAATGCAATTGACT
pri-let-7c_rev	GGCAGCCATACACCTAAGGG
pri-let-7e_fwd	CCTCCTTCCCCTGAAATCTG
pri-let-7e_rev	GGGGCAGAGACCTAGAAAGC
pri-let-7f-2_fwd	GGACAGAGTTGCAGTCAGGA
pri-let-7f-2_rev	CGACTGGCTCTGTTCAGGTT

4.8 Immunofluorescence microscopy assay

Stimulated MM6 cells (see chapter 4.2) were seeded onto Poly-D-Lysine coated cover slips (10^6 cells per well). After culturing the cells for at least 30 min (37°C; 5% CO_2), 2.5 µM Ca^{2+}-ionophore A23187 and 0.1 mM calcium chloride were added. The cells were spun down by centrifugation (2000 rpm; 5 min) and fixed by treatment with 4% paraformaldehyde for 20 min at room temperature. Then, the cells were washed with PBS twice and permeabilized with acetone for 4 min. After two washing steps with PBS, the cells were also permeabilized with 0.25% triton X-100 for 20 min followed by one washing step with PBS.

The cells were incubated with primary antibodies (diluted 1:100 in goat serum) overnight or for the weekend at 4°C. The following combination of primary antibodies was used: mouse monoclonal anti 5-LO (Steinhilber lab, Goethe-University Frankfurt) and rabbit polyclonal anti Dicer (Bethyl lab/Dicer A301-936A).

Then, the cells were washed several times with PBS and incubated with the following secondary antibodies (diluted 1:1000 in PBS) for 30 min at room temperature and protected from light: green fluorescent Alexa Fluor 488 anti rabbit II antibody and red fluorescent Alexa Fluor 555 anti-mouse II antibody. After again washing the cells several times with PBS, the cover slips were mounted on slides with 20 µL Mowiol containing 2.5% n-propyl gallate and DAPI. Then, the slides were examined under the fluorescence microscope (Axiovert 200M microsope with Plan Neofluar X100/1.30 Pol (DIC III) objective and AxioCam MR camera) and analyzed with the related software (Axio Vision 4).

4.9 Proximity ligation assay

Stimulated MM6 cells (see chapter 4.2) were seeded onto coated cover slips, fixed with paraformaldehyde and permeabilized with acetone and triton X-100 as described in chapter 4.6. However, the cells were stimulated neither with Ca^{2+}-ionophore A23187 nor with calcium chloride.

The cells were incubated with following primary antibodies (diluted 1:100 in goat serum) overnight or for the weekend at 4°C: mouse monoclonal anti 5-LO (Steinhilber lab, Goethe-University Frankfurt) and rabbit polyclonal anti Dicer (Bethyl lab/Dicer A301-936A). Then the Duolink® In Situ Red Starter Kit Mouse/Rabbit was performed according to the manufacturer's protocol. In short, the cells are incubated with Duolink® PLA Probes, followed by ligation, amplification, and final washing steps. Prior to examining the cells under the fluorescence microscope (Axiovert 200M microsope with Plan Neofluar X100/1.30 Pol (DIC III) objective and AxioCam MR camera), the cover slips were mounted on slides as described in chapter 4.6. For analysis of the slides, the related software (Axio Vision 4) was used.

4.10 FITC-labeled opsonized zymosan

First, zymosan was heated in a boiling water bath for 20 min. Then, the heated zymosan was sonicated (20 s with 11 µm peak to peak amplitude) to disintegrate agglomerates. After washing twice with HBSS buffer, the zymosan was resuspended in HBSS buffer at a concentration of 20 mg/mL. The pretreated zymosan was stored at -80°C.

The pretreated zymosan was thawed and precipitated by centrifugation (400 x g, 10 min). After resuspending in 0.1 M carbonate buffer pH 9.5, the suspension was sonicated to get a homogeneous distribution. The sonicated pretreated zymosan was incubated with 5 µg/mL FITC in 0.1 M carbonate buffer pH 9.5 at 37°C for 30 min. Then, the FITC-labeled zymosan was precipitated by centrifugation (400 x g, 10 min) and the precipitate was washed twice with 0.1 M carbonate buffer pH 9.5 and twice with HBSS buffer.

For opsonization, the FITC-labeled zymosan was incubated with 65% serum dilution (diluted in HBSS buffer) at 37°C for 60 min (20 mg FITC-labeled zymosan per mL serum dilution). After precipitation by centrifugation (400 x g, 10 min) and after washing twice with HBSS buffer, the opsonized FITC-labeled zymosan was resuspended in HBSS buffer at a concentration of 20 mg/mL.

Then, MM6 wildtype cells ($0.2x10^6$ cells/mL) were differentiated with 1 ng/mL TGF-β and 50 nM calcitriol for four days. Additionally, the cells were stimulated with 25 µg/mL FITC-labeled opsonized zymosan. Samples were collected after 0, 0.5, 1, 3, 6, 24, 48, 72, and 96 h. The samples were seeded onto Poly-D-Lysine coated cover slips. After spinning down the cells by centrifugation (2000 rpm, 5 min), the cover slips were mounted on slides with 20 µL Mowiol containing 2.5% n-propyl gallate and DAPI. The slides were examined under the fluorescence microscope (Camera: AxioCam MR, Carl Zeiss Jena) and analyzed with the related software (Axio Vision 4).

4.11 Cell lysis

Stimulated MM6 cells (see chapter 4.2) were lysed on ice for 30 min in 50 µL T-PER tissue protein extraction reagent per 1 Mio cells. Then, cells were spun down (13300 rpm, 5 min, 4°C) and the supernatant was used for protein measurement and further experiments.

4.12 Protein measurement

The protein concentration was determined by Bradford assay. 190 µL Bradford reagent was added to 10 µL cell lysate (diluted 1:20 in water) (see chapter 4.9). The absorption at 595 nm was measured using

a Tecan Infinite M 200. For calculation of the protein concentration, a standard curve with BSA concentrations of 50-500 µg/mL was also determined.

4.13 SDS-PAGE and Western blot

60-120 µg cell lysate (see chapter 4.9) was separated by 12% sodium dodecyl sulfate polyacrylamide gel electrophoresis (SDS-PAGE) and transferred to a HyBond ECL nitrocellulose membrane. After blocking with Odyssey blocking buffer at room temperature for 1 h, the membrane was incubated with the primary antibody (rabbit monoclonal anti 5-LO (Cell signaling Technology, 5-LO C49G1) or rabbit polyclonal anti Dicer (Bethyl lab/Dicer A301-936A)) at 4°C overnight. Then, the membrane was washed with PBS and incubated with the IRDye conjugated secondary antibody (anti-mouse or anti-rabbit) at room temperature for 45 min. After washing the membrane with PBS-T, the Odyssey Infrared Imaging System was used for visualization and quantitative analysis. β-actin was used as the reference protein.

4.14 5-LO activity assay

Stimulated MM6 cells (see Chapter 4.2) were harvested by centrifugation (2000 rpm; 4°C; 4 min) and resuspended in PG-buffer (PBS/0.1% glucose). Then, 1 mM calcium chloride was added and cells (10^6 cells in total) were pre-incubated with 100 nM PMA and inhibitors (3 µM Zileuton, 0.3 µM MK886, 1 µM diflapolin, 5 µM AUDA, or 1 µM TK04a), if indicated, at 37°C for 10 min. Subsequently, the cells were stimulated with 2.5 µM Ca^{2+}-ionophore A23187 and 10 µM arachidonic acid at 37°C for 10 min. The reaction was stopped on ice by adding 1 mL methanol. After adding 530 µL acidified PBS and 200 ng PGB_1 as internal standard, the samples were subjected to solid phase extraction.

Samples were centrifugated (2000 rpm; 4°C; 10 min) and the supernatant was transferred to the Clean-Up Extraction Columns (UCT (Bristal, PA, USA)), which were previously equilibrated with water. The columns were washed with 1 mL water and 1 mL methanol (25%). 5-LO metabolites were eluted with 300 µL methanol (100%). After adding 120 µL water, samples were analyzed by RP-HPLC.

The 5-LO metabolites were separated on a C18 Column (Nova-Pak C18 Radial-Pak Column, 60 Å, 4 µm, 5 mm X 100 mm, 1/pkg; Waters (Eschborn, Germany)) isocratically by running the HPLC with methanol/water/TFA (73/27/0.007) at a speed of 1.2 mL/min. The separated metabolites were subsequently subjected to UV detection at 280 nm (PGB_1, leukotrienes) and 235 nm (15/12/5-H(p)ETE). The analytes were eluted in the following order: PGB_1 – trans isomer of LTB_4 – LTB_4 – LTC_4 – 15/12/5-H(p)ETE.

4.15 Design and cloning of pHDV_pre-miR

The pHDV_pre-miR plasmid (see Fig. 4.1) was used to produce precursor miRNA. The transcription is controlled by a T7 promotor, that requires at least one guanine residue at the beginning of the transcribed sequence. Therefore, the first nucleotide of the used sequences was changed to a guanine residue, if necessary. The corresponding nucleotide was also adjusted so that the secondary structure of the pre-miRNA remained unaffected.

The phosphorylated oligonucleotides pre-let-7e_fwd and pre-let-7e_rev, pre-miR-125a_fwd and pre-miR-125a_rev, pre-miR-99b_fwd and pre-miR-99b_rev, respectively, were cloned into the pHDV backbone, using the restriction enzymes EcoRI and NcoRI, straight after hybridization. The oligonucleotides (see Table 4.7) were designed in such a way that the sticky ends fit perfectly to EcoRI and NcoRI. Sequencing was used to check whether the sequence is correct.

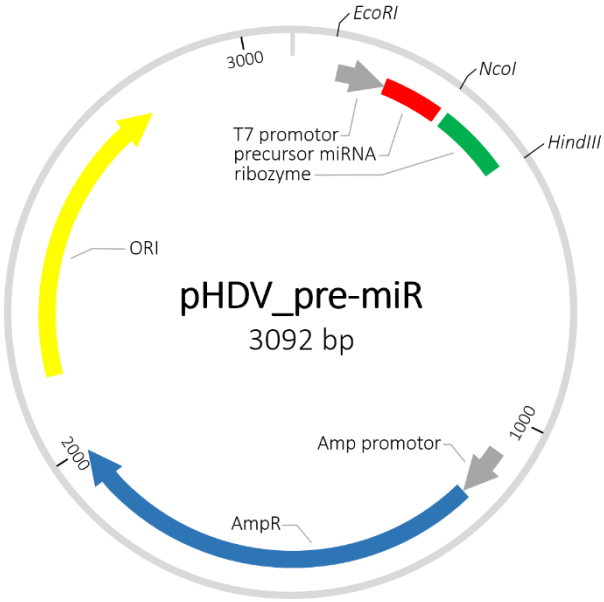

Figure 4.1 Map of pHDV_pre-miR plasmid
The genes located on the pHDV_pre-miR plasmid are indicated as arrows: T7 promotor (grey), precursor miRNA (red), ribozyme (green), ampicillin resistance (blue) as well as its promotor (grey), and the origin of replication (yellow). The restrictions sites for EcoRI, NcoI, and HindIII are also displayed.

Table 4.7 Sequences of the oligonucleotides used for the cloning of the pHDV_pre-miR plasmid

Name	Sequence (5'→3')
pre-miR-125a_fwd	AATTCTAATACGACTCACTATAGCCCTGAGACCCTTTAACCTGTGAGGAC ATCCAGGGTCACAGGTGAGGTTCTTGGGATCCGCCGGC
pre-miR-125a_rev	CATGGCCGGCGGATCCCAAGAACCTCACCTGTGACCCTGGATGTCCTCA CAGGTTAAAGGGTCTCAGGGCTATAGTGAGTCGTATTAG
pre-miR-99b_fwd	AATTCTAATACGACTCACTATAGACCCGTAGAACCGACCTTGCGGGGCC TTCGCCGCACACAAGCTCGTGTCTGTGGGTGCGGCCGGC
pre-miR-99b_rev	CATGGCCGGCCGCACCCACAGACACGAGCTTGTGTGCGGCGAAGGCCC CGCAAGGTCGGTTCTACGGGTCTATAGTGAGTCGTATTAG
pre-let-7e_fwd	AATTCTAATACGACTCACTATAGGAGGTAGGAGGTTGTATAGTTGAGGA GGACACCCAAGGAGATCACTATACGGCCTCCTAGCTTTCCGCCGGC
pre-let-7e_rev	CATGGCCGGCGGAAAGCTAGGAGGCCGTATAGTGATCTCCTTGGGTGT CCTCCTCAACTATACAACCTCCTACCTCCTATAGTGAGTCGTATTAG

4.16 *In vitro* transcription and purification of pre-miRNA

100 µg linearized plasmid was mixed with 200 mM Tris-HCl (pH 8.0), 20 mM magnesium acetate, 20 mM DTT, 2 mM spermidine, 6.25 µL T7 polymerase, and 4 mM each of ATP, CTP, GTP, and UTP. The mixture was incubated at 37°C overnight. The plasmid was linearized using the restriction enzyme HindIII.

For purification, the produced RNA was ethanol-precipitated, dissolved in formamide loading dye containing 25 mM EDTA, and loaded on a 12% denaturing polyacrylamide gel containing 8 M urea. The product was visualized by UV shadowing, excised, eluted overnight in 300 mM sodium acetate (pH 6.5), and ethanol-precipitated. The purified RNA (see Table 4.8) was dissolved in a suitable amount of water and molarity was determined.

Table 4.8 Sequences of the pre-miRNAs

Name	Sequence (5'→3')
pre-miR-125a	GCCCUGAGACCCUUUAACCUGUGAGGACAUCCAGGGUCACAGGUGA GGUUCUUGGGAUCC
pre-miR-99b	GACCCGUAGAACCGACCUUGCGGGGCCUUCGCCGCACACAAGCUCGU GUCUGUGGGUGCG
pre-let-7e	GGAGGUAGGAGGUUGUAUAGUUGAGGAGGACACCCAAGGAGAUCA CUAUACGGCCUCCUAGCUUUCC

4.17 Phosphorylation and dephosphorylation of the pre-miRNA's 5' end

Dephosphorylation of 20 pmol pre-miRNA was performed using alkaline phosphatase according to the manufacturer's protocol. In order to generate radioactive labelled pre-miRNA, phosphorylation was carried out using 10 pmol of previously dephosphorylated pre-miRNA, 3 µL (10 mM) of [γ-^{32}P] ATP, and polynucleotide kinase according to the manufacturer's instructions.

To purify the radioactive labelled pre-miR, it was precipitated by adding 0.5x solution volume of 7.5 M ammonium acetate and 2.5x solution volume of ethanol. Then, the mixture was incubated on ice for 10 min and spun down by centrifugation (13300 rpm; 10 min). The pellet was washed with 70% (v/v) ethanol twice and resuspended in a suitable amount of water.

4.18 *In vitro* Dicer Assay

The *in vitro* Dicer assay was performed according to *Dincbas-Renqvist et al.*[32]. 0.05 µM recombinant human Dicer 1650-1912 mutant protein was preincubated at 21°C for 5 min without or with increasing amounts (0.05-5 µM) of human wildtype 5-LO or mutant 5-LO_3W. After adding 40000 counts of radioactive labelled pre-miRNA (see chapter 4.15), the samples were incubated at 37°C for 1 h. The control sample was incubated in the absence of Dicer 1650-1912 and 5-LO. The reaction was carried out in a buffer containing 20 mM Tris-HCl (pH 7.5), 5 mM magnesium chloride, 1 mM DTT, 1 mM ATP, and 15 µM BSA. To stop the reaction, formamide loading dye containing 25 mM EDTA was added and the sample was heated up to 95°C for 5 min.

For generating size markers, radioactive labelled pre-miRNA was incubated under alkaline conditions at 96°C for 2 min or 6 min (pre-miR-125a/pre-miR-99b: 2 min; pre-let-7e: 6 min) in 50 mM sodium carbonate (pH 9.0). A marker enabling the identification of guanine residues was generated by incubating radioactive labelled pre-miRNA at 55°C for 6 min with 20 units of RNase T1 at denaturing conditions. Then, the RNA samples were ethanol-precipitated and dissolved in formamide loading dye containing 25 mM EDTA.

All reactions were applied on a 10% denaturing polyacrylamide gel containing 8 M urea and separated by gel electrophoresis. Then, the gels were dried and analyzed by phosphorimaging.

5 Summary

5.1 Summary

MicroRNAs (miRNA) are prominent players of the gene silencing pathway that control the majority of human protein-coding genes and thus are involved in almost every physiological process. The biosynthesis of these important posttranscriptional regulators of gene expression needs to be tightly controlled. In addition to the transcriptional regulation of miRNAs, it becomes more and more evident that the miRNA processing can also be modulated. For instance, the enzyme 5-lipoxygenase (5-LO), which is mainly known for its catalyzing properties in the biosynthesis of inflammatory leukotrienes and specialized pro-resolving mediators, and whose expression is also controlled by miRNAs, interferes with the miRNA pathway through its interaction with Dicer, a key enzyme of the miRNAs' processing. Thus, this thesis aims to further investigate the interaction of 5-LO and Dicer, as well as its functional impact on the miRNA processing.

The 5-LO binding to Dicer was previously characterized using *in vitro* methods. Performing proximity ligation assays, that allow monitoring of endogenous protein complexes in their natural environment, demonstrated an *in situ* interaction of the target proteins in Mono Mac 6 cells, a human monocytic cell line that exerts a heavily increased 5-LO protein expression upon stimulation with TGF-β, calcitriol, and LPS or zymosan. Sequencing of small noncoding RNAs identified the clustered miRNAs miR-99b, let-7e, and miR-125a as potential 5-LO targets. Real-time quantitative PCR experiments were used to show that 5-LO acts both as a transcriptional as well as a posttranscriptional regulator by modifying both processing levels in opposing directions. More precisely, 5-LO exerts stimulatory effects on the transcription of the primary miRNA encoding for the miR-99b/let-7e/miR-125a cluster, but in turn also exerts inhibitory effects on the Dicer-mediated cleavage of the let-7e precursor. The processing of the other clustered miRNAs, namely miR-99b and miR-125a, is unaffected or just slightly enhanced, revealing a pre-miRNA specific and dose-dependent 5-LO effect, which was confirmed by performing *in vitro* Dicer assays. The mutually overlapping effects result in an upregulation of mature miR-99b and miR-125a with simultaneously unchanged let-7e levels. Since the cluster members exert different biological functions, especially in the context of stem cells, these observations might describe a mechanism to modulate the expression of each member within miRNA clusters individually.

It is worth noting that LPS and zymosan share the exceptional characteristic of contrastingly modulating one pathway at different regulatory levels. Real-time quantitative PCR experiments were utilized to demonstrate that whenever the TLR activators LPS or zymosan stimulate the transcription of a miRNA they also inhibit its subsequent processing, resulting in increased levels of the NF-κB-dependent TLR-response miRNAs miR-146a, miR-21, miR-125a, and let-7e, all of which function as negative feedback regulators of the TLR signaling. This precise regulation of the miRNA processing by LPS and zymosan, which seems to be independent of 5-LO, provides further evidence for the tight interconnections between miRNAs and the innate immune responses mediated via TLR signaling.

In conclusion, the opposing modulation at multiple levels by a single determinant within one pathway could potentially be a generally valid principle which allows fine tuning of the miRNA expression through opposing effects that dampen each other. Furthermore, the findings gained within the course of this study contribute to characterizing 5-LO's role within the miRNA pathway.

5.2 Zusammenfassung

MicroRNAs (miRNA) sind bedeutsame Akteure des Gen-Silencing Signalwegs, da sie die Mehrzahl der humanen Protein-kodierenden Gene kontrollieren und demzufolge in nahezu jeden physiologischen Prozess involviert sind. Die Biosynthese dieser wichtigen posttranskriptionellen Regulatoren der Genexpression bedarf daher einer strikten Kontrolle. Wissenschaftliche Erkenntnisse zeigen, dass nicht nur die Transkription der miRNAs reguliert werden kann, sondern auch deren Prozessierung. Beispielsweise interagiert das Enzym die 5-Lipoxygenase (5-LO), welches vor allem für seine katalytische Aktivität in der Biosynthese der inflammatorischen Leukotriene und SPMs (specialized pro-resolving mediators) bekannt ist und dessen Expression ebenfalls durch miRNAs reguliert wird, mit Dicer. Da es sich bei Dicer um ein Schlüsselenzym der miRNA-Prozessierung handelt, beeinflusst die 5-LO möglicherweise durch die Interaktion mit Dicer die Synthese der miRNAs. Die vorliegende Doktorarbeit dient dem Zweck, die Interaktion zwischen 5-LO und Dicer, sowie deren funktionalen Einfluss auf die miRNA-Biosynthese näher zu untersuchen

Die Bindung von 5-LO zu Dicer wurde bereits unter Verwendung von *in vitro* Methoden charakterisiert. Die Durchführung von Proximity Ligation Assays, eine Methode, welche das Monitoring endogener Proteinkomplexe in ihrer natürlichen Umgebung ermöglicht, bestätigte eine *in situ* Interaktion zwischen den Zielproteinen in Mono Mac 6 (MM6) Zellen. Bei den MM6-Zellen handelt es sich um eine humane monozytische Zelllinie, welche einen starken Anstieg der 5-LO-Proteinexpression nach Stimulierung mit TGF-β, Calcitriol und LPS oder Zymosan zeigt. Die Sequenzierung kurzer nicht-kodierender RNAs identifizierte das miRNA-Cluster miR-99b, let-7e und miR-125a als ein potenzielles Ziel der 5-LO. Durch die Durchführung der quantitativen Echtzeit-PCR konnte gezeigt werden, dass die 5-LO sowohl als transkriptioneller als auch als posttranskriptioneller Regulator agiert, indem das Enzym beide Prozessierungsebenen in unterschiedliche Richtungen modifiziert. Einerseits stimuliert die 5-LO das Primärtranskript, welches für das miR-99b/let-7e/miR-125a Cluster kodiert, andererseits inhibiert das Enzym die Dicer-vermittelte Prozessierung des let-7e Vorläufers. Die Reifung der anderen miRNAs, miR-99b und miR-125a, wird nicht beeinflusst beziehungsweise leicht stimuliert. Dies verdeutlicht, dass die 5-LO pre-miRNA-spezifische sowie dosisabhängige Effekte ausübt, welche durch die Durchführung von *in vitro* Dicer Assays bestätigt werden konnten. Die gegenläufigen und sich überschneidenden Effekte resultieren in einer Hochregulierung der reifen miRNAs miR-99b und miR-125a mit gleichzeitig unveränderten let-7e-Spiegeln. Angesichts der divergierenden biologischen Funktionen der beschriebenen miRNAs, insbesondere im Kontext von Stammzellen, beschreiben diese Beobachtungen einen Mechanismus zur individuellen Regulierung der Expression einzelner miRNAs innerhalb eines Clusters.

Es ist bemerkenswert, dass LPS und Zymosan ebenso wie 5-LO die außergewöhnliche Fähigkeit besitzen, einen Signalweg auf verschiedenen Ebenen gegenläufig zu regulieren. Die Ergebnisse quantitativer Echtzeit-PCR-Experimente zeigen, dass, wann immer die TLR-Aktivatoren LPS oder Zymosan die Transkription einer miRNA stimulieren, sie nachfolgend deren Prozessierung hemmen. Dies resultiert in einer erhöhten Expression der NF-κB-abhängigen und TLR-responsiven miRNAs miR-146a, miR-21, miR-125a und let-7e, welche als negative Feedback-Regulatoren des TLR-Signalwegs fungieren. Diese präzise und scheinbar von 5-LO-unabhängige Regulation der miRNA-Prozessierung durch LPS und Zymosan verdeutlicht die enge Verflechtung zwischen miRNAs und der über den TLR-Signalweg vermittelten angeborenen Immunantwort.

Zusammenfassend kann festgehalten werden, dass die gegensätzliche Modulation auf multiplen Ebenen durch einen einzelnen Akteur innerhalb eines Signalwegs ein allgemein gültiges Prinzip darstellen könnte, welches die Feinregulierung der miRNA-Expression durch gegenläufige Effekte, die sich gegenseitig abmildern, erlaubt. Die anhand dieser Doktorarbeit gewonnenen Erkenntnisse tragen zur Charakterisierung der Rolle der 5-LO innerhalb des miRNA-Signalwegs bei.

6 References

6 References

1. Meister, G. & Tuschl, T. Mechanisms of gene silencing by double-stranded RNA. *Nature* **431,** 343–349; 10.1038/nature02873 (2004).
2. Carthew, R. W. & Sontheimer, E. J. Origins and Mechanisms of miRNAs and siRNAs. *Cell* **136,** 642–655; 10.1016/j.cell.2009.01.035 (2009).
3. Fire, A. *et al.* Potent and specific genetic interference by double-stranded RNA in Caenorhabditis elegans. *Nature* **391,** 806–811; 10.1038/35888 (1998).
4. NobelPrize.org. Nobel Media AB 2019. MLA style: The Nobel Prize in Physiology or Medicine 2006. Available at https://www.nobelprize.org/prizes/medicine/2006/summary/ (2006).
5. Lee, R. C., Feinbaum, R. L. & Ambros, V. The C. elegans heterochronic gene lin-4 encodes small RNAs with antisense complementarity to lin-14. *Cell* **75,** 843–854 (1993).
6. Ha, M. & Kim, V. N. Regulation of microRNA biogenesis. *Nature reviews. Molecular cell biology* **15,** 509–524; 10.1038/nrm3838 (2014).
7. Kozomara, A. & Griffiths-Jones, S. miRBase. Annotating high confidence microRNAs using deep sequencing data. *Nucleic acids research* **42,** D68-73; 10.1093/nar/gkt1181 (2014).
8. U.S. National Library of Medicine. ClincalTrials.gov. database of privately and publicly funded clinical studies conducted around the world. Available at https://clinicaltrials.gov/ct2/home.
9. Rupaimoole, R. & Slack, F. J. MicroRNA therapeutics. Towards a new era for the management of cancer and other diseases. *Nature reviews. Drug discovery* **16,** 203–222; 10.1038/nrd.2016.246 (2017).
10. U.S. Food and Drug Administration. FDA approves first-of-its kind targeted RNA-based therapy to treat a rare disease. Press Announcement. Available at https://www.fda.gov/news-events/press-announcements/fda-approves-first-its-kind-targeted-rna-based-therapy-treat-rare-disease (2018).
11. European Medicines Agency. Onpattro. European public assessment report. Available at https://www.ema.europa.eu/en/medicines/human/EPAR/onpattro (2018).
12. Pharmazeutische Zeitung. Patisiran: EU-Zulassung für erstes RNAi-Medikament. Available at https://www.pharmazeutische-zeitung.de/2018-08/patisiran-eu-zulassung-fuer-erstes-rnai-medikament/ (2018).
13. Monteys, A. M. *et al.* Structure and activity of putative intronic miRNA promoters. *RNA (New York, N.Y.)* **16,** 495–505; 10.1261/rna.1731910 (2010).
14. Han, J. *et al.* The Drosha-DGCR8 complex in primary microRNA processing. *Genes & development* **18,** 3016–3027; 10.1101/gad.1262504 (2004).
15. Han, J. *et al.* Posttranscriptional crossregulation between Drosha and DGCR8. *Cell* **136,** 75–84; 10.1016/j.cell.2008.10.053 (2009).
16. Shiohama, A., Sasaki, T., Noda, S., Minoshima, S. & Shimizu, N. Molecular cloning and expression analysis of a novel gene DGCR8 located in the DiGeorge syndrome chromosomal region. *Biochemical and Biophysical Research Communications* **304,** 184–190; 10.1016/S0006-291X(03)00554-0 (2003).
17. Davis, B. N., Hilyard, A. C., Nguyen, P. H., Lagna, G. & Hata, A. Smad proteins bind a conserved RNA sequence to promote microRNA maturation by Drosha. *Molecular cell* **39,** 373–384; 10.1016/j.molcel.2010.07.011 (2010).

18. Guil, S. & Cáceres, J. F. The multifunctional RNA-binding protein hnRNP A1 is required for processing of miR-18a. *Nature structural & molecular biology* **14,** 591–596; 10.1038/nsmb1250 (2007).

19. Michlewski, G., Guil, S., Semple, C. A. & Cáceres, J. F. Posttranscriptional regulation of miRNAs harboring conserved terminal loops. *Molecular cell* **32,** 383–393; 10.1016/j.molcel.2008.10.013 (2008).

20. Trabucchi, M. *et al.* The RNA-binding protein KSRP promotes the biogenesis of a subset of microRNAs. *Nature* **459,** 1010–1014; 10.1038/nature08025 (2009).

21. Yi, R., Qin, Y., Macara, I. G. & Cullen, B. R. Exportin-5 mediates the nuclear export of pre-microRNAs and short hairpin RNAs. *Genes & development* **17,** 3011–3016; 10.1101/gad.1158803 (2003).

22. Fougerolles, A. de, Vornlocher, H.-P., Maraganore, J. & Lieberman, J. Interfering with disease. A progress report on siRNA-based therapeutics. *Nature reviews. Drug discovery* **6,** 443–453; 10.1038/nrd2310 (2007).

23. Bartel, D. P. MicroRNAs. Target recognition and regulatory functions. *Cell* **136,** 215–233; 10.1016/j.cell.2009.01.002 (2009).

24. Liu, Z. *et al.* Cryo-EM Structure of Human Dicer and Its Complexes with a Pre-miRNA Substrate. *Cell* **173,** 1191-1203.e12; 10.1016/j.cell.2018.03.080 (2018).

25. Lau, P.-W. *et al.* The molecular architecture of human Dicer. *Nature Structural and Molecular Biology* **19,** 436; 10.1038/nsmb.2268 (2012).

26. Takeshita, D. *et al.* Homodimeric structure and double-stranded RNA cleavage activity of the C-terminal RNase III domain of human dicer. *Journal of molecular biology* **374,** 106–120; 10.1016/j.jmb.2007.08.069 (2007).

27. Zhang, H., Kolb, F. A., Jaskiewicz, L., Westhof, E. & Filipowicz, W. Single processing center models for human Dicer and bacterial RNase III. *Cell* **118,** 57–68; 10.1016/j.cell.2004.06.017 (2004).

28. Ma, J.-B., Ye, K. & Patel, D. J. Structural basis for overhang-specific small interfering RNA recognition by the PAZ domain. *Nature* **429,** 318–322; 10.1038/nature02519 (2004).

29. Park, J.-E. *et al.* Dicer recognizes the 5' end of RNA for efficient and accurate processing. *Nature* **475,** 201–205; 10.1038/nature10198 (2011).

30. Heo, I. *et al.* Lin28 mediates the terminal uridylation of let-7 precursor MicroRNA. *Molecular cell* **32,** 276–284; 10.1016/j.molcel.2008.09.014 (2008).

31. Tokumaru, S., Suzuki, M., Yamada, H., Nagino, M. & Takahashi, T. let-7 regulates Dicer expression and constitutes a negative feedback loop. *Carcinogenesis* **29,** 2073–2077; 10.1093/carcin/bgn187 (2008).

32. Dincbas-Renqvist, V. *et al.* Human Dicer C-terminus functions as a 5-lipoxygenase binding domain. *Biochimica et biophysica acta* **1789,** 99–108; 10.1016/j.bbagrm.2008.10.002 (2008).

33. Provost, P., Samuelsson, B. & Rådmark, O. Interaction of 5-lipoxygenase with cellular proteins. *Proceedings of the National Academy of Sciences of the United States of America* **96,** 1881–1885 (1999).

34. Doyle, M. *et al.* The double-stranded RNA binding domain of human Dicer functions as a nuclear localization signal. *RNA (New York, N.Y.)* **19,** 1238–1252; 10.1261/rna.039255.113 (2013).

35. Ma, E., Zhou, K., Kidwell, M. A. & Doudna, J. A. Coordinated activities of human dicer domains in regulatory RNA processing. *Journal of molecular biology* **422,** 466–476; 10.1016/j.jmb.2012.06.009 (2012).

36. Lee, H., Han, S., Kwon, C. S. & Lee, D. Biogenesis and regulation of the let-7 miRNAs and their functional implications. *Protein & cell* **7,** 100–113; 10.1007/s13238-015-0212-y (2016).

37. Emmrich, S. *et al.* miR-99a/100~125b tricistrons regulate hematopoietic stem and progenitor cell homeostasis by shifting the balance between TGFβ and Wnt signaling. *Genes & development* **28,** 858–874; 10.1101/gad.233791.113 (2014).

38. Gerrits, A. *et al.* Genetic screen identifies microRNA cluster 99b/let-7e/125a as a regulator of primitive hematopoietic cells. *Blood* **119,** 377–387; 10.1182/blood-2011-01-331686 (2012).

39. Guo, S. *et al.* MicroRNA miR-125a controls hematopoietic stem cell number. *Proceedings of the National Academy of Sciences of the United States of America* **107,** 14229–14234; 10.1073/pnas.0913574107 (2010).

40. Potenza, N. *et al.* Molecular mechanisms governing microRNA-125a expression in human hepatocellular carcinoma cells. *Scientific reports* **7,** 10712; 10.1038/s41598-017-11418-3 (2017).

41. La Rica, L. de *et al.* NF-κB-direct activation of microRNAs with repressive effects on monocyte-specific genes is critical for osteoclast differentiation. *Genome biology* **16,** 2; 10.1186/s13059-014-0561-5 (2015).

42. Curtale, G. *et al.* Multi-Step Regulation of the TLR4 Pathway by the miR-125a~99b~let-7e Cluster. *Frontiers in immunology* **9,** 2037; 10.3389/fimmu.2018.02037 (2018).

43. Johnson, S. M. *et al.* RAS is regulated by the let-7 microRNA family. *Cell* **120,** 635–647; 10.1016/j.cell.2005.01.014 (2005).

44. Kumar, M. S. *et al.* Suppression of non-small cell lung tumor development by the let-7 microRNA family. *Proceedings of the National Academy of Sciences of the United States of America* **105,** 3903–3908; 10.1073/pnas.0712321105 (2008).

45. Yu, F. *et al.* let-7 Regulates Self Renewal and Tumorigenicity of Breast Cancer Cells. *Cell* **131,** 1109–1123; 10.1016/j.cell.2007.10.054 (2007).

46. Sampson, V. B. *et al.* MicroRNA let-7a down-regulates MYC and reverts MYC-induced growth in Burkitt lymphoma cells. *Cancer research* **67,** 9762–9770; 10.1158/0008-5472.CAN-07-2462 (2007).

47. Wang, Z. *et al.* MYC protein inhibits transcription of the microRNA cluster MC-let-7a-1~let-7d via noncanonical E-box. *The Journal of biological chemistry* **286,** 39703–39714; 10.1074/jbc.M111.293126 (2011).

48. Chang, T.-C. *et al.* Widespread microRNA repression by Myc contributes to tumorigenesis. *Nature genetics* **40,** 43–50; 10.1038/ng.2007.30 (2008).

49. Heo, I. *et al.* TUT4 in concert with Lin28 suppresses microRNA biogenesis through pre-microRNA uridylation. *Cell* **138,** 696–708; 10.1016/j.cell.2009.08.002 (2009).

50. Hagan, J. P., Piskounova, E. & Gregory, R. I. Lin28 recruits the TUTase Zcchc11 to inhibit let-7 maturation in mouse embryonic stem cells. *Nature structural & molecular biology* **16,** 1021–1025; 10.1038/nsmb.1676 (2009).

51. Newman, M. A., Thomson, J. M. & Hammond, S. M. Lin-28 interaction with the Let-7 precursor loop mediates regulated microRNA processing. *RNA (New York, N.Y.)* **14,** 1539–1549; 10.1261/rna.1155108 (2008).

52. Heo, I. *et al.* Mono-uridylation of pre-microRNA as a key step in the biogenesis of group II let-7 microRNAs. *Cell* **151,** 521–532; 10.1016/j.cell.2012.09.022 (2012).

53. Takashima, Y. *et al.* Suppression of lethal-7b and miR-125a/b Maturation by Lin28b Enables Maintenance of Stem Cell Properties in Hepatoblasts. *Hepatology (Baltimore, Md.)* **64,** 245–260; 10.1002/hep.28548 (2016).

54. Wu, L. & Belasco, J. G. Micro-RNA regulation of the mammalian lin-28 gene during neuronal differentiation of embryonal carcinoma cells. *Molecular and cellular biology* **25,** 9198–9208; 10.1128/MCB.25.21.9198-9208.2005 (2005).

55. O'Connell, R. M., Rao, D. S. & Baltimore, D. microRNA regulation of inflammatory responses. *Annual review of immunology* **30,** 295–312; 10.1146/annurev-immunol-020711-075013 (2012).

56. Taganov, K. D., Boldin, M. P., Chang, K.-J. & Baltimore, D. NF-kappaB-dependent induction of microRNA miR-146, an inhibitor targeted to signaling proteins of innate immune responses. *Proceedings of the National Academy of Sciences of the United States of America* **103,** 12481–12486; 10.1073/pnas.0605298103 (2006).

57. O'Connell, R. M., Taganov, K. D., Boldin, M. P., Cheng, G. & Baltimore, D. MicroRNA-155 is induced during the macrophage inflammatory response. *Proceedings of the National Academy of Sciences of the United States of America* **104,** 1604–1609; 10.1073/pnas.0610731104 (2007).

58. Sheedy, F. J. *et al.* Negative regulation of TLR4 via targeting of the proinflammatory tumor suppressor PDCD4 by the microRNA miR-21. *Nature immunology* **11,** 141–147; 10.1038/ni.1828 (2010).

59. Curtale, G. *et al.* Negative regulation of Toll-like receptor 4 signaling by IL-10-dependent microRNA-146b. *Proceedings of the National Academy of Sciences of the United States of America* **110,** 11499–11504; 10.1073/pnas.1219852110 (2013).

60. O'Neill, L. A., Sheedy, F. J. & McCoy, C. E. MicroRNAs. The fine-tuners of Toll-like receptor signalling. *Nature reviews. Immunology* **11,** 163–175; 10.1038/nri2957 (2011).

61. Androulidaki, A. *et al.* The kinase Akt1 controls macrophage response to lipopolysaccharide by regulating microRNAs. *Immunity* **31,** 220–231; 10.1016/j.immuni.2009.06.024 (2009).

62. O'Connell, R. M., Chaudhuri, A. A., Rao, D. S. & Baltimore, D. Inositol phosphatase SHIP1 is a primary target of miR-155. *Proceedings of the National Academy of Sciences of the United States of America* **106,** 7113–7118; 10.1073/pnas.0902636106 (2009).

63. McCoy, C. E. *et al.* IL-10 inhibits miR-155 induction by toll-like receptors. *The Journal of biological chemistry* **285,** 20492–20498; 10.1074/jbc.M110.102111 (2010).

64. Zhao, J. L. *et al.* NF-kappaB dysregulation in microRNA-146a-deficient mice drives the development of myeloid malignancies. *Proceedings of the National Academy of Sciences of the United States of America* **108,** 9184–9189; 10.1073/pnas.1105398108 (2011).

65. Boldin, M. P. *et al.* miR-146a is a significant brake on autoimmunity, myeloproliferation, and cancer in mice. *The Journal of experimental medicine* **208,** 1189–1201; 10.1084/jem.20101823 (2011).

66. El-Gabalawy, H., Guenther, L. C. & Bernstein, C. N. Epidemiology of immune-mediated inflammatory diseases. Incidence, prevalence, natural history, and comorbidities. *The Journal of rheumatology. Supplement* **85,** 2–10; 10.3899/jrheum.091461 (2010).

67. NobelPrize.org Nobel Media AB 2019. Press release -The Nobel Prize in Physiology or Medicine 1982. Available at https://www.nobelprize.org/prizes/medicine/1982/press-release/ (1982).

68. Dennis, E. A. & Norris, P. C. Eicosanoid storm in infection and inflammation. *Nature reviews. Immunology* **15,** 511–523; 10.1038/nri3859 (2015).

69. Häfner, A.-K., Kahnt, A. S. & Steinhilber, D. Beyond leukotriene formation-The noncanonical functions of 5-lipoxygenase. *Prostaglandins & other lipid mediators* **142,** 24–32; 10.1016/j.prostaglandins.2019.03.003 (2019).

70. Rådmark, O., Werz, O., Steinhilber, D. & Samuelsson, B. 5-Lipoxygenase, a key enzyme for leukotriene biosynthesis in health and disease. *Biochimica et biophysica acta* **1851,** 331–339; 10.1016/j.bbalip.2014.08.012 (2014).

71. Rådmark, O. & Samuelsson, B. 5-Lipoxygenase. Mechanisms of regulation. *Journal of lipid research* **50 Suppl,** S40-5; 10.1194/jlr.R800062-JLR200 (2009).

72. Steinhilber, D., Schubert-Zsilavecz, M. & Roth, H. J. *Medizinische Chemie. Targets, Arzneistoffe, chemische Biologie; 191 Tabellen.* 2nd ed. (2010).

73. Mutschler, E. *Mutschler Arzneimittelwirkungen. Lehrbuch der Pharmakologie, der klinischen Pharmakologie und Toxikologie: mit einführenden Kapiteln in die Anatomie, Physiologie und Pathophysiologie: mit 349 Abbildungen, 257 Tabellen und 1417 Strukturformeln.* 10th ed. (2013).

74. Pace, S. *et al.* Androgen-mediated sex bias impairs efficiency of leukotriene biosynthesis inhibitors in males. *The Journal of clinical investigation* **127,** 3167–3176; 10.1172/JCI92885 (2017).

75. U.S. Food and Drug Administration. Drugs@FDA: FDA Approved Drug Products. Drug Database. Available at https://www.accessdata.fda.gov/scripts/cder/daf/index.cfm.

76. Rote Liste. Rote Liste. Available at https://www.rote-liste.de/ (2019).

77. Basavarajappa, D. *et al.* Roles of coactosin-like protein (CLP) and 5-lipoxygenase-activating protein (FLAP) in cellular leukotriene biosynthesis. *Proceedings of the National Academy of Sciences of the United States of America* **111,** 11371–11376; 10.1073/pnas.1410983111 (2014).

78. Brock, T. G. Regulating leukotriene synthesis. The role of nuclear 5-lipoxygenase. *Journal of cellular biochemistry* **96,** 1203–1211; 10.1002/jcb.20662 (2005).

79. Luo, M. *et al.* Phosphorylation by protein kinase a inhibits nuclear import of 5-lipoxygenase. *The Journal of biological chemistry* **280,** 40609–40616; 10.1074/jbc.M507045200 (2005).

80. Flamand, N., Luo, M., Peters-Golden, M. & Brock, T. G. Phosphorylation of serine 271 on 5-lipoxygenase and its role in nuclear export. *The Journal of biological chemistry* **284,** 306–313; 10.1074/jbc.M805593200 (2009).

81. Rådmark, O., Werz, O., Steinhilber, D. & Samuelsson, B. 5-Lipoxygenase. Regulation of expression and enzyme activity. *Trends in biochemical sciences* **32,** 332–341; 10.1016/j.tibs.2007.06.002 (2007).

82. Brungs, M., Rådmark, O., Samuelsson, B. & Steinhilber, D. Sequential induction of 5-lipoxygenase gene expression and activity in Mono Mac 6 cells by transforming growth factor beta and 1,25-dihydroxyvitamin D3. *Proceedings of the National Academy of Sciences of the United States of America* **92,** 107–111 (1995).

83. Stoffers, K. L. *et al.* Calcitriol upregulates open chromatin and elongation markers at functional vitamin D response elements in the distal part of the 5-lipoxygenase gene. *Journal of molecular biology* **395,** 884–896; 10.1016/j.jmb.2009.10.022 (2010).

84. Steinhilber, D. *et al.* 5-lipoxygenase. Underappreciated role of a pro-inflammatory enzyme in tumorigenesis. *Frontiers in pharmacology* **1,** 143; 10.3389/fphar.2010.00143 (2010).

85. Moore, G. Y. & Pidgeon, G. P. Cross-Talk between Cancer Cells and the Tumour Microenvironment. The Role of the 5-Lipoxygenase Pathway. *International journal of molecular sciences* **18**; 10.3390/ijms18020236 (2017).

86. DeKelver, R. C. *et al.* Cooperation between RUNX1-ETO9a and novel transcriptional partner KLF6 in upregulation of Alox5 in acute myeloid leukemia. *PLoS genetics* **9,** e1003765; 10.1371/journal.pgen.1003765 (2013).

87. Chen, Y., Hu, Y., Zhang, H., Peng, C. & Li, S. Loss of the Alox5 gene impairs leukemia stem cells and prevents chronic myeloid leukemia. *Nature genetics* **41,** 783–792; 10.1038/ng.389 (2009).

88. Roos, J. *et al.* 5-Lipoxygenase is a candidate target for therapeutic management of stem cell-like cells in acute myeloid leukemia. *Cancer research* **74,** 5244–5255; 10.1158/0008-5472.CAN-13-3012 (2014).

89. Busch, S. *et al.* 5-lipoxygenase is a direct target of miR-19a-3p and miR-125b-5p. *Journal of immunology (Baltimore, Md. : 1950)* **194,** 1646–1653; 10.4049/jimmunol.1402163 (2015).

90. Wang, D., Li, Y., Zhang, C., Li, X. & Yu, J. MiR-216a-3p inhibits colorectal cancer cell proliferation through direct targeting COX-2 and ALOX5. *Journal of cellular biochemistry* **119,** 1755–1766; 10.1002/jcb.26336 (2018).

91. Recchiuti, A., Krishnamoorthy, S., Fredman, G., Chiang, N. & Serhan, C. N. MicroRNAs in resolution of acute inflammation. Identification of novel resolvin D1-miRNA circuits. *FASEB journal : official publication of the Federation of American Societies for Experimental Biology* **25,** 544–560; 10.1096/fj.10-169599 (2011).

92. Fredman, G., Li, Y., Dalli, J., Chiang, N. & Serhan, C. N. Self-limited versus delayed resolution of acute inflammation. Temporal regulation of pro-resolving mediators and microRNA. *Scientific reports* **2,** 639; 10.1038/srep00639 (2012).

93. Gonsalves, C. S. & Kalra, V. K. Hypoxia-mediated expression of 5-lipoxygenase-activating protein involves HIF-1alpha and NF-kappaB and microRNAs 135a and 199a-5p. *Journal of immunology (Baltimore, Md. : 1950)* **184,** 3878–3888; 10.4049/jimmunol.0902594 (2010).

94. Provost, P., Samuelsson, B. & Rådmark, O. Interaction of 5-lipoxygenase with cellular proteins. *Proceedings of the National Academy of Sciences of the United States of America* **96,** 1881–1885; 10.1073/pnas.96.5.1881 (1999).

95. Scholl, F. C. Dissertation. Goethe-Universität Frankfurt, 2015.

96. Jinek, M. *et al.* A programmable dual-RNA-guided DNA endonuclease in adaptive bacterial immunity. *Science (New York, N.Y.)* **337,** 816–821; 10.1126/science.1225829 (2012).

97. Kreiß, M. Master thesis. Goethe-Universität Frankfurt, 2016.

98. Söderberg, O. *et al.* Direct observation of individual endogenous protein complexes in situ by proximity ligation. *Nature methods* **3,** 995–1000; 10.1038/nmeth947 (2006).

99. Gerstmeier, J. *et al.* Time-resolved in situ assembly of the leukotriene-synthetic 5-lipoxygenase/5-lipoxygenase-activating protein complex in blood leukocytes. *FASEB journal : official publication of the Federation of American Societies for Experimental Biology* **30,** 276–285; 10.1096/fj.15-278010 (2015).

100. Sigma-Aldrich (Merck KGaA, D. How Proximity Ligation Assay (PLA) Works. Available at https://www.sigmaaldrich.com/technical-documents/protocols/biology/how-pla-works.html.

101. Müller, S. *et al.* omiRas. A Web server for differential expression analysis of miRNAs derived from small RNA-Seq data. *Bioinformatics (Oxford, England)* **29,** 2651–2652; 10.1093/bioinformatics/btt457 (2013).

102. Zuker, M. & Stiegler, P. Optimal computer folding of large RNA sequences using thermodynamics and auxiliary information. *Nucleic acids research* **9,** 133–148 (1981).

103. Esser, J. *et al.* Zymosan suppresses leukotriene C_4 synthase activity in differentiating monocytes. Antagonism by aspirin and protein kinase inhibitors. *FASEB journal : official publication of the Federation of American Societies for Experimental Biology* **25,** 1417–1427; 10.1096/fj.10-175828 (2011).

104. Bell, R. L. *et al.* The discovery and development of zileuton. An orally active 5-lipoxygenase inhibitor. *International journal of immunopharmacology* **14,** 505–510 (1992).

105. Gillard, J. *et al.* L-663,536 (MK-886) (3-1-(4-chlorobenzyl)-3-t-butyl-thio-5-isopropylindol-2-yl-2,2 - dimethylpropanoic acid), a novel, orally active leukotriene biosynthesis inhibitor. *Canadian journal of physiology and pharmacology* **67,** 456–464 (1989).

106. Garscha, U. *et al.* Pharmacological profile and efficiency in vivo of diflapolin, the first dual inhibitor of 5-lipoxygenase-activating protein and soluble epoxide hydrolase. *Scientific reports* **7,** 9398; 10.1038/s41598-017-09795-w (2017).

107. Ketting, R. F. *et al.* Dicer functions in RNA interference and in synthesis of small RNA involved in developmental timing in C. elegans. *Genes & development* **15,** 2654–2659; 10.1101/gad.927801 (2001).

108. Sigma-Aldrich (Merck KGaA, D. Duolink® PLA Troubleshooting Guide. Available at https://www.sigmaaldrich.com/technical-documents/protocols/biology/duolink-troubleshooting-guide.html.

109. Wang, D. J., Legesse-Miller, A., Johnson, E. L. & Coller, H. A. Regulation of the let-7a-3 promoter by NF-κB. *PloS one* **7,** e31240; 10.1371/journal.pone.0031240 (2012).

110. García, R. *et al.* p-SMAD2/3 and DICER promote pre-miR-21 processing during pressure overload-associated myocardial remodeling. *Biochimica et biophysica acta* **1852,** 1520–1530; 10.1016/j.bbadis.2015.04.006 (2015).

111. Blahna, M. T. & Hata, A. Smad-mediated regulation of microRNA biosynthesis. *FEBS letters* **586,** 1906–1912; 10.1016/j.febslet.2012.01.041 (2012).

112. Sürün, D. *et al.* High Efficiency Gene Correction in Hematopoietic Cells by Donor-Template-Free CRISPR/Cas9 Genome Editing. *Molecular therapy. Nucleic acids* **10,** 1–8; 10.1016/j.omtn.2017.11.001 (2018).

7 Supplement

7.1 Sequencing of small noncoding RNAs

Table S1 5-LO alters the miRNA expression profile

id	WT+/+	5-LOΔ+/+	x-fold	log [x-fold]
hsa-miR-99b-3p	4.189790	0.748449	5.597963	0.748030
hsa-miR-99b-5p	36.452100	7.879830	4.626001	0.665206
hsa-miR-361-3p	5.531400	1.247410	4.434308	0.646826
hsa-miR-26b-3p	2.134400	0.498966	4.277646	0.631205
hsa-miR-1908	1.867600	0.498966	3.742940	0.573213
hsa-let-7f-2-3p	1.723860	0.498966	3.454865	0.538431
hsa-miR-193a-3p	6.355690	1.909940	3.327691	0.522143
hsa-miR-130b-3p	3.303970	0.997932	3.310817	0.519935
hsa-miR-132-3p	2.199130	0.705488	3.117176	0.493761
hsa-miR-760	1.509250	0.498966	3.024755	0.480690
hsa-miR-195-5p	1.411280	0.498966	2.828409	0.451542
hsa-let-7e-5p	196.665000	71.247600	2.760304	0.440957
hsa-miR-1226-3p	1.821820	0.705488	2.582354	0.412016
hsa-miR-1226-5p	1.821820	0.705488	2.582354	0.412016
hsa-miR-203a	3.110040	1.204450	2.582125	0.411977
hsa-miR-125a-5p	45.548400	18.048000	2.523737	0.402044
hsa-miR-146a-3p	1.867600	0.748449	2.495294	0.397122
hsa-miR-4521	1.190260	0.498966	2.385453	0.377571
hsa-miR-23b-3p	1.739610	0.748449	2.324287	0.366290
hsa-miR-130b-5p	3.889760	1.703420	2.283500	0.358601
hsa-miR-191-3p	1.600800	0.705488	2.269068	0.355847
hsa-miR-574-3p	4.328600	1.978160	2.188195	0.340086
hsa-miR-421	5.408340	2.623340	2.061624	0.314209
hsa-miR-193a-5p	7.545950	3.827800	1.971354	0.294765
hsa-miR-484	18.596200	10.142500	1.833493	0.263279
hsa-miR-342-3p	7.828500	4.326760	1.809322	0.257516
hsa-miR-98-3p	3.512450	2.128340	1.650324	0.217569
hsa-miR-30b-3p	1.509250	0.919925	1.640623	0.215009
hsa-miR-222-5p	0.800398	0.498966	1.604113	0.205235
hsa-miR-34a-5p	3.356160	2.124380	1.579830	0.198610
hsa-miR-15b-5p	76.104300	48.398800	1.572442	0.196575
hsa-miR-25-5p	2.211680	1.418890	1.558740	0.192774
hsa-let-7f-1-3p	3.754150	2.408910	1.558443	0.192691
hsa-miR-1468	0.754623	0.498966	1.512374	0.179659
hsa-miR-29b-3p	0.754623	0.498966	1.512374	0.179659
hsa-miR-338-3p	0.754623	0.498966	1.512374	0.179659
hsa-miR-362-5p	0.754623	0.498966	1.512374	0.179659
hsa-miR-548l	0.754623	0.498966	1.512374	0.179659
hsa-miR-660-5p	11.583900	7.866080	1.472639	0.168096
hsa-miR-664a-5p	158.781000	109.532000	1.449631	0.161258
hsa-miR-941	12.739700	9.109530	1.398502	0.145663
hsa-miR-664a-3p	123.350000	88.644200	1.391518	0.143489
hsa-miR-301b	3.573980	2.623340	1.362378	0.134298
hsa-miR-30b-5p	46.702700	34.364300	1.359047	0.133234
hsa-miR-744-5p	8.687220	6.529150	1.330528	0.124024
hsa-miR-18a-5p	107.064000	80.513600	1.329763	0.123774
hsa-let-7i-3p	3.278880	2.469210	1.327906	0.123167
hsa-miR-183-5p	0.656657	0.498966	1.316036	0.119268
hsa-miR-769-3p	0.656657	0.498966	1.316036	0.119268
hsa-miR-345-5p	32.532300	24.738400	1.315053	0.118943
hsa-miR-339-5p	0.910911	0.705488	1.291179	0.110986
hsa-miR-196b-5p	563.281000	440.215000	1.279559	0.107060
hsa-miR-7-5p	47.485400	37.315100	1.272552	0.104675
hsa-miR-625-5p	1.082950	0.851710	1.271501	0.104317

hsa-miR-223-3p	93.842000	74.324800	1.262593	0.101264
hsa-miR-107	52.288000	41.558000	1.258193	0.099747
hsa-miR-18a-3p	57.439400	46.558400	1.233706	0.091212
hsa-miR-191-5p	2214.010000	1811.960000	1.221887	0.087031
hsa-miR-590-3p	1.723860	1.410980	1.221747	0.086981
hsa-miR-320b	5.990930	4.932950	1.214472	0.084388
hsa-miR-148b-3p	130.716000	109.151000	1.197570	0.078301
hsa-miR-27b-3p	57.677200	48.346100	1.193006	0.076643
hsa-miR-28-5p	9.926460	8.482050	1.170290	0.068294
hsa-miR-199b-3p	9.834910	8.618480	1.141142	0.057340
hsa-miR-17-5p	1004.710000	887.842000	1.131632	0.053705
hsa-miR-103a-3p	481.487000	432.851000	1.112362	0.046246
hsa-miR-3613-5p	1.334000	1.204450	1.107559	0.044367
hsa-miR-143-3p	58.739200	53.222300	1.103658	0.042834
hsa-miR-199a-3p	19.669800	17.839200	1.102617	0.042425
hsa-miR-3607-5p	22198.400000	20288.100000	1.094159	0.039080
hsa-miR-3607-3p	22224.800000	20323.100000	1.093573	0.038848
hsa-miR-30a-3p	2.088620	1.913900	1.091290	0.037940
hsa-miR-19b-1-5p	0.754623	0.705488	1.069647	0.029240
hsa-miR-500a-3p	1.288220	1.204450	1.069550	0.029201
hsa-miR-190b	1.067200	0.997932	1.069412	0.029145
hsa-miR-181d	183.313000	173.405000	1.057138	0.024132
hsa-miR-642a-5p	1.785380	1.703420	1.048115	0.020409
hsa-miR-210	7.469870	7.174340	1.041193	0.017531
hsa-miR-23a-3p	26.601700	25.553200	1.041032	0.017464
hsa-miR-223-5p	80.137800	77.513600	1.033855	0.014460
hsa-miR-142-3p	97.893900	95.216900	1.028115	0.012042
hsa-miR-3653	479.227000	468.110000	1.023749	0.010193
hsa-miR-301a-3p	49.173300	48.036700	1.023661	0.010156
hsa-miR-361-5p	19.357000	18.924900	1.022832	0.009804
hsa-miR-16-5p	1059.530000	1037.560000	1.021175	0.009100
hsa-miR-24-3p	265.253000	260.669000	1.017586	0.007571
hsa-miR-454-3p	25.030900	24.738400	1.011824	0.005105
hsa-miR-20a-5p	1360.960000	1347.420000	1.010049	0.004342
hsa-miR-181b-5p	469.717000	465.676000	1.008678	0.003752
hsa-let-7a-3p	0.754623	0.748449	1.008249	0.003568
hsa-miR-629-5p	4.251320	4.283800	0.992418	-0.003305
hsa-miR-29a-3p	5.092560	5.139470	0.990873	-0.003982
hsa-miR-589-5p	6.635040	6.717960	0.987657	-0.005394
hsa-miR-148a-3p	356.231000	362.137000	0.983691	-0.007141
hsa-miR-92b-3p	31.203200	31.975100	0.975859	-0.010613
hsa-miR-146b-3p	7.997330	8.218820	0.973051	-0.011864
hsa-miR-339-3p	4.046050	4.223500	0.957985	-0.018641
hsa-miR-335-3p	6.975910	7.294940	0.956267	-0.019421
hsa-miR-1248	157.635000	165.196000	0.954230	-0.020347
hsa-miR-296-3p	1.190260	1.247410	0.954185	-0.020367
hsa-miR-152	36.503300	38.788800	0.941078	-0.026374
hsa-miR-27a-3p	64.718400	68.863800	0.939803	-0.026963
hsa-miR-17-3p	12.420700	13.251100	0.937334	-0.028106
hsa-miR-26b-5p	509.015000	544.310000	0.935156	-0.029116
hsa-miR-28-3p	52.246700	56.201200	0.929637	-0.031687
hsa-miR-221-5p	10.517200	11.319800	0.929098	-0.031939
hsa-miR-664b-5p	115.943000	125.871000	0.921126	-0.035681
hsa-miR-128	5.880410	6.390840	0.920131	-0.036150
hsa-miR-221-3p	557.281000	610.829000	0.912336	-0.039845
hsa-miR-181a-5p	2173.250000	2387.300000	0.910338	-0.040797
hsa-miR-425-5p	94.056600	103.617000	0.907733	-0.042042
hsa-miR-181c-5p	144.622000	159.369000	0.907466	-0.042169
hsa-miR-181a-3p	19.411200	21.481800	0.903611	-0.044018
hsa-miR-148a-5p	11.489100	12.744200	0.901516	-0.045027
hsa-miR-19a-3p	102.385000	114.469000	0.894434	-0.048452
hsa-miR-15a-5p	10.417500	11.732900	0.887888	-0.051642

hsa-miR-222-3p	209.570000	236.541000	0.885977	-0.052577
hsa-miR-15b-3p	5.092560	5.844960	0.871274	-0.059845
hsa-miR-21-3p	62.043900	71.675400	0.865623	-0.062671
hsa-miR-425-3p	28.259100	32.768400	0.862389	-0.064297
hsa-miR-1291	9633.470000	11288.600000	0.853380	-0.068857
hsa-miR-532-5p	20.726200	24.418600	0.848787	-0.071201
hsa-miR-423-5p	67.620300	79.723200	0.848188	-0.071508
hsa-miR-340-5p	17.889400	21.323700	0.838944	-0.076267
hsa-miR-20a-3p	8.570580	10.220100	0.838600	-0.076445
hsa-miR-106a-5p	4.690160	5.599430	0.837614	-0.076956
hsa-miR-98-5p	664.344000	796.134000	0.834463	-0.078593
hsa-miR-769-5p	35.887200	43.132600	0.832020	-0.079866
hsa-miR-27a-5p	8.781980	10.631700	0.826018	-0.083010
hsa-miR-30c-5p	64.836000	78.526400	0.825659	-0.083199
hsa-miR-1307-3p	86.563100	104.947000	0.824827	-0.083637
hsa-miR-142-5p	323.269000	394.473000	0.819496	-0.086453
hsa-miR-24-2-5p	3.720930	4.541200	0.819372	-0.086519
hsa-miR-106b-5p	21.262500	26.207800	0.811304	-0.090816
hsa-miR-664b-3p	71.954400	88.775800	0.810518	-0.091237
hsa-miR-92a-3p	9989.790000	12461.400000	0.801659	-0.096010
hsa-miR-181c-3p	24.881000	31.085900	0.800395	-0.096696
hsa-miR-33a-3p	8.441100	10.606400	0.795850	-0.099169
hsa-miR-378a-5p	2.641180	3.328830	0.793426	-0.100494
hsa-miR-185-5p	4.233840	5.353910	0.790794	-0.101937
hsa-miR-26a-5p	332.331000	424.748000	0.782419	-0.106560
hsa-miR-19b-3p	496.766000	641.983000	0.773799	-0.111372
hsa-let-7g-5p	1313.920000	1747.630000	0.751830	-0.123881
hsa-let-7d-5p	158.247000	218.123000	0.725494	-0.139366
hsa-miR-93-5p	538.957000	743.697000	0.724700	-0.139842
hsa-miR-140-3p	108.827000	151.790000	0.716958	-0.144507
hsa-miR-3651	51.490600	71.944700	0.715697	-0.145271
hsa-let-7f-5p	5748.790000	8062.920000	0.712991	-0.146916
hsa-miR-106b-3p	60.837600	85.433900	0.712101	-0.147458
hsa-miR-1307-5p	13.184700	18.605000	0.708664	-0.149559
hsa-let-7d-3p	10.902100	15.593800	0.699130	-0.155442
hsa-miR-378c	1.506040	2.163380	0.696151	-0.157296
hsa-miR-155-5p	1357.550000	1998.120000	0.679414	-0.167866
hsa-miR-423-3p	125.507000	185.288000	0.677362	-0.169179
hsa-miR-146a-5p	66.853400	100.140000	0.667599	-0.175484
hsa-miR-320a	166.751000	251.452000	0.663152	-0.178387
hsa-miR-140-5p	12.697100	19.349100	0.656211	-0.182956
hsa-miR-30e-5p	206.419000	317.296000	0.650557	-0.186715
hsa-miR-93-3p	1.723860	2.658390	0.648460	-0.188117
hsa-let-7i-5p	1623.700000	2514.820000	0.645653	-0.190001
hsa-miR-378a-3p	455.338000	706.320000	0.644662	-0.190668
hsa-miR-21-5p	2499.160000	3885.150000	0.643260	-0.191614
hsa-miR-22-3p	50.662800	79.077400	0.640674	-0.193363
hsa-let-7a-5p	3885.530000	6075.150000	0.639578	-0.194107
hsa-miR-192-5p	18.095800	28.396300	0.637259	-0.195684
hsa-miR-186-5p	121.548000	191.623000	0.634308	-0.197700
hsa-miR-30d-5p	599.944000	947.909000	0.632913	-0.198656
hsa-miR-146b-5p	1267.880000	2130.850000	0.595011	-0.225475
hsa-miR-25-3p	343.037000	580.864000	0.590563	-0.228733
hsa-miR-3615	10.935300	19.213000	0.569162	-0.244764
hsa-miR-6087	86.394300	151.793000	0.569159	-0.244767
hsa-miR-92a-1-5p	105.070000	186.818000	0.562419	-0.249940
hsa-miR-548k	3.499900	6.222960	0.562417	-0.249941
hsa-miR-335-5p	1.190260	2.124380	0.560286	-0.251590
hsa-miR-3909	1.190260	2.159420	0.551194	-0.258695
hsa-miR-374b-5p	0.533599	0.997932	0.534705	-0.271886
hsa-miR-30a-5p	0.266799	0.498966	0.534704	-0.271887
hsa-miR-181a-2-3p	65.811600	126.939000	0.518451	-0.285293

hsa-let-7c	30.551000	60.061600	0.508661	-0.293571
hsa-miR-196a-5p	0.984986	1.952900	0.504371	-0.297250
hsa-miR-301a-5p	0.533599	1.058230	0.504237	-0.297365
hsa-miR-16-2-3p	6.807080	13.917600	0.489099	-0.310603
hsa-miR-15a-3p	1.288220	2.761650	0.466468	-0.331179
hsa-miR-101-3p	48.760500	105.234000	0.463353	-0.334088
hsa-miR-4449	0.656657	1.453940	0.451640	-0.345208
hsa-miR-1304-3p	1.867600	4.550990	0.410372	-0.386822
hsa-miR-30e-3p	44.577700	109.192000	0.408251	-0.389073
hsa-miR-378i	0.861928	2.163380	0.398417	-0.399662
hsa-miR-3609	14.221800	36.853300	0.385903	-0.413522
hsa-miR-199b-5p	4.484890	11.654900	0.384807	-0.414757
hsa-miR-1246	8.876740	23.118800	0.383962	-0.415712
hsa-miR-9-5p	16.209300	42.304200	0.383161	-0.416619
hsa-miR-153	0.800398	2.128340	0.376067	-0.424735
hsa-miR-671-5p	1.288220	3.436050	0.374913	-0.426069
hsa-miR-3620-3p	1.067200	3.036390	0.351470	-0.454112
hsa-miR-3620-5p	1.067200	3.036390	0.351470	-0.454112
hsa-miR-598	2.791050	8.261780	0.337827	-0.471306
hsa-miR-374a-3p	1.411280	4.330720	0.325877	-0.486947
hsa-let-7b-5p	51.421200	163.164000	0.315150	-0.501482
hsa-miR-4677-3p	0.533599	1.839850	0.290023	-0.537567
hsa-miR-148b-5p	1.785380	6.447190	0.276924	-0.557640
hsa-miR-374a-5p	0.533599	1.952900	0.273234	-0.563465
hsa-miR-197-3p	0.533599	2.159420	0.247103	-0.607122
hsa-miR-182-5p	4.767440	22.227800	0.214481	-0.668611
hsa-miR-125b-2-3p	0.800398	4.928990	0.162386	-0.789452
hsa-miR-577	0.533599	3.553060	0.150180	-0.823388

Sequencing of small noncoding RNAs was performed on an Illumina platform in wildtype and 5-LOΔ MM6 cells, differentiated with 1 ng/mL TGF-β and 50 nM calcitriol for three days. The omiRas tool[101] was used to analyze the data. Column 2 and 3 report the normalized mean expression. The effect of 5-LO on the miRNA expression profile is reported as x-fold (column 4) and as the base 10 logarithm of the x-fold (column 5). Results are representative for three independent experiments.

Table S2 LPS alters the miRNA expression profile

id	WT+/+	WT+/+/L	x-fold	log [x-fold]
hsa-miR-146b-3p	7.899920	171.330000	21.687561	1.336211
hsa-miR-146a-3p	1.850040	22.481400	12.151845	1.084642
hsa-miR-146a-5p	66.176800	521.219000	7.876159	0.896314
hsa-miR-301a-5p	0.528584	2.781260	5.261718	0.721128
hsa-miR-577	0.528584	2.781260	5.261718	0.721128
hsa-miR-125b-2-3p	0.792876	3.107860	3.919730	0.593256
hsa-let-7a-3p	0.757169	2.695980	3.560605	0.551524
hsa-miR-766-3p	0.638044	2.262100	3.545367	0.549661
hsa-miR-197-3p	0.528584	1.784270	3.375566	0.528347
hsa-miR-146b-5p	1256.500000	4126.230000	3.283908	0.516391
hsa-miR-29c-3p	0.528584	1.696580	3.209670	0.506460
hsa-miR-21-3p	61.428500	180.131000	2.932369	0.467219
hsa-miR-500a-3p	1.285750	3.686790	2.867424	0.457492
hsa-miR-345-3p	0.528584	1.446670	2.736878	0.437255
hsa-miR-374a-3p	1.395210	3.794050	2.719340	0.434463
hsa-miR-221-5p	10.443000	25.073900	2.401025	0.380397
hsa-miR-30b-3p	1.514340	3.346780	2.210059	0.344404
hsa-miR-1225-3p	0.528584	1.109070	2.098191	0.321845
hsa-miR-374b-5p	0.528584	1.109070	2.098191	0.321845
hsa-miR-30a-5p	0.264292	0.554534	2.098187	0.321844
hsa-miR-374a-5p	0.528584	1.084680	2.052048	0.312188
hsa-miR-4521	1.166630	2.325400	1.993263	0.299565
hsa-miR-125a-3p	1.285750	2.432670	1.892024	0.276927
hsa-miR-222-3p	207.392000	350.150000	1.688349	0.227462
hsa-let-7f-1-3p	3.742970	6.174410	1.649602	0.217379
hsa-miR-182-5p	4.714220	7.706360	1.634705	0.213439
hsa-miR-125a-5p	45.059200	72.815600	1.615999	0.208441
hsa-miR-181a-3p	19.252500	30.635300	1.591238	0.201735
hsa-miR-590-3p	1.695210	2.695980	1.590352	0.201493
hsa-miR-193a-3p	6.304810	9.976810	1.582412	0.199320
hsa-miR-378i	0.847606	1.337000	1.577384	0.197937
hsa-miR-671-5p	1.285750	1.976810	1.537476	0.186808
hsa-miR-3609	14.045100	21.322500	1.518145	0.181313
hsa-miR-27a-5p	8.673770	12.905500	1.487877	0.172567
hsa-miR-193a-5p	7.471440	10.652000	1.425696	0.154027
hsa-miR-128	5.807100	8.032970	1.383301	0.140917
hsa-miR-652-3p	1.135750	1.564920	1.377874	0.139209
hsa-miR-9-5p	15.980700	21.922100	1.371786	0.137286
hsa-miR-15a-3p	1.285750	1.759880	1.368758	0.136327
hsa-miR-301b	3.523740	4.817840	1.367252	0.135849
hsa-miR-4677-3p	0.528584	0.675196	1.277367	0.106316
hsa-miR-153	0.792876	1.012790	1.277362	0.106314
hsa-miR-21-5p	2474.250000	3138.010000	1.268267	0.103211
hsa-miR-199b-5p	4.430910	5.545340	1.251513	0.097435
hsa-let-7e-5p	194.387000	241.426000	1.241986	0.094117
hsa-miR-22-3p	50.035100	61.793500	1.235003	0.091668
hsa-miR-106a-5p	4.640470	5.696580	1.227587	0.089052
hsa-miR-15a-5p	10.321400	12.650800	1.225686	0.088379
hsa-miR-140-5p	12.612000	15.079900	1.195679	0.077614
hsa-miR-1248	155.911000	184.078000	1.180661	0.072125
hsa-miR-19b-1-5p	0.757169	0.867744	1.146037	0.059199
hsa-miR-221-3p	550.901000	631.325000	1.145986	0.059179
hsa-miR-454-3p	24.742700	27.945300	1.129436	0.052862
hsa-miR-155-5p	1343.450000	1514.970000	1.127671	0.052183
hsa-miR-1244	0.792876	0.892133	1.125186	0.051224
hsa-miR-3615	10.831000	12.167000	1.123350	0.050515
hsa-miR-195-5p	1.395210	1.564920	1.121638	0.049853
hsa-let-7i-3p	3.245260	3.517350	1.083842	0.034966

hsa-miR-15b-3p	5.009390	5.350390	1.068072	0.028601
hsa-miR-132-3p	2.192920	2.338800	1.066523	0.027970
hsa-miR-99b-5p	35.963800	38.297300	1.064885	0.027303
hsa-miR-320a	164.931000	173.081000	1.049415	0.020947
hsa-miR-1225-5p	1.057170	1.109070	1.049093	0.020814
hsa-let-7b-5p	50.897500	53.354100	1.048266	0.020471
hsa-miR-664b-5p	114.716000	118.950000	1.036909	0.015740
hsa-miR-1291	9504.340000	9783.520000	1.029374	0.012573
hsa-miR-30e-3p	44.099800	45.270100	1.026538	0.011375
hsa-miR-98-5p	657.044000	672.684000	1.023804	0.010217
hsa-miR-4449	0.638044	0.650808	1.020005	0.008602
hsa-miR-29a-3p	5.009390	5.106660	1.019418	0.008352
hsa-miR-664b-3p	71.233000	72.447500	1.017050	0.007342
hsa-miR-25-5p	2.188090	2.193750	1.002587	0.001122
hsa-let-7f-5p	5684.860000	5693.920000	1.001594	0.000692
hsa-miR-1307-5p	13.004600	12.993500	0.999146	-0.000371
hsa-miR-301a-3p	48.745300	48.370900	0.992319	-0.003349
hsa-miR-148a-3p	352.343000	348.696000	0.989649	-0.004519
hsa-miR-361-5p	19.066300	18.837300	0.987989	-0.005248
hsa-miR-3607-5p	21944.600000	21677.000000	0.987806	-0.005328
hsa-miR-3607-3p	21970.700000	21696.700000	0.987529	-0.005450
hsa-let-7c	30.111400	29.704000	0.986470	-0.005916
hsa-miR-27a-3p	64.119100	63.250500	0.986453	-0.005923
hsa-miR-19a-3p	101.419000	99.894400	0.984967	-0.006578
hsa-miR-3651	50.902200	50.114400	0.984523	-0.006774
hsa-let-7i-5p	1606.170000	1563.890000	0.973677	-0.011585
hsa-miR-92a-3p	9872.300000	9573.970000	0.969781	-0.013326
hsa-miR-200c-3p	1.166630	1.131050	0.969502	-0.013451
hsa-miR-664a-3p	122.040000	118.067000	0.967445	-0.014374
hsa-let-7a-5p	3842.090000	3705.720000	0.964506	-0.015695
hsa-miR-3653	473.167000	455.534000	0.962734	-0.016494
hsa-miR-27b-3p	57.080700	54.926500	0.962260	-0.016707
hsa-miR-148b-3p	129.434000	124.501000	0.961888	-0.016876
hsa-miR-143-3p	58.011300	55.763700	0.961256	-0.017161
hsa-miR-191-5p	2188.150000	2096.280000	0.958015	-0.018628
hsa-miR-185-5p	4.185640	4.002400	0.956222	-0.019441
hsa-miR-199a-3p	19.466600	18.550900	0.952960	-0.020925
hsa-miR-30e-5p	204.160000	193.805000	0.949280	-0.022606
hsa-miR-664a-5p	157.083000	148.056000	0.942534	-0.025703
hsa-miR-30d-5p	593.132000	558.260000	0.941207	-0.026315
hsa-miR-941	12.623800	11.849000	0.938624	-0.027508
hsa-miR-199b-3p	9.733280	9.106660	0.935621	-0.028900
hsa-miR-26b-5p	503.899000	470.096000	0.932917	-0.030157
hsa-miR-181c-3p	24.640400	22.937300	0.930882	-0.031105
hsa-miR-296-3p	1.166630	1.084680	0.929755	-0.031632
hsa-let-7d-3p	10.790400	10.031800	0.929697	-0.031659
hsa-miR-181b-5p	464.354000	428.422000	0.922619	-0.034977
hsa-miR-181a-5p	2149.520000	1982.590000	0.922341	-0.035109
hsa-miR-92b-3p	30.804500	28.359600	0.920632	-0.035914
hsa-miR-1226-3p	1.814340	1.663600	0.916917	-0.037670
hsa-miR-1226-5p	1.814340	1.663600	0.916917	-0.037670
hsa-let-7g-5p	1299.280000	1191.130000	0.916762	-0.037744
hsa-miR-20a-5p	1346.320000	1233.240000	0.916008	-0.038101
hsa-miR-181c-5p	142.913000	129.984000	0.909532	-0.041182
hsa-miR-106b-5p	21.002100	19.044600	0.906795	-0.042491
hsa-let-7d-5p	156.733000	142.119000	0.906759	-0.042508
hsa-miR-26a-5p	328.655000	297.490000	0.905174	-0.043268
hsa-miR-28-3p	51.680700	46.720600	0.904024	-0.043820
hsa-miR-25-3p	339.026000	306.419000	0.903822	-0.043917
hsa-miR-103a-3p	476.281000	429.540000	0.901863	-0.044860
hsa-miR-17-5p	993.932000	896.106000	0.901577	-0.044997
hsa-miR-92a-1-5p	103.660000	92.894000	0.896141	-0.047624

hsa-miR-7-5p	46.914000	42.028200	0.895856	-0.047762
hsa-miR-362-5p	0.757169	0.675196	0.891738	-0.049763
hsa-miR-425-3p	27.925900	24.832300	0.889221	-0.050990
hsa-miR-1307-3p	85.609100	75.629900	0.883433	-0.053826
hsa-miR-142-5p	319.478000	282.237000	0.883432	-0.053827
hsa-miR-423-3p	124.061000	109.387000	0.881719	-0.054670
hsa-miR-16-5p	1047.590000	923.552000	0.881597	-0.054730
hsa-miR-181a-2-3p	64.987500	56.964200	0.876541	-0.057228
hsa-miR-223-5p	79.199400	69.316500	0.875215	-0.057885
hsa-miR-378a-3p	450.542000	394.090000	0.874702	-0.058140
hsa-miR-186-5p	120.208000	104.955000	0.873112	-0.058930
hsa-miR-196b-5p	556.732000	482.782000	0.867171	-0.061895
hsa-miR-425-5p	93.016000	80.569300	0.866188	-0.062388
hsa-miR-142-3p	96.679900	83.446900	0.863126	-0.063926
hsa-miR-19b-3p	491.915000	420.787000	0.855406	-0.067828
hsa-miR-340-5p	17.743000	15.165200	0.854715	-0.068179
hsa-miR-181d	181.139000	154.248000	0.851545	-0.069792
hsa-miR-93-5p	532.931000	452.050000	0.848234	-0.071485
hsa-miR-6087	85.464000	71.435600	0.835856	-0.077869
hsa-miR-24-3p	262.590000	218.312000	0.831380	-0.080201
hsa-miR-378c	1.490480	1.216330	0.816066	-0.088275
hsa-miR-744-5p	8.578500	6.998190	0.815782	-0.088426
hsa-miR-532-5p	20.531000	16.598500	0.808460	-0.092341
hsa-miR-30b-5p	46.242800	37.375000	0.808234	-0.092463
hsa-miR-769-5p	35.497500	28.648400	0.807054	-0.093097
hsa-miR-106b-3p	60.142600	48.118200	0.800069	-0.096873
hsa-miR-107	51.771500	41.115200	0.794167	-0.100088
hsa-miR-192-5p	17.873600	14.141400	0.791189	-0.101720
hsa-miR-18a-5p	105.725000	82.990000	0.784961	-0.105152
hsa-miR-1246	8.769040	6.866540	0.783044	-0.106214
hsa-miR-17-3p	12.276100	9.520950	0.775568	-0.110380
hsa-miR-15b-5p	75.197000	57.707500	0.767418	-0.114968
hsa-miR-339-3p	3.997590	3.022580	0.756101	-0.121420
hsa-miR-140-3p	107.769000	81.299400	0.754386	-0.122407
hsa-miR-130b-3p	3.235590	2.432670	0.751847	-0.123870
hsa-miR-30c-5p	64.120900	48.115800	0.750392	-0.124712
hsa-miR-423-5p	66.725300	50.000300	0.749345	-0.125318
hsa-miR-345-5p	32.099600	23.785500	0.740991	-0.130187
hsa-miR-223-3p	92.716000	67.207900	0.724879	-0.139734
hsa-miR-589-5p	6.564270	4.672790	0.711852	-0.147610
hsa-miR-629-5p	4.207150	2.989610	0.710602	-0.148373
hsa-miR-378a-5p	2.650090	1.880540	0.709614	-0.148978
hsa-miR-99b-3p	4.152420	2.915320	0.702077	-0.153615
hsa-miR-18a-3p	56.670300	39.137300	0.690614	-0.160765
hsa-miR-19a-5p	0.638044	0.433872	0.680003	-0.167489
hsa-miR-769-3p	0.638044	0.433872	0.680003	-0.167489
hsa-miR-148a-5p	11.323600	7.697780	0.679800	-0.167619
hsa-miR-152	36.226400	24.288800	0.670472	-0.173619
hsa-miR-16-2-3p	6.733290	4.508160	0.669533	-0.174228
hsa-miR-20a-3p	8.516750	5.663600	0.664995	-0.177181
hsa-miR-23b-3p	1.714240	1.131050	0.659797	-0.180590
hsa-miR-598	2.752380	1.781860	0.647389	-0.188835
hsa-miR-574-3p	4.280910	2.748280	0.641985	-0.192475
hsa-miR-23a-3p	26.311800	16.806800	0.638755	-0.194666
hsa-miR-148b-5p	1.749940	1.109070	0.633776	-0.198064
hsa-miR-210	7.318790	4.604430	0.629124	-0.201263
hsa-miR-342-3p	7.754750	4.793450	0.618131	-0.208920
hsa-miR-3620-3p	1.057170	0.650808	0.615613	-0.210692
hsa-miR-3620-5p	1.057170	0.650808	0.615613	-0.210692
hsa-miR-101-3p	48.123200	29.569700	0.614458	-0.211508
hsa-miR-98-3p	3.469010	2.121860	0.611662	-0.213489
hsa-miR-660-5p	11.418800	6.827630	0.597929	-0.223350

hsa-miR-361-3p	5.442710	3.252920	0.597666	-0.223542
hsa-miR-3143	1.135750	0.675196	0.594494	-0.225853
hsa-miR-338-3p	0.757169	0.433872	0.573019	-0.241831
hsa-miR-335-5p	1.166630	0.650808	0.557853	-0.253480
hsa-miR-9-3p	0.792876	0.433872	0.547213	-0.261844
hsa-miR-28-5p	9.804690	5.336990	0.544330	-0.264137
hsa-miR-421	5.333240	2.844560	0.533364	-0.272976
hsa-miR-30a-3p	2.078630	0.999398	0.480796	-0.318039
hsa-miR-34a-5p	3.319010	1.542940	0.464880	-0.332660
hsa-miR-33a-3p	8.359580	3.881740	0.464346	-0.333158
hsa-miR-320b	5.921390	2.673990	0.451581	-0.345264
hsa-miR-24-2-5p	3.702430	1.663600	0.449327	-0.347438
hsa-miR-181b-3p	1.057170	0.433872	0.410409	-0.386783
hsa-miR-3909	1.166630	0.433872	0.371902	-0.429572
hsa-miR-335-3p	6.878460	2.432670	0.353665	-0.451408
hsa-miR-3613-5p	1.321460	0.433872	0.328328	-0.483692
hsa-miR-26b-3p	2.114330	0.675196	0.319343	-0.495743
hsa-miR-548k	3.473840	1.109070	0.319263	-0.495851
hsa-miR-484	18.361700	4.865340	0.264972	-0.576800
hsa-miR-130b-5p	3.847590	0.867744	0.225529	-0.646797
hsa-miR-203a	3.100090	0.433872	0.139955	-0.854013

Sequencing of small noncoding RNAs was performed on an Illumina platform in wildtype MM6 cells, differentiated with 1 ng/mL TGF-β and 50 nM calcitriol for three days. Cells were also stimulated with 1 µg/mL LPS. The omiRas tool[101] was used to analyze the data. Column 2 and 3 report the normalized mean expression. The effect of LPS on the miRNA expression profile is reported as x-fold (column 4) and as the base 10 logarithm of the x-fold (column 5). Results are representative for three independent experiments.

7.2 5-LO product formation in MM6 cells

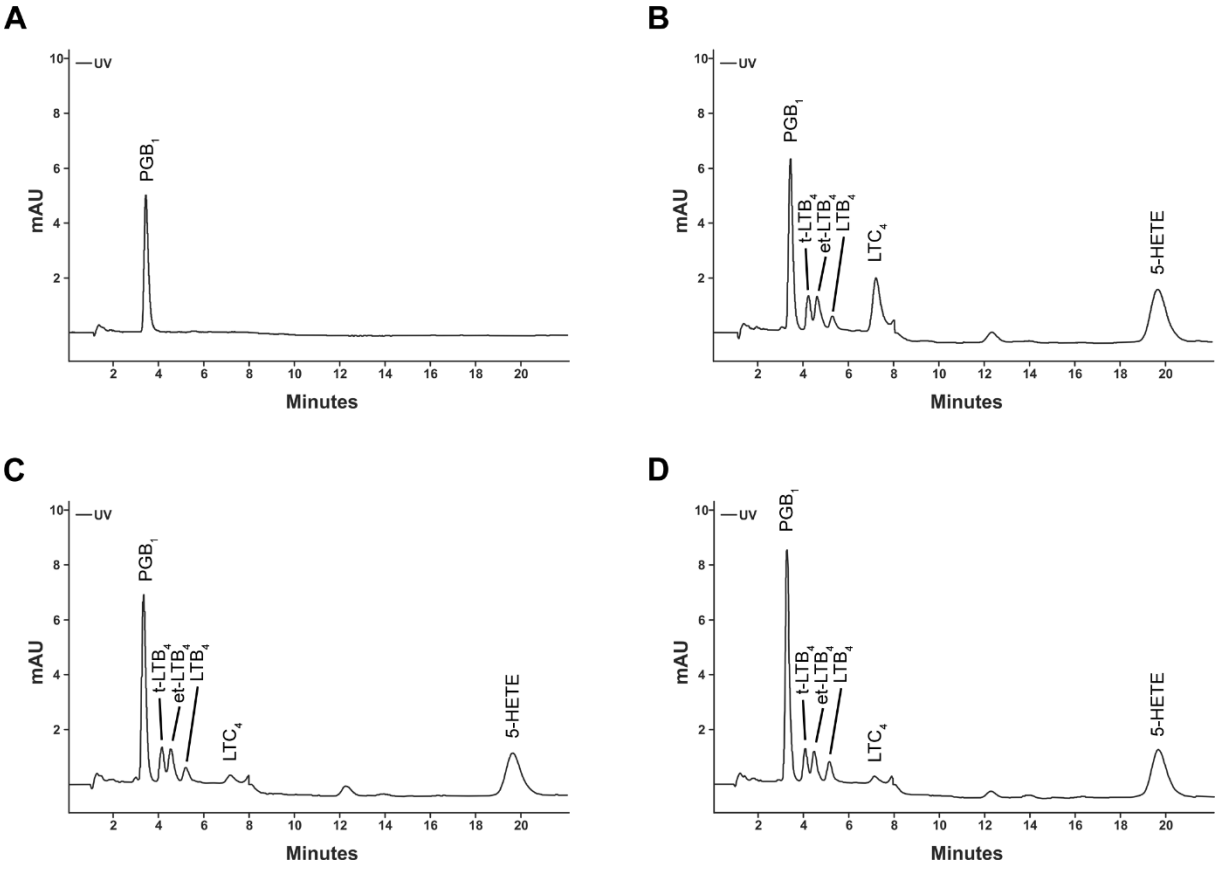

Figure S1 5-LO product formation in wildtype MM6 cells

(A-D) 5-LO product formation was analyzed by reverse-phase HPLC in 1 Mio wildtype MM6 cells, differentiated with 1 ng/mL TGF-β and 50 nM calcitriol for four days. Additionally, cells were stimulated with 1 µg/mL LPS (C) or 25 ng/mL zymosan (D). (A) Cells were preincubated (37°C, 10 min) with 100 nM PMA. (B-D) After preincubation (37°C, 10 min) with 100 nM PMA, cells were also incubated (37°C, 10 min) with 2.5 µM Ca^{2+}-ionophore A23187 and 10 µM arachidonic acid.